

UNIVERSITA' DEGLI STUDI DI PARMA

Dottorato di ricerca in Fisiopatologia Sistemica

Ciclo XXV

**ROLE OF PROTEOGLYCANS AND
GLYCOSAMINOGLYCANS IN TUMORIGENESIS**

Coordinatore:

Chiar.mo Prof Enrico Maria Silini

Tutor:

Chiar.mo Prof. Roberto Perris

Dottoranda: Dott.ssa Alessandra D'Angelo

a mio nonno

CONTENTS

ABSTRACT	3
ABBREVIATION	4
1. INTRODUCTION	6
1.1 Cell proliferation	18
1.2 Cell-cell adhesion	27
1.3 Cell-matrix interaction	28
1.4 Cell motility	33
1.5 Neurite outgrowth	38
1.6 Matrix assembly	41
1.7 Apoptosis	47
1.8 Cell differentiation	48
1.9 Angiogenesis	49
1.10 Coagulation	54
1.11 Immune response	55
2. MATERIALS AND METHODS	60
2.1 RNA extraction and reverse transcription-polymerase chain reaction (RT-PCR)	61
2.2 Purification of HSs	62
2.3 Cell culture and transfection	62
2.4 ECM molecule-cell adhesion	64
2.5 Flow cytometry	64
2.6 Western blotting	64
2.7 ELISA	65
2.8 Immunofluorescence and confocal microscopy	66
2.9 <i>In vitro</i> proliferation assay	67
2.10 Anchorage-independent growth assay	67
2.11 <i>In vivo</i> tumorigenesis	68
2.12 Immunohistochemistry	69
2.13 Vessel density and perfusion	71
2.14 Data and statistical analysis	71

3. RESULTS	72
3.1 Glypican 5 control of cancer growth and dissemination	73
3.1.1 Proteoglycan surface patter in sarcoma cells	73
3.1.2 GPC5 distribution on cell surface	75
3.1.3 GPC5 influences cell adhesion and proliferation	80
3.1.4 Inhibition of <i>in vivo</i> tumor formation	82
3.2 Immunomapping of highly sulfated heparan moieties in human tissues	91
3.2.1 Specificity of mAb 4D1	91
3.2.2 The epitope of mAb 4D1 encompasses highly sulfated tetrasaccharide repeat	91
3.2.3 Distribution of mAb 4D1-reactive HS chains in human adult tissue	95
3.3 Immunomapping of KSs	108
3.3.1 Definition of the specificity of the anti-KS mAb 373E1	108
3.3.2 Immunohistochemical staining pattern	110
4. DISCUSSION	117
5. ACKNOWLEDGEMENTS	122
6. BIBLIOGRAPHY	124

ABSTRACT

Structural-functional diversity of proteoglycans is the pivot of their biological importance during the embryonic development, in the adult and also in pathological conditions such as cancer. proteoglycans may be involved in different cell behavior by binding and modulating a broad spectrum of growth factors. In particular, among proteoglycans, glypicans are listed as both tumor-inhibitors and promoters and seems to be closely tumor-type specific. Our study on glypican 5 in a particular soft tissue sarcoma, human osteosarcoma, support the hypothesis that this molecule may be considered as a tumor-suppressor, inhibiting cancer cell growth and motility. Glycosaminoglycans participate to many of the proteoglycan biological processes and their functional complexity is in part due to their structural and chemical characteristics. For this reason we decided to investigate two particular glycosaminoglycan chains, highly sulfated heparan sulfate moieties and a specific keratan sulfate structure, using the monoclonal antibody technique. Our goal is to understand the correlation between the chemical structures of these moieties and their distribution in the human adult tissues. These may be the first steps in the comprehension of the structural-functional relationship of proteoglycans that could be considered as an attractive target for therapeutic intervention in different pathological conditions.

ABBREVIATIONS

AchR	acetylcholine receptor	FGFR	fibroblast growth factor receptor
ADAM	A disintegrin and metalloproteinase	FITC	fluorescein isothiocyanate
AIS	axonal initial segment	Fz	Frizzled
APC	antigen presenting cells	GAG	glycosaminoglycan
BBB	blood brain barrier	GDF	growth differentiation factor
b FGF	basic fibroblast growth factor	GM-CSF	granulocyte macrophage-colony stimulating factor
BMP	bone morphogenic protein	GPC	glypican
BMPR	bone morphogenic protein receptor	GPI	glycosyl phosphatidyl inositol
BKHS	bovine kidney heparan sulfate	Ha	hyaluronan
BSA	bovine serum albumin	HA	hemagglutinin
BWS	Beckwith Wiedemann Syndrome	HB-GAM	heparin-binding growth-associated molecule
C4-BP	C4-binding protein	Hep	heparin
CHO	Chinese Hamsted ovary	HGF	hepatocyte growth factor
CS	chondroitin sulfate	HGFR	hepatocyte growth factor receptor
Dlp	Dally-like protein	HGF/SF	hepatocyte growth factor/scatter factor
DMEM	Dulbecco's modified Eagle's medium	HNSCC	head and neck squamous cell carcinoma
DS	dermatan sulfate	HRP	horseradish peroxidase
ECM	extracellular matrix	HS	heparan sulfate
EGF	epidermal growth factor	IGF	insulin-like growth factor
EGFR	epidermal growth factor receptor	IGFR	insulin-like growth factor receptor
ERM	ezrin/radixin/moesin	IL-8	interleukin-8
FAK	focal adhesion kinase	KS	keratan sulfate
FBS	fetal bovine serum	LDL	low density lipoprotein
FGF	fibroblast growth factor		
FGF-BP	fibroblast growth factor-binding protein		

LRR	leucine rich region	Shh	Sonic hedgehog
MAPK	mitogen-activated protein kinase	ShS	sheep serum
MASC	myotube-associated specificity component	SMC	smooth muscle cell
MMP	metalloprotease	TAFI	thrombin activatable fibrinolysis inhibitor
MuSK	muscle-specific tyrosin kinase	TGFβ	transforming growth factor β
NFκB	nuclear transcription factor-kappa B	TGFβR	transforming growth factor β receptor
NGS	normal goat serum	TMA	tissue macroarray
NMJ	neuromuscular junction	TNF	tumor necrosis factor
PG	proteoglycan	TRITC	tetramethyl rhodamine isothiocyanate
PDGF	platelet-derived growth factor	VEGF	Vascular endothelial growth factor
PDGFR	platelet-derived growth factor receptor	VEGFR	Vascular endothelial growth factor receptor
PE	phycoerythrin	VLDL	very low density lipoprotein
PIHS	porcine instinal heparan sulfate	WISP-1	Wnt1 inducible signaling pathway protein
PKC	protein kinase C	Wg	Wingless
SD	syndecan		
SGBS	Simpson-Golabi-Behemel Syndrome		

1. INTRODUCTION

Proteoglycans are macromolecules composed of a central protein structure substituted with covalently attached glycosaminoglycan chains. GAGs may be divided in three main families: heparin/heparan sulfate, chondroitin sulfate and its epimerized homolog dermatan sulfate and keratan sulfate. Inside these families there are different subtypes on the basis of the chemical structure and the tissue localization (Tab.1). All GAGs are characterized by disaccharide units repetition, in particular acetylated hexosamine (N-acetyl-galactosamine or N-acetyl-glucosamine) and uronic acids (D-glucuronic acid or L-iduronic-acid). Only keratan sulfate is comprised of N-acetyl-glucosamine and galactose unit [Theocharis et al., 2010]. The linkage of GAGs to the core protein involves a specific tetrasaccharide of two Galactose residues and a Xylose residue, coupled to the core protein through an O-glycosidic bond to a serine residue except for KS type I that is linked to the core protein through an N-asparagine bond. GAGs may be modified at various positions by sulfation, epimerization and acetylation. Size and ratio of the GAG chains may change with development, aging or during particular pathological conditions [Hardingham and Fosand, 1992]. There is no an unifying structural feature to form a unique and knowable PG family. This is due to the fact that many PGs have structural forms and sequences similar to those found in other protein families. In the past different PG classifications were done, on the basis of their localization and the type and number of GAG chains attached, the size, the modular composition or the gene homology. A new classification is here proposed on the basis of PG structural characteristics (Tab.2). PGs function as coreceptor for different ligands and at first it was believed that PG functions could be related exclusively to the presence of the GAG chains. The capacity of GAG chains to differently bind molecules involved in cell-cell and cell-matrix adhesion, cell proliferation and cell motility, appears to be charge-dependent because it is determined by the degree of sulfation of the chain. Another important parameter that influences PG binding capacity is the number and the size of the GAG chains attached to the core protein [Ruoslahti, 1989]. Now the PG family includes different molecules that may exist in glycosylated or unglycosylated isoforms, or molecules that are considered as PG also if they are free of any glycosylation. For this reason the attention of researcher now become to move toward a new way of visualization of this macromolecule family. It becomes increasingly important to focus also the structural and functional characteristics of the core protein. In the next section it will follow a large study on the PG ligands and the related functions with a particular attention to the sites which are directly responsible for the binding.

Table 1. GAG species and their structural characteristics

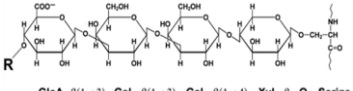
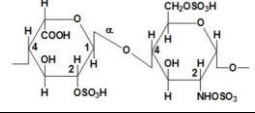
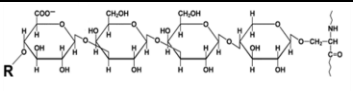
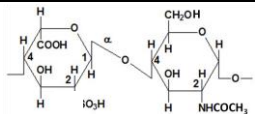
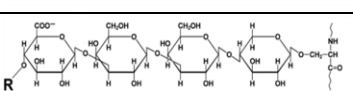
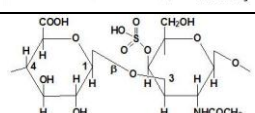
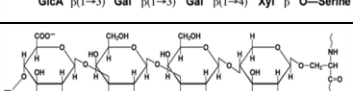
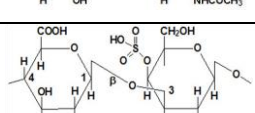
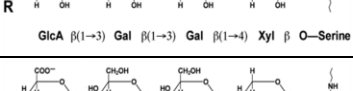
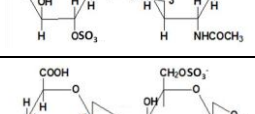
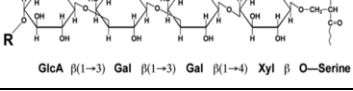
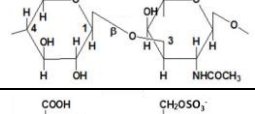
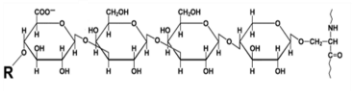
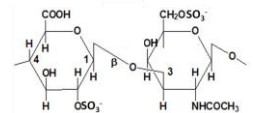
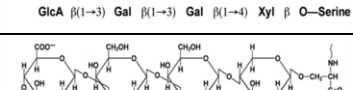
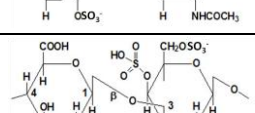
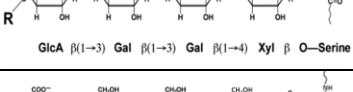
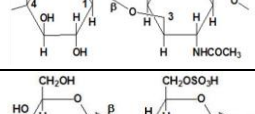
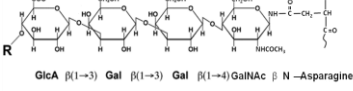
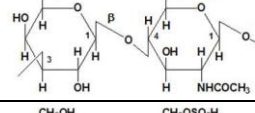
GAG	Size range	Core protein linkage	Disaccharide structure
Heparin	10-17 disaccharide units	 GlcA $\beta(1\rightarrow3)$ Gal $\beta(1\rightarrow3)$ Gal $\beta(1\rightarrow4)$ Xyl β O-Serine	
HS	10-17 disaccharide units	 GlcA $\beta(1\rightarrow3)$ Gal $\beta(1\rightarrow3)$ Gal $\beta(1\rightarrow4)$ Xyl β O-Serine	
CS-A	More than 100 disaccharide units	 GlcA $\beta(1\rightarrow3)$ Gal $\beta(1\rightarrow3)$ Gal $\beta(1\rightarrow4)$ Xyl β O-Serine	
CS-B/DS	More than 100 disaccharide units	 GlcA $\beta(1\rightarrow3)$ Gal $\beta(1\rightarrow3)$ Gal $\beta(1\rightarrow4)$ Xyl β O-Serine	
CS-C	More than 100 disaccharide units	 GlcA $\beta(1\rightarrow3)$ Gal $\beta(1\rightarrow3)$ Gal $\beta(1\rightarrow4)$ Xyl β O-Serine	
CS-D	More than 100 disaccharide units	 GlcA $\beta(1\rightarrow3)$ Gal $\beta(1\rightarrow3)$ Gal $\beta(1\rightarrow4)$ Xyl β O-Serine	
CS-E	More than 100 disaccharide units	 GlcA $\beta(1\rightarrow3)$ Gal $\beta(1\rightarrow3)$ Gal $\beta(1\rightarrow4)$ Xyl β O-Serine	
KS-I	8-9 disaccharide units	 GlcA $\beta(1\rightarrow3)$ Gal $\beta(1\rightarrow3)$ Gal $\beta(1\rightarrow4)$ GalNAc β N-Asparagine	
KS-II	5-11 disaccharide units	 GlcA $\beta(1\rightarrow3)$ Gal $\beta(1\rightarrow3)$ Gal $\beta(1\rightarrow4)$ Xyl β O-Serine	
KSIII	5-11 disaccharide units	 GlcA $\beta(1\rightarrow3)$ Gal $\beta(1\rightarrow3)$ Gal $\beta(1\rightarrow4)$ Xyl β O-Serine	

Table 2. Revisited PG nomenclature based upon combined GAG and core protein structural-functional traits

PG class	PG name	Core protein size (kDa)	Chromosomal location		Number and type of GAG chain	Human gene designation
			Human	mouse		
Matrix-associated						
Basement membrane	Perlecan	400	1p36.1-p34	4	3 HS/CS	HSPG2
	Agrin	220	1p36.33	4	3-6 HS	AGRN
	Leprecan	82	1p34.1	4	1-2 CS	LEPRE1
	Bamacan	138	10q25	19	3 CS	SMC3
Hyaluronan-binding	Versican	74-370	5q14.3	13	no GAGs/ 5-17 CS	CSPG2
	Neurocan	135	19p12	8	1-2 CS	NCAN
	Aggrecan	250	15q26.1	7	50-100 CS/KS	ACAN
	Brevican	96	1q31	3	no GAGs/ 1-3 CS	BCAN
Collagen-binding	Opticin	90	1q32.1	1	HS/CS	OPTC
	Lumican	38	12q21.3-q22	10	2-3 KS	LUM
	Decorin	42	12q21.3-q23	10	1 DS/CS	DCN
	Biglycan	38	Xq28	X	1-2 DS/CS	BGN

	Epiphycan	36	12q21	10	2 CS/DS	EPYC
	Keratocan	37	12q22	10	KS	KERA
	Fibromodulin	42	1q32	1	4 KS	FMOD
	Mimecan/ osteoglycin	34	9q22	13	KS	OGN
	Osteoadheri/osteomodu- dulin	47	9q22.31	13	KS	OMD
	Asporin	45	9q22	13	no GAGs	ASPN
	PRELP	58	1q32	1	no GAGs	PRELP
Interstitial	Chondro-adherin	36	17q21.33	11	no GAGs	CHAD
	Bikunin	25	9q32-q33	n.d.	1 CS	AMBP
	Testican1/ osteonectin	44	5q31.2	13	1-2 HS/CS	SPOCK1
	Testican2/ osteonectin	44	10pter-q25.3	10	1-2 HS/CS	SPOCK2
	Testican3/ osteonectin	44	4q32.3	8	1-2 HS/CS	SPOCK3
	Endocan	20	5q11.2	13	1 DS	ESM1
Neural	Interphoto receptor1	135	6q14.2-q15	9	N.D.	IMPG1
	Interphoto receptor2	135	3q12.2-q12.3	16	N.D.	IMPG2

	Neuroglycan C	60	3p21.3	9	no GAGs/ 1CS	CSPG5
	Phosphacan	175	7q31.3	6	2-5 CS	PTPRZ1
Cell surface anchored	Glypican 1	57-69	2q35-q37	1	1-3 HS	GPC1
	Glypican 2	57-69	7q22.1	5	1-3 HS	GPC2
	Glypican 3	60	Xq26.1	X	1-3 HS	GPC3
	Glypican 4	57-69	Xq26.1	X	1-3 HS	GPC4
	Glypican 5	65	13q32	14	1-3 HS/CS	GPC5
	Glypican 6	60	13q32	14	1-3 HS	GPC6
Transmembrane	Syndecan 1	33	2p24.1	12	1-2 HS/1-3 CS	SDC1
	Syndecan 2	23	8q22-q23	15	1-2 HS/1-3 CS	SDC2
	Syndecan 3	43	1pter-p22.3	4	1-2 HS/1-3 CS	SDC3
	Syndecan 4	22	20q12	2	1-2 HS/1-3 CS	SDC4
	CD44	90-250	11p13	2	no GAGs/ HS/CS	CD44 molecule
	NG2/CSPG4	300	15q24.2	9	1 CS	NG2
	SV2	80	1q21.2	N.D.	KS	SV2A
	Betaglycan	110	1p33-p32	5	1 HS/CS/ DS	TGFBR3
Intracellular	Serglycin	18	10q22.1	10	10-15 Hep or HS/CS	SRGN
Hybrid	Collagen type IX	65	6q12-q14	1	no GAGs/ 1CS	COL9A1

Collagen type XV	225-250	9q21-q22	4	1-4 HS/CS	COL15A1
Collagen type XVIII	180-200	21q22.3	10	3 HS	COL18A1
Thrombomodulin	57	20p11.2	2	no GAGs/ 1CS	THBD

Table 3. GAG chain- versus core protein-mediated interactions of PGs

PG	GAG	Core Protein
Perlecan	FGFs, PRELP, VEGF, PDGF, FGFR3, bFGF	Laminin, collagen type IV, collagen type XVIII, fibronectin, thrombomodulin, fibrillin-1, PRELP, FGF7, FGF18, FGF-BP, N-CAM, nidogens, fibulin 2, $\alpha\beta 1$ integrin, α -dystroglycan, LDL, VLDL
Agrin	N.D.	α -dystroglycan, laminins 1,2 and 4, PDGF, TGF β , MASC, acetylcholine receptor
Leprecan	N.D.	Collagens
Bamacan	N.D.	Histone deacetylases, acetyltransferases
Versican	P-selectin, L-selectins, chemokines, CD44, $\beta 1$ integrin, EGFR, toll-like receptor 2	Hyaluronan, lectins, fibronectin, collagen type I, $\beta 1$ integrin, tenascin R, fibulin 1, fibulin 2, fibrillin 1
Neurocan	HB-GAM, amphoterin	Hyaluronan, lectins, tenascins C and R, Ng-CAM, N-CAM, TAG1/axonin1, heparin, FGF2
Aggrecan	collagens	Hyaluronan, lectins, collagen type II, collagen type IX, collagen type XI, COMP, matrilin, CMP
Brevican	N.D.	Hyaluronan, lectins, tenascins, EGFR, fibulin 2, Bral2, neurofascin 186
Opticin	Collagens type IX, collagen type XVIII	N.D.
Lumican	N.D.	Collagens, cytokines, $\alpha\beta 1$ integrin receptor, cytokines
Decorin	TNF- β , WISP-1, FGF-2, collagen type I, collagen type VI	TGF β s, TNF-b, WISP-1, collagens type I, collagen type II, MMPs, EGFR, IGFR, EGF, IGF
Biglycan	BMP2, BMP4, WISP-1	Collagen type VI
Epiphycan	N.D.	Collagens
Keratocan	N.D.	Collagens
Fibromodulin	N.D.	Collagen type I, collagen type II
Mimecan//osteoglycin	N.D.	BMP2, BMP3, TGF $\beta 1$, TGF $\beta 2$
Osteoadherin/osteomodulin	N.D.	$\alpha\beta 3$ integrin, EGFR
Asporin	N.A.	TGF $\beta 1$, BMP2, collagen type II
PRELP	N.A.	Perlecan, collagen type I, collagen type II, C4-BP, C9

Chondroadherin	N.A.	$\alpha 2\beta 1$ integrins, collagen type II
Bikunin	N.D.	Cathepsin G, acrosin, chymotrypsin, trypsin, granulocyte elastase, plasmin
Testicans 1-3	N.D.	Protease, cathepsin L
Endocan	Cytokines, fibronectin, collagens, HGF/SF	VEGF-A, VEGFR2, FGF2, TGF β , IGF2, EGF, integrins
Interphoto receptors 1-2	N.D.	N.D.
Neuroglycan C	N.D.	ErbB3
Phosphacan	N.D.	CAMs, pleiothropin
Glypicans 1-6	FGFs, FGFR, Wnt, BMPs, IGF-2, TGF β	Wnt, bFGF
Syndecams 1-4	MMP7, ADAM, fibronectin, laminin, vitronectin, plasma protein, anti thrombin 1, FGFs, VEGF, PDGF, HGF, TGF β , thrombospondin, chemokine, IL8, pathogens, integrins, collagens, Wnt	MMP7, integrins, PDZ proteins, FGF2, TGF β , anti-elastase, $\alpha 1$ -antitrypsin
CD44	N.D.	Hyaluronan, collagens type I and IV, laminin, fibronectin, osteopontin, integrins, HGF, EGF, FGFs, VEGF-A, TGF β , MMPs, VEGFR2, ErbB family receptors, ezrin, radixin, moesin, merlin
NG2/CSPG4	N.D.	Collagens type V and VI, FGF2, PDGF-AA, PDGFR α , FGFR1, FGFR3, laminin 2, $\alpha 3\beta 1$ integrin
SV2	N.D.	N.D.
Betaglycan	FGFs, TGF- β	TGF $\beta 1$, TGF $\beta 2$, TGF $\beta 3$, TGF β Rs, inhibin A, inhibin B, BMP2, BMP4, BMP7, BMPRs, endoglin, β -arrestin 2, GAIP-protein
Serglycin	CD44, granzyme B, proteases	N.D.
Collagens	N.D.	Integrins, MMPs, MT1-MMP, FGF2, VEGF, C4-BP, factor H, thrombomyosin
Thrombomodulin	Antithrombin, thrombin	Anti-thrombin, anti-coagulant protein C, thrombin, TAFI

N.D.: not detected; N.A.: not applicable

Table 4. GAG chain- versus core protein-mediated function of PGs

PG	GAG	Core protein	Context
Perlecan	Cell proliferation, cell motility, matrix assembly, angiogenesis	Cell proliferation, cell-matrix interaction	NIH-3T3 fibroblasts, SMCs, engineered human skin model, Zebrafish model, null mice models
Aggrin	N.D.	Cell-matrix interaction, neurite outgrowth, immune response	Mutant mice models
Leprecan	N.D.	Cell proliferation	NIH-3T3 fibroblasts
Bamacan	N.D.	Cell proliferation	
Versican	Cell-cell adhesion	Cell proliferation, cell-matrix interaction, cell motility	NIH-3T3 fibroblasts
Neurocan	N.D.	Cell-matrix interaction, neurite outgrowth, matrix assembly	
Aggrecan	Matrix assembly	Cell-matrix interaction, matrix assembly	Nanomelic chicken model, mutant mice models
Brevican	N.D.	Cell motility, matrix assembly	
Opticin	Matrix assembly, angiogenesis	N.D.	
Lumican	Matrix assembly	Cell motility	CHO cells
Decorin	Matrix assembly	Cell proliferation, matrix assembly	CHO cell line, SMCs, null mice models
Biglycan	Cell proliferation, cell differentiation	Matrix assembly	C2C12 cells, knockout mice models
Epiphycan	N.D.	N.D.	
Keratocan	N.D.	N.D.	
Fibromodulin	N.D.	Matrix assembly	Null mouse models
Mimecan/osteoglycin	N.D.	Matrix assembly	Knockout mouse models
Osteoadherin/osteomodulin	N.D.	Cell-matrix interaction	MC3T3E1 cells
Asporin	N.A.	Matrix assembly	
PRELP	N.A.	Cell proliferation, cell-matrix interaction, immune response	Mouse osteoblasts, mouse osteoblasts, <i>in vivo</i> mouse models
Chondroadherin	N.A.	Cell-matrix interaction	K9 cells
Bikunin	N.D.	Cell motility, coagulation	

Testicans 1-3	N.D.	Cell motility, neurite outgrowth	
Endocan	Cell proliferation, cell-matrix adhesion	Cell-matrix interaction, angiogenesis	HEK-293 cells
Interphoto receptor 1-2	N.D.	N.D.	
Neuroglycan C	N.D.	Cell proliferation	MDA-MB 453 cells, CHO cells, Escherichia Coli model
Phosphacan	N.D.	Neurite outgrowth	
Glypicans 1-6	Cell proliferation, apoptosis	Cell proliferation, apoptosis	Drosophila model, Xenopus model, mutant mouse models
Syndecans 1-4	Cell proliferation, cell-cell adhesion, cell-matrix interaction, cell motility, matrix assembly, cell differentiation, angiogenesis, immune response	Cell-cell adhesion, matrix assembly, cell differentiation, angiogenesis	CHO cell line, syndecans null fibroblasts, Huh7 cells, HT1080 cells, mutant mice models, Zebrafish model, quail model
CD44	N.D.	Cell proliferation, cell-matrix interaction, cell motility, cell differentiation	
NG2/CSPG4	N.D.	Cell-matrix interaction, cell motility, neurite outgrowth, apoptosis, angiogenesis	Glioma cells, C57Bl/6 mice models
SV2	N.D.	N.D.	
Betaglycan	Cell motility	Cell proliferation	MCF10A and MDA-MB-231 cell lines, 3T3 fibroblasts, <i>in vivo</i> xenograft mice model, null mice model
Serglycin	Cell-cell adhesion, cell motility, immune response	N.D.	Serglycin deficient mast cells, monocyte-like THP-1 cells, knockout mouse models, NDST-2 knockout mouse models
Collagens	N.D.	Cell motility, apoptosis, angiogenesis, immune response	Umbilical vein endothelial cells, chick chorioallantoic membranes
Thrombomodulin	Coagulation	Cell proliferation, coagulation, immune response	Mutant mouse models

Table 5. GAG- chain versus core protein- involvement in disease

PG	GAG	Core protein	Context
Perlecan	Cell proliferation, cell motility, angiogenesis	Angiogenesis	Tumor cells
Aggrin	Matrix assembly	N.D.	Alzheimer's disease
Leprecan	N.D.	N.D.	
Bamacan	N.D.	Tumor progression	
Versican	N.D.	Cell proliferation, cell-matrix interaction, cell motility, metastasis	NIH-3T3 fibroblasts, tumor cells
Neurocan	N.D.	N.D.	
Aggrecan	Matrix assembly	Matrix assembly	Nanomelic chicken model, mutant mice models
Brevican	N.D.	Cell motility	9L cells
Opticin	Angiogenesis	N.D.	CAM assay
Lumican	Tumor progression	Cell motility, metastasis	A375 cells, B16F1 cells
Decorin	N.D.	Tumor progression, angiogenesis, metastasis	Colon carcinoma cells, HT1080 cells, Saos2 cells, breast cancer animal models
Biglycan	Tumor progression	N.D.	
Epiphycan	N.D.	N.D.	
Keratocan	N.D.	N.D.	
Fibromodulin	N.D.	N.D.	
Mimecan/osteoglycin	N.D.	N.D.	
Osteoadherin/osteomodulin	N.D.	Cell proliferation, cell migration	
Asporin	N.A.	Matrix assembly	Osteoarthritis
PRELP	N.A.	Immune response	Rheumatoid arthritis
Chondroadherin	N.A.	N.D.	
Bikunin	N.D.	Cell motility, metastasis	Bladder carcinoma
Testicans 1-3	N.D.	Cell motility	
Endocan	Tumor progression	Angiogenesis	Bladder cancer, vascular endothelial cells, transgenic mice mdels
Interphoto receptor 1-2	N.D.	N.D.	

Neuroglycan C	N.D.	Cell proliferation	T47D cells, MDAMB-453 cells
Phosphacan	N.D.	N.D.	
Glypicans 1-6	Cell proliferation	N.D.	
Syndecans 1-4	Cell proliferation, cell-matrix interaction	Tumor progression, angiogenesis	Tumor cells
CD44	N.D.	Tumor progression, cell motility, angiogenesis	SCC25 cells, CAL 27 cells, MCF7 cells, B-CCL cells, <i>in vivo</i> models
NG2/CSPG4	N.D.	Tumor progression, cell-matrix interaction, cell motility, apoptosis, angiogenesis	
SV2	N.D.	N.D.	
Betaglycan	N.D.	Tumor progression	
Serglycin	Cell motility, metastasis, immune response	N.D.	
Collagens	N.D.	Angiogenesis	
Thrombomodulin	Coagulation	N.D.	

1.1. Cell proliferation

ONLY CORE PROTEIN

In CHO cells decorin directly inhibits cell proliferation and this function depends on its capacity to bind TGF- β 1, β 2 and β 3 with the same efficiency, via its core protein [Baghy et al., 2012; Hardingham and Foseng, 1992; Iozzo and Murdoch, 1996; Iozzo, 1998]. Decorin is up-regulated when cells reach quiescence and it has been identified as one of the genes, named quiescins, that are overexpressed by lung fibroblasts during the stationary phase of contact inhibition and quiescence [Iozzo and Murdoch, 1996]. Decorin may also inhibit cell proliferation in a directly way independent of TGF β . In fact when decorin is ectopically expressed into colon carcinoma cells which do not synthesize decorin, the cells become quiescent, form small colonies in soft agar and do not generate tumors in immunocompromised hosts. Overexpression of decorin or its addition in culture media has been shown to cause a severe cytostatic effect on many cancer cells including glioma, ovarian and colon cancer cells. Increased decorin expression *in vivo*, achieved

with gene transfer techniques, causes growth inhibition in various tumors and it prevents metastasis in particular in breast cancer animal models. It is shown that a number of clones are arrested in G1 phase of the cell cycle and their growth suppression can be restored by treatment with decorin antisense oligodeoxynucleotides [Iozzo, 1998]. A tumor xenograft approach using decorin-expressing cell lines, such as HT1080 and Saos2, showed a significant reduction of growth and neovascularization, in particular at the tumor invasive front compared to the decorin expressing counterpart. *De novo* expression of decorin or exogenous recombinant decorin, down-regulated the endogenous expression of the pro-angiogenic factor VEGF and suppressed the tumorigenicity of human colon carcinoma cells both *in vitro* and *in vivo*. Another mechanism of cell growth modulation by decorin is through interaction with growth factor receptors such as EGFR and IGFR. The decorin-induced growth arrest is associated with an induction of p21, a potent inhibitor of cyclin-dependent kinase activity. Ectopic expression of decorin proteoglycan or decorin core protein fraction, a mutated form lacking any GAG side chains, induces growth suppression in neoplastic cells of various histogenetic origins [Iozzo, 1998]. The induction of p21 occurs due to a rapid phosphorylation of the EGF receptor and a concurrent activation of the MAP kinase signal pathway. This leads to a protracted induction of endogenous p21 and ultimate cell cycle arrest [Iozzo, 1998]. The ability of secreted decorin to induce growth suppression gives further support to the concept that abnormal production of this PG around invading carcinomas represents a specialized biological response of the host designed to counterbalance the invading tumor cells [Iozzo, 1998]. Decorin is also essential for smooth muscle cells proliferation and synthetic functions. In particular the effect of decorin on SMCs is mediated via inhibition of TGF β activity and leading to decreased proliferation and less synthetic activity of these cells [Singla et al., 2011]. Decorin also has an important effect on the vascular calcification and it increases calcium deposition in cultured bovine arterial SMCs [Fischer et al. 2004].

A subpopulation of 3T3 fibroblasts that express a form of betaglycan lacking the GAG chains binds different growth factors with equal affinity compared with the fully glycosylated species [Couchman, 2010; Hardingham and Fosang, 1992]. Betaglycan ectodomain may be regulated by shedding via proteolytic cleavage, producing a soluble form that is proposed to sequester growth factors from their signaling receptors, antagonizing the signaling [Bilandzic and Stenvers, 2011]. The C-terminal of the betaglycan cytoplasmic domain may bind the C-terminal domain of the protein GAIP, an inducible phosphoprotein, and this interaction stabilizes the PG molecule at the cell membrane and increase TGF β responsiveness in Mv1Lu mink lung epithelial cells and L6 myoblasts [Bilandzic and Stenvers, 2011]. T β R2 null mice die at embryonic stages by heart and liver defects caused by an altered TGF β 2-induced mesenchymal transformation process

and the incidence of apoptotic events. Betaglycan orchestrates the TGF β , BMP and inhibin-mediated signals in different cell types enhancing the binding of all the TGF β isoforms with their receptors, in particular the TGF β 2. On the other hand, betaglycan enhances the binding of BMP2, 4, 7 and GDF5 to BMPRI leading to an increase in Smad1 phosphorylation. The capacity of this PG to bind TGF β may be the reason of its tumor suppressor function in different cell types. In particular its loss is related with the loss of sensitivity to TGF β and inhibin-mediated control of cancer cell growth and migration. It is demonstrated that cancer cells show a downregulation or loss of betaglycan expression at the mRNA and/or protein levels which correlates with increasing tumor progression [Bilandzic and Stenvers, 2011]. Betaglycan also binds β -arrestin2 in a GAG-independent manner. Arrestin is a regulator of G protein-coupled receptors which bind to activated receptor, targeting them for internalization and desensitization. Arrestin requires betaglycan to be phosphorylated by the TGF β R2. As result of betaglycan-arrestin association, betaglycan and the TGF β R2 are co-internalized via a clathrin-independent/lipid raft pathway and TGF β signaling is suppressed. The association of betaglycan with β -arrestin2 also results in the internalization of ALK6 type I BMP receptor, conversely, enhancing BMP signaling [Bilandzic and Stenvers, 2011].

Thrombomodulin EGF-like repeats in the extracellular part of the core protein, has mitogenic effects on cultured fibroblasts and vascular smooth muscle cells mediated via activation of protein kinase C and MAPKs [Anastasiou et al., 2012].

N-terminal domain of PRELP is a type-specific NF κ B inhibitor, in particular in the bone tissues [Happonen et al., 2001]. Studies on *in vitro* cultures of mouse osteoblasts and osteoclasts and *in vivo* mouse models of bone loss confirm that PRELP involvement in osteogenesis requires its internalization and its inhibition of the transcription nuclear factor NF κ B [Rucci et al., 2009]. The binding of PRELP inhibits the p65NF κ B transcriptional activity and blocks osteoclasts formation by a direct mechanism affecting perfusion osteoclasts. In this way it becomes an active regulator of bone resorption [Rucci et al., 2009].

Versican structurally consists of N- and C-terminal globular domains and two chondroitin sulfate domains (CS- α and CS- β), which are encoded by differential splicing exons. Alternative splicing generates at least four isoforms of versican known as V0, V1, V2, and V3. V0 contains both CS- α and CS- β ; V1 and V2 possess only CS- β and CS- α , respectively; and V3 solely has the globular domains. Versican isoforms V0/V1 are mainly expressed in the late stage of embryonic development, whereas versican V2 is one of the main constituents of the mature neural ECM. The different versican isoforms show different function in enhancing or inhibiting cell proliferation. In particular the V1 isoform has been shown to enhance cell proliferation and protect NIH-3T3 fibroblasts from apoptosis [Ricciardelli et al., 2009]. In fact *in vivo* studies on V1-induced NIH-3T3

tumor formation in nude mice is associated with apoptotic resistance and down-regulated Fas mRNA and protein levels and unexpectedly, sensitization to a wide range of cytotoxic agents [Ricciardelli et al., 2009]. Both the G1 and G3 versican domains have been shown to promote cell proliferation of NIH-3T3 fibroblasts and tumor cells. The G1 domain of versican is thought to stimulate proliferation by destabilizing cell adhesion whilst the G3 induced proliferation is mediated, at least in part, by the action of EGF-like motifs in the G3 domain activating EGF receptors [Ricciardelli et al., 2009]. By contrast, the V2 isoform exhibits opposing biological activities by inhibiting cell proliferation and lacking any association with apoptotic resistance [Ricciardelli et al., 2009]. The smallest splice variant, V3, consisting only of the amino- and carboxy-terminal G1 and G3 domains and lacking CS chains, was found to be expressed in primary endothelial cell cultures only following activation by pro-inflammatory cytokines or growth factors. The role of V3 in activated endothelium is not yet known. The overexpression of V3 in arterial SMCs resulted in their increased adhesion to culture flasks but reduced proliferation and slower migration in scratch wound assays [Ricciardelli et al., 2009]. In the same way, the overexpression of the V3 isoform in melanoma cancer cells markedly reduces cell growth *in vitro* and *in vivo* and promotes metastasis to the lung. These findings suggest that the V3 isoform may have a dual role as an inhibitor of tumor growth and a stimulator of metastasis [Ricciardelli et al., 2009]. Elevated levels of versican have been reported in most malignancies to date, including; brain tumors, melanomas, osteosarcomas, lymphomas, breast, prostate, colon, lung, pancreatic, endometrial, oral, and ovarian cancers. Even non-solid cancers, such as human acute monocytic leukemia cells, express and secrete V0 and V1 isoforms [Ricciardelli et al., 2009]. In all of these cases versican expression is related with poor prognosis. Epithelial versican expression has also been described in endometrial cancer and ovarian cancer. In ovarian cancer, high stromal versican levels correlated with serous cancers and were associated with reduced overall survival, while high versican levels in the epithelial cancer cells correlated with clear cell histology and increased recurrence-free survival [Ricciardelli et al., 2009]. The knockdown of versican expression in A549 lung cancer cells by RNA interference significantly inhibited tumor growth *in vivo* but not *in vitro*.

Neuroglycan C is expressed predominantly in the brain where it can directly bind and activate ErbB tyrosine kinase, one of the component of the EGF receptor family. This is confirmed also in *in vitro* studies on MDA-MB-453 cells, where the treatment with an anti ErbB3 antibody completely block neuroglycan C activity. This PG is not able to bind ErbB 1, 2 and 4. It was demonstrated that recombinant extracellular domains of NGC produced in *Escherichia coli* and CHO cells induce cell proliferation of the human breast cancer cell lines, T47D and MDAMB-453, via direct binding to ErbB3 and transactivation of ErbB2 [Kinugasa et al., 2004].

NIH-3T3 fibroblasts were transfected with mouse leprecan cDNA or with a truncated form encoding only the N terminal region of leprecan core protein or with an antisense construct. Clones expressing high level of both the isoforms and the antisense derivatives that showed negligible expression of the endogenous leprecan transcript, show an elevated capacity to form colonies and the clones transfected with the truncated form, lacking the carboxy-terminus, exhibited colony forming efficiencies comparable to that of vector transfected clones. These data suggest a growth suppressive function of leprecan attributable to its core protein portion [Kaul et al., 2000].

Bamacan is important in the formation of cohesin complexes that stabilize the cell during the cell cycle. During the S phase of cell cycle, bamacan bind the other components of cohesin complex such histone deacetylases or acetyltransferases via its core protein. *In vitro* studies show that histone deacetylases can directly deacetylate bamacan. Overexpression of deacetylases leads to under-acetylation of bamacan and cohesion defects, consistent with the idea that acetylation promotes cohesion and deacetylation reduces it cohesion. The ATPase activity of the bamacan subunits is critical for chromosome cohesion and it has been suggested that acetylation of bamacan by acetyltransferases modulates its ATPase activity [Xiong et al., 2010]. The involvement of this proteoglycan in chromatid cohesion during metaphase play an important role also in tumorigenesis and in tumor progression. Increased levels of bamacan have been reported in human tumors, primarily those of epithelial origin, such as breast, colon and lung. Moreover during tumor formation, extracellular bamacan forms abnormal accumulation, also if its exact extracellular function is not yet known.

NG2 proteoglycan binds to FGF2 and PDGF-AA with high affinity. The core protein of NG2, rather than the chondroitin sulfate chain, serves as a co receptor for FGF family members, with putative binding sites scattered throughout the D2 and D3 domains. Both FGF2 and PDGF-AA are critical for expansion of the oligodendrocyte progenitor population. In addition, phosphorylation of NG2 plays a role in cell proliferation. Extracellular signal-regulated kinase catalyzes the phosphorylation of NG2 at Thr2314, stimulating cell proliferation. Interestingly, $\alpha 3 \beta 1$ integrin activation is also required for this NG2-dependent increase in proliferation. NG2 phosphorylated at Thr2314 is co-localized with $\alpha 3 \beta 1$ integrin on microprojections on the apical cell surface. The integrin interacts with a set of signaling molecules, different from those needed in the motility mechanism [Xu et al., 2011]. Under non-stimulatory conditions, NG2-transfected U251 glioma cells are more proliferative than parental U251 cells due to basal levels of NG2 phosphorylation at Thr2314. Thr2314-Glutamine mutants exhibit even higher rates of proliferation, while Thr2314-Valine mutants are indistinguishable from non-transfected U251 cells [Stallcup and Huang, 2008]. In *in vivo* studies it was induce glioma formation via injection of a PDGF-B expressing

retrovirus into the white matter of adult wild type C57Bl/6 mice and NG2 null C57Bl/6 mice. The study underlines the important effect of NG2 in promoting glioma progression [Stallcup and Huang, 2008]. In a second *in vivo* assay it was utilized microinjection of CT2A mouse glioma cells into the white matter of five adult wild type and five adult NG2 null C57Bl/6 mice [Stallcup and Huang, 2008]. It shows a dramatic difference in the size of the tumors that develop in the two mouse lines after three weeks. Tumors in wild type mice are on average 10-fold larger than tumors in NG2 null mice [Stallcup and Huang, 2008]. Since CT2A cells express NG2, the differential effects of NG2 on tumor progression in wild type and NG2 null mice must come from elements of the host stroma, possibly including pericytes in the tumor vasculature and oligodendrocyte progenitors recruited to the tumor mass [Stallcup and Huang, 2008].

CD44 extracellular region interacts with hyaluronan and different ErbB family members, representing a pathway to EGFR inhibitor resistance by cross-activation of related pathways. Together with its ability to bind different cytoskeletal elements, such as ezrin, radixin, moesin and merlin, by its cytoplasmic domain, CD44 acts as a promoter of tumor cell proliferation and motility. CD44 role is evaluated in particular in head and neck squamous cell carcinomas. The transfection of CD44 low cell line SCC25 with CD44 gene, induces aggressive tumor morphology and appear to enhance tumor initiation. In these cells, CD44 complexes with RhoA-specific guanine nucleoside exchange factor to induce RhoA signaling, phospholipase C epsilon activity and cancer cell migration. The complex also interact with EGFR to stimulate Ras-mediated signaling and HSNCC cell growth. This interaction may be related with the chemotherapy resistance that is characteristics of this tumor type. Knockdown of CD44 in the overexpressing cell line CAL 27, validates these data by reducing tumor growth. The interaction between CD44 and ErbB2 has been shown in other tumors and could potentially provide a mechanism to bypass EGFR inhibition.

It has been shown that the core protein of endocan interacts *in vitro* with lymphocyte and monocyte LFA-1 and inhibits the LFA-1/ICAM-1 interaction, thereby regulating leukocyte recruitment and adhesion into inflammatory sites. Endocan is over expressed in a number of malignant tumors, including non small cell lung cancer, glioblastoma and hepatocellular carcinoma, with the expression level positively correlating with the severity of the disease. Within such tissues, endocan has been detected in endothelial cells at the tumor periphery. In severe combined immunodeficiency mice, injection of nontumorigenic HEK-293 cells, which have been engineered to express endocan, forms tumors, whereas HEK-293 cells expressing the S137A mutant form of endocan did not. This suggests that the tumor-promoting activity of endocan is, at least partly, caused by the GAG chain, presumably through promoting the activity of growth factors, including HGF/SF.

ONLY GAG CHAINS

HS chains of glypicans can bind both FGF2 and its receptor, promoting the receptor dimerization and increasing the growth factor mitogenic activity [Filmus, 2001]. The use of heparin-sulfate degrading enzymes reduces the FGFs binding of more than 95%, and this confirms the involvement of the GAG chains in the FGF binding of glypicans [Midorikawa et al., 2003]. Glypicans are also involved in BMP binding and regulation. The same studies in *Drosophila* with dally mutants, showed also that glypican regulates the signaling of dpp, the *Drosophila* corresponding form of BMP [Filmus, 2001]. In particular glypican 3 seems to be involved in the negative control of cellular proliferation [Midorikawa et al., 2003]. For this function, IGF2 and FGFs in general are suggested as putative GPC3 ligands. More deeply this PG seems to inhibit IGF2 signaling pathway, by competing for IGF2 binding with the signaling receptor [Midorikawa et al., 2003]. The existence of diseases due to GPC3 mutations and characterized by cell growth disorders, validates the important role of glypican 3 expression as cell proliferation modulator. In fact mutations in GPC3 are associated with the Simpson-Golabi-Behmel syndrome characterized by pre- and post-natal overgrowth. SGBS is caused by a nonfunctional GPC3 protein and its study is supported by the generation of GPC3-deficient mice [Filmus, 2001]. In these mice there is an increase in the proliferation rate of epithelial cells in the ureteric bud/collecting system. This support the idea that GPC3 is involved negatively in the regulation of cell proliferation and it can induce apoptosis in a cell type-specific manner [Filmus, 2001]. The same clinical evidence of SGBS are present also in Beckwith-Wiedemann syndrome, that is related to an overexpression of IGF2 factor. The loss-of-function mutation of GPC3 is equivalent to overexpression of IGF2 [Filmus, 2001]. To validate this data mice overexpressing IGF2 were generated and they showed together with the phenotypic features of BWS, also the skeletal defects that are typical of SGBS. An elegant *in vivo* study with a double mutant mice lacking the IGFR and H19 locus was generated to clarify the GPC3 function in the IGF signaling pathway. IGFR is a negative regulator of IGF2 and, binding the growth factor, it is able to downregulate its endocytosis and degradation. H19 locus regulates IGF2 imprinting. The double mutant mice show developmental growth typical of SGBS, caused by the mutation of the glypican-3 gene on the X chromosome. IGF2R-deficient mice display a degree of developmental overgrowth similar to the GPC3^{-/-} mice and this support the hypothesis of a direct cooperation between the glypican and IGF2 [Yan et al., 2009].

Syndecans bind different growth factors involved in the cell proliferation, like FGFs, VEGFs, PDGF, via their HS chains. CS chains may cooperate with HS for the binding. Post-translation HS chain modification or modification of the enzymes involved in HS modification, may

deeply influence the syndecan-mediated growth factors signaling [Tkachenko et al., 2005]. For example, in quail, Qsulf1, the avian homolog of Sulf1 and Sulf2, has been shown to remodel HS on the cell surface promoting Wnt1 signaling. In human cancer cell lines, Hsulf1 expression inhibited HGF stimulation of cell proliferation [Tkachenko et al., 2005]. The inhibition of HS formation attributable to mutations of EXT1 and EXT2 genes, results in hereditary multiple exostoses, an autosomal skeletal disorder characterized by inappropriate chondrocyte proliferation and bone growth due to an abnormal diffusion of hedgehog proteins [Tkachenko et al., 2005]. Also in pathological conditions, GAG modification result really fundamental for syndecans functions. For example during liver fibrosis and carcinogenesis, the degree of 3-*O*-sulfation of syndecans heparan sulfate is increased [Choi et al., 2011]. Also if structural modifications of heparan sulfate chains make an important contribution to the ability of syndecans to encode such enormous molecular and functional diversity, this structural diversity can be further increased through structural variability of chondroitin sulfate chains covalently attached to syndecan1, 3, and 4 [Choi et al., 2011]. syndecan 1 is known to associate with HGF and promote activation of phosphoinoside 3-kinase and mitogen-activated protein kinase pathways in multiple myeloma [Choi et al., 2011]. The involvement of the interaction of syndecans with their ligands in cell proliferation are well studied in different *in vivo* mutant mice models. For example homozygous disruption of syndecans 1 gene in mice determines an abnormally slow re-epithelialization after injury and an increased leukocyte adhesion involving the Wnt 1 signaling pathway; in syndecans 1 knockout mice mammary gland specific expression of Wnt1 do not lead to development of tumor as happens in wild type mice [Tkachenko et al., 2005].

Biglycan GAG chains are essential for its capacity to modulate cell proliferation and tumor progression. In facts this PG binds WISP-1 through its chains, in particular DS and CS-4 sulfated chains. *In vitro* solid phase assays demonstrate that the use of dermatan sulfate or chondroitin-4 sulfate moieties abolishes the binding of biglycan with WISP-1 demonstrating that a sulfate group is only required at position 4 of the *N*-acetylgalactosamine. By binding to biglycan, WISP-1 prevents its inhibitory activity on tumor cell proliferation favouring the tumor progression [Desnoyers et al., 2001].

COOPERATION

Perlecan functions as a gatekeeper to limit access of growth factors to subjacent target cells controlling cell replication and proliferation, as happens for the smooth muscle cells in vasculogenesis. So perlecan could modify the behavior of replicative cells by controlling the amount of growth factors involved in vascular morphogenesis [Iozzo, 1998]. Murine perlecan is

capable of downregulating Oct-1, a transcription factor involved in vascular smooth cell growth control, in *in vitro* experiments. Because the addition of soluble heparin does not elicit the same response, it is plausible that the ability of perlecan to alter smooth muscle cell function resides in the coordinated binding of the N-terminal domain of the protein core (SEA module and three SGD tripeptides) and HS chains [Iozzo, 1998]. In particular the function of HS chains seem to be the binding of FGF2 and its protection from proteolytic degradation [Bix and Iozzo, 2008]. The role of HS in smooth muscle cell proliferation has been shown to be important, when it is removed by a combination of bacterial heparinase digestions, the cells at a site of injury no longer respond to introduced FGF2 [Whiterlock et al., 2008]. It has been shown that the HS chains are responsible for the binding of other components of FGF family, like FGF1, 7, 9, 10, 18 and such interactions may lead to enhanced angiogenesis and chondrogenesis [Iozzo, 1998; Whiterlock et al., 2008]. Different *in vivo* studies show the importance of perlecan-FGFs binding. For example colon carcinoma cells, in which the perlecan gene is disrupted by targeted homologous recombination, grow slowly, fail to respond to exogenous FGF7 with or without heparin and are less tumorigenic when injected in immunocompromised mice. In an engineered human skin model, perlecan-deficient keratinocytes form a poorly-organized epidermis which is partially restored by exogenous FGF7 [Whiterlock et al., 2008]. The protein core of perlecan binds to FGF18, a key factor for chondrogenesis, and alters the mitogenic effect of FGF18 on growth plate chondrocytes. This finding is also supported by the similarity in cartilage phenotype between perlecan null and the FGF18 null mice which both exhibit a defect in endochondral ossification [Whiterlock et al., 2008]. Finally, Perlecan HS is also involved in branching morphogenesis of the submandibular salivary gland by specifically interacting with FGF10. In *ex vivo* models, heparanase co-localizes with perlecan in the glandular basement membrane and liberates FGF10 that is bound to the heparan sulfate. This chains leads to a signaling cascade which activates MAPK, stimulates the formation of epithelial clefts and ultimately enhances branching morphogenesis. The specificity of this interaction was demonstrated by surface plasmon resonance studies showing that FGF10 and FGF10/FGFR2b complexes bound to HS chains on perlecan, and that these complexes could be liberated by heparanase [Whiterlock et al., 2008]. Interestingly, perlecan is also able to act on the PDGF signaling pathway. In fact PDGF has been shown to contain an alternatively spliced exon that contains “heparin-binding” or matrix localization sequences. Both PDGF homodimers bind to perlecan HS derived from endothelial cells, and the inhibition of smooth muscle cell growth by perlecan may involve the inhibition of PDGF signaling which has downstream effects on FGF2 signaling [Whiterlock et al., 2008].

It is well known, also in *in vivo* studies, that glypicans bind Wnt and, like in the FGF2 binding, also in this case the HS chains are involved. Studies on dally-like, a *Drosophila* glypican,

show that dally mutation or the use of siRNA is associated with segment polarity defects similar to the ones caused by the loss of Wnt activity [Filmus, 2001; Yan et al, in 2009]. In these studies are investigated the interactions of dally-like with the *Drosophila* corresponding wingless morphogen, Wingless. It is shown that dally like may have a biphasic activity in the binding of Wg and that this behaviour is due to the ratio of dally-like and Fz2 (the Wg signalling receptor) on the cells. More deeply while a low ratio of Dlp:Fz2 can help Fz2 to bind Wg activating the signal cascade, a high ratio of Dlp:Fz2 prevents Fz2 from capturing Wg while Dlp may bind and sequester the morphogen factor. Also if previous studied showed that mutant models for the HS chains biosynthesis enzymes, have a defective Wg signalling, Yan demonstrates that Dlp core protein is involved in Wg binding, so it is possible to say that the specificity of Dlp in Wg signaling and biphasic activity results from its core protein. In particular the N terminal domain of core protein is essential for Wg binding. These conclusions are consistent with previous ones indicating that *Xenopus* GPC4 interacts with Wnt11 via N-terminal region of its core protein, and that GPC3 core protein binds directly Wnt and Shh without GAG chains interaction. As well as if Dlp core protein is responsible for Wg signalling, HS chains are also important for the binding affinity. Wg Dlp shows significantly stronger binding for Wg than the core protein alone [Yan et al., 2009].

To better study the domains involved in the interaction of syndecans with FGF2, different *in vivo* mouse models were generated. Expression of a full-length SDC4, SDC1 and GPC1 or of chimera constructs consisting of the ectoplasmic domain of GPC1 linked to the transmembrane/cytoplasmic domain of SDC4 (G1-S4c) or of the ectoplasmic domain of SDC4 linked to the GPC1 GPI anchor (S4-GPI), significantly increases cell associated HS mass and the number of FGF2-binding sites. However only cells expressing SDC4 and G1-S4c construct but not GPC1, SDC1 or S4-GPI cells demonstrated enhanced responsiveness to FGF2. Through this *in vivo* evidences, it is possible to conclude that the presence of SDC4 cytoplasmic domain and not simply an increase in the cell surface HS mass, that correspond to an increase in FGF-binding site number, is required for signaling. The cleavage of syndecans-4 HS chains also blocked enhanced FGF2 responsiveness, demonstrating that both SDC4 HS chains and SDC4 cytoplasmic domain are required for FGF2 signaling [Tkachenko et al., 2005].

1.2. Cell-cell adhesion

ONLY GAG CHAINS

Serglycin is proposed to be one of the most important PG essential in cell-cell interaction during the immune response. It is released by immune cells and binds to CD44 expressed on

lymphoid cells. This interaction is mediated by both serglycin CS-4 sulfated and CS-6 sulfated chains, but it is not dependent on the presence of heparin or HS chains. The interaction of serglycin with its extracellular ligands determines lymphoid cells activation [Kolset and Tveit, 2008; Kolset and Pejler, 2011].

Also in the case of versican, CS chains are identified as the principal binding sites for different cell surface molecules, such as P- and L-selectin, β 1 integrin, EGFR, CD44 and other ligands like chemokines that may be down regulated by versican binding [Ricciardelli et al., 2009].

COOPERATION

Syndecans, in particular syndecans 4, binds of different cell membrane proteins, such as integrins, happens via both GAG chains and core protein. For example, *in vitro* studies show that syndecans 4 expressing cells are able to bind specifically human foreskin fibroblasts and mouse aortic endothelial cells [Tkachenko et al., 2005].

1.3. Cell-matrix interaction

ONLY CORE PROTEIN

The adhesion of cells to the matrix is mainly mediated by the PG core protein. For example, the extracellular domain of the CD44 core protein binds different matrix component, like hyaluronan, collagens type I and II, laminin, fibronectin and osteopontin [Hardingham and Fosang, 1992; Hertweck et al., 2011; Louderbough and Schroeder, 2011]. The N-terminal domain of core protein is involved in hyaluronan binding giving it a different binding affinity for hyaluronan. The different glycosylation of the core protein and the molecular weight of Ha, in particular during inflammation seem to be implicated in the variation of the hyaluronan-binding affinity [Hardingham and Fosang, 1992]. In particular, while low molecular weight Ha stimulates cell growth, high molecular weight Ha inhibits proliferation [Hertweck et al., 2011]. This binding activates several pathway involved in cell proliferation, adhesion and migration. More precisely, it activates Rho and Rac1 GTPase that cause a reorganization of the actin cytoskeleton, ErbB2 tyrosine kinases, which lead to cell proliferation, and nuclear factor NF κ B [Wu et al., 2005]. Osteopontin selectively binds to CD44 isoforms v6 and v7 and triggers signaling that promotes cell survival, migration and invasion and angiogenesis.

Versican binds hyaluronan molecules via its N-terminal globular domain and lectins via the C terminal region and it may also interact with fibronectin, tenascin R, fibulin 1 and 2, fibrillin 1 and collagen type I reducing cell adhesion [Iozzo and Murdoch, 1996; Iozzo, 1998; Wight, 2002; Wu et

al., 2005; Ricciardelli et al., 2009]. The versican C-terminal G3 domain is involved in the binding of $\beta 1$ integrins increasing phosphorylation of FAK and reducing H_2O_2 -induced apoptosis [Wu et al., 2005]. The increased FAK phosphorylation causes an increased cell adhesion and spreading and a reduced migratory capacity [Wu et al., 2005]. *In vitro* experiments on NIH-3T3 fibroblasts and cancer cells show that soluble versican may reduce prostate cancer and melanoma cells adhesion to fibronectin-coated surfaces, promoting cancer cell proliferation and motility [Theocharis et al., 2010].

Also aggrecan, neurocan and brevican bind hyaluronan via their N-terminal globular domain I, in particular the G1 region, that binds lectins via the C-terminal region [Hardingham and Fosang, 1992; Iozzo and Murdoch, 1996; Iozzo, 1998]. Brevican upregulation and proteolytic cleavage affect cancer cell adhesion and promote cancer cell motility and its core protein is also involved in EGFR activation that determines an increasing in cell-adhesion molecules expression and secretion of fibronectin fibrils on the cell surface [Theocharis et al., 2010].

Perlecan may have different functions in the cell-matrix adhesion on the basis of the type of cell involved. In fact cells like endothelial cells or chondrocytes are urged by perlecan expression to adhere to the ECM while other cell types like that of the hematopoietic system may be rejected by the presence of the perlecan [Iozzo and Murdoch, 1996]. Some adhesive properties described for perlecan can be attributed to N-terminal domain [Iozzo and Murdoch, 1996]. For example perlecan N-terminal SEA module and the SGD tripeptides may bind laminin 111, collagen type IV, fibronectin, thrombomodulin, fibrillin 1 and PRELP [Bix and Iozzo, 2008]. The domain II contains the LDL attachment sites and the domain III, that is present in mouse but not conserved in human, contains an RGDS region that binds FGF7 and FGF-BP [Bix and Iozzo, 2008], whereas the domain IV of perlecan core protein is involved in neural cell adhesion via contact with N-CAM molecules [Iozzo, 1998] and it also binds nidogens, fibulin 2, fibronectin and collagen type IV [Bix and Iozzo, 2008]. The C-terminal domain V contains EGF repeats and binds nidogen 1, fibulin 2, $\beta 1$ integrin, $\alpha 2$ integrin, FGF7, collagen XVIII, PRELP and α -dystroglycan [Bix and Iozzo, 2008]. To support the core protein functions, also GAG chains of perlecan are involved with the core protein in the binding of FGF7 and PRELP stabilizing the binding.

The LG2 region of core protein C-terminus of agrin is responsible of the binding with α -dystroglycan, a component of dystrophin glycoprotein complex, [Bezakova et al., 2003] that crosses the plasma membrane and becomes a structural link between cell cytoskeleton and extracellular matrix binding laminin. In the basal lamina of the brain microvasculature and in the muscle basement membranes, agrin core protein binds the laminin 1, 2 and 4 throughout its N-terminal domain [Bezakova et al., 2003; Iozzo, 1998; Jury and Kabouridis, 2010]. Agrin is present in two

different isoforms, the secreted form and the transmembrane one, that takes a non cleaved signal peptide. While the secreted agrin isoform is able to bind laminin, the transmembrane agrin isoform is not able to do it. The presence or not of this signal peptide influences the localization of agrin in tissues that do or do not contain a basal laminin [Bezakova et al., 2003]. Agrin is essential in motoneurons and in the brain; in the first it plays an important role in the formation of neuromuscular junctions, while in the second it is essential for the integrity of the blood brain barrier. Mutant mice deficient in agrin show non-functional NMJs and an uncontrolled immune cell infiltration in the brain throughout the BBB and they die before or shortly after birth [Jury and Kabouridis, 2010].

NG2/CSPG4 extended central D2 domain binds to type V and VI collagen, acting as a linkage between the cell surface and the extracellular matrix. Similar results have been achieved on laminin 2-coated surfaces. The roles of collagen VI and laminin 2 in brain vasculature and their association with axonal processes provide a means for migration of NG2-positive glioma cells along blood vessels and nerve fiber tracts [Couchman, 2010; Xu et al., 2011].

Also for syndecans, the core proteins is involved in integrins binding, in particular unglycosylated syndecan 1, 2 and 4 ectodomains can promote integrins-mediated adhesion. In the case of syndecan-1, a specific region approximately in the middle of the ectodomain interacts directly with $\beta 3$ or $\beta 5$ integrins, instead syndecan 2 and 4 ectodomains are able to activate $\beta 1$ integrins in an indirect way [Couchman, 2010]. Syndecan 1 is responsible for the impaired cell spreading on vitronectin but not on fibronectin thanks to its ability to modulate vitronectin interaction with $\alpha 5\beta 3$ integrin receptors [Tkachenko et al., 2005]. The region of the syndecan 1 ectodomain that interacts with integrin has been identified, it is termed synstatin and located between the heparan sulfate substitution sites and the transmembrane domain. Synstatin is so called for its ability to act as a competitor of intact proteoglycans and inhibitor of angiogenesis and tumor progression [Choi et al., 2011]. Syndecans not only bind their ligands through their extracellular domain, but they can influence integrins-mediated adhesion also through the intracellular signaling routes [Couchman, 2010]. In this way syndecans can modulate different integrin-dependent processes like fibronectin matrix assembly.

Chondroadherin is mainly found in the territorial matrix of articular cartilage where it binds the $\alpha 2\beta 1$ integrins on the cell surface of chondrocytes and induces cells to remain round. Studies on a chondrosarcoma cell line, K9 cells, show that these cells are able to bind both native and unfolded chondroadherin, suggesting that the binding is due to a linear amino acid segment of the chondroadherin molecule [Haglund et al., 2011]. This segment is shown to be located in one of the two cysteine loops in the C terminus of chondroadherin [Haglund et al., 2011]. The binding induces

ERK phosphorylation in human articular cartilage chondrocytes, mediating signals between the chondrocytes and the cartilage matrix. Chondroadherin also interact with collagen type II influencing the collagen fibrillogenesis [Haglund et al., 2011]. It is demonstrated that complexes of monomeric collagen type II and chondroadherin can be released from articular cartilage to activate resident matrix metalloproteinases. Both chondroadherin and collagen interact with chondrocytes, partly via the same receptor, but give rise to different cellular responses. By also interacting with each other, a complex system is created which may be of functional importance for the communication between the cells and its surrounding matrix and/or in the regulation of collagen fibril assembly.

PRELP is present in or close to several basement membranes. This structure is found as a thin sheet of extracellular matrix separating epithelial cells from the underlying connective tissue. PRELP binds the HS chains of perlecan and bridges the collagens type I and II fibres of matrix with these HSPGs at the cell surface, showing an important role in cell-matrix adhesion [Happonen et al., 2011; Rucci et al., 2009]. This binding occurs via N-terminal region of PRELP, because full-length PRELP, but not truncated PRELP lacking the amino-terminal domain, bound perlecan, while the bind with collagen occurs via its LRR domain and truncation of PRELP had not disturbed the protein conformation. By binding to perlecan HS chains in the basement membrane via its amino-terminal part and to collagen in the connective tissue via its LRR domain, PRELP is a likely candidate as one of the anchoring molecules at basement membrane-connective tissue junctions.

Osteoadherin/osteomodulin was firstly extracted from bovine cartilage and then it was discovered also in human cartilage and bone matrices, where it seems to be osteoblasts-specific. It binds to hydroxyapatite and its potential function is to bind cells, since it is showed to be as efficient as fibronectin in promoting osteoblasts attachment *in vitro*. Its involvement in osteoblasts attachment is due to its interaction with $\alpha 5\beta 1$ integrin [Bleicher et al., 2000]. *In vitro* experiments on rat osteosarcoma cells suggest that the integrins-binding is due to the core protein RGD region of osteoadherin. Moreover *in vitro* experiments on MC3T3E1 osteoblasts show that osteoadherin overexpression in these cells increase the cell differentiation and mineralization and reduces their proliferation and migration. Probably this anti-motility function may berelated with the osteoadherin capacity to bind and blocking EGFR. EGFR deficient mice demonstrate a reduced osteoblasts migration and proliferation and EGFR expression is upregulated in bone metastatic cancers. LRR domain of the OSD core protein is indicated as the EGFR-binding site.

ONLY GAG CHAINS

In some cases GAG chains binding capacity may play a pivotal role in cell-matrix adhesion. In particular cell surface syndecans may interact with different ECM molecules like fibronectin, vitronectin, laminin, collagens, plasma protein and antithrombin 1 and with different growth factors and morphogens. The binding is due to their GAG chains that are able to recognize and bind the heparin-binding sites of these molecules. More deeply, in myeloma cells syndecan 1 binds tenascin with different affinities depending on its degree of glycosylation and modification of its GAG chains [Choi et al., 2011]. In focal adhesions both integrins and proteoglycans are present together and it is well-known that focal adhesion formation during cell spreading on fibronectin depends upon engagement of an integrin and a cell-surface proteoglycan [Choi et al., 2011]. So the cooperation between integrins and syndecans became really crucial for cell adhesion to different matrices. In particular syndecan 1-mediated signaling promotes cell spreading in human mammary carcinoma cells, a process that requires cooperation with $\alpha 5\beta 3$ integrin, and it supports $\alpha 2\beta 1$ integrin-mediated adhesion on collagen type I and type II. It is shown that syndecan 1 and $\beta 1$ integrin cooperatively regulate adhesion and MMPs production by human salivary gland tumors on the laminin $\alpha 1$ -derived peptide AG73 [Choi et al., 2011]. Syndecan 2 cooperates with $\alpha 5\beta 1$ integrin in cell adhesion to fibronectin and regulates actin cytoskeletal organization in Lewis lung carcinoma cells. In human colon cancer cells, syndecan 2 regulates adhesion and migration through cooperation with $\alpha 2\beta 1$ integrin. Moreover syndecan 4 binds through its GAG chains to the heparin-binding domain of fibronectin and promotes the formation of focal adhesions and stress fibers. Some studies suggest that CS chains may cooperate with HSs in binding to extracellular matrix protein laminin but they have not a principle role in the binding [Tkachenko et al., 2005]. Fibronectin interactions with heparan sulfate that mediate proteoglycan-based cell adhesion both *in vitro* and *in vivo* require *N*-sulfation, but not *2-O*-sulfation, of the chains [Choi et al., 2011]. More deeply, integrin $\alpha 5\beta 1$, but not $\alpha 4\beta 1$ integrin or its close relative $\alpha 9\beta 1$, requires syndecan 4 as a co-receptor and can signal to induce focal adhesion formation and migration by increasing PKC α activation. Syndecan 4 is involved also in the regulation of astrocyte adhesion through a cooperative interaction with $\alpha 5\beta 3$ integrin, and clustering of syndecan 4 and $\beta 1$ integrin by laminin $\alpha 3$ chain-derived peptide promotes keratinocyte migration [Choi et al., 2011]. RNAi knockdown and mutagenesis studies have subsequently revealed cooperation of $\alpha 5\beta 3$ integrin and $\alpha 5\beta 5$ integrin with syndecan 1 during adhesion to vitronectin 7, 8, and $\alpha 2\beta 1$ integrin and $\alpha 6\beta 4$ integrin with syndecans during adhesion to laminin [Morgan et al., 2007]. So the role of the complexes syndecan-integrin became really fundamental in the process of matrix assembly.

COOPERATION

The cooperation of GAG chains and core protein is the basis of endocan functions. In particular it binds fibronectin, collagens and cytokines via its GAG chain. Instead the EGF-like domain of core protein is involved in the binding of integrins, in particular of $\alpha 5\beta 3$ integrins, a cell surface receptor that is present on the apical side of endothelial cells. This bind occurs in the presence of divalent cations. So endocan may cooperate with integrins to promote focal adhesion complexes assembly and disassembly influencing cell adhesion and migration that are really important during the endothelial-mesencymal transition [Carrillo et al., 2011].

1.4. Cell motility

ONLY CORE PROTEIN

V0 and V1 isoforms of versican are mainly expressed in embryonic tissues, where they act as barriers to neural crest cell migration and axonal outgrowth. In these tissues, it interferes with the attachment of embryonic fibroblasts to various substrata like fibronectin, laminin and collagen. The expression of versican core protein domain G1 within barrier tissues may be linked to guidance of migratory neural crest cells and outgrowth axons [Iozzo, 1998]. Versican is important in promoting also cancer cell motility and invasion. This hypothesis is supported by functional studies demonstrating that versican can increase cancer cell motility, proliferation and metastasis. In addition, purified versican is able to reduce attachment of prostate cancer cells and melanoma to fibronectin-coated surfaces *in vitro* [Ricciardelli et al., 2009]. Versican was selectively excluded from podosomes of human osteosarcoma cells and that inhibition of versican biosynthesis by an antisense method suppresses a malignant cell-adhesive phenotype [Ricciardelli et al., 2009]. Stable transfection of G1 versican into the H460M lung cancer cell line did not alter tumor growth rate *in vivo*, and interestingly clones expressing low or high levels of G1 versican had opposing effects on cancer cell motility *in vitro* and the incidence of metastasis in nude mice [Ricciardelli et al., 2009]. Only the cells expressing low levels of G1 versican demonstrated increased motility and metastasis to the lung. Interestingly, in MT-1 human breast cancer cells, overexpression of G3 versican resulted in larger tumors and the promotion of metastasis to bones and soft tissues [Ricciardelli et al., 2009]. Studies in astrocytoma cancer cell lines have demonstrated that the G1 domain, but not the G3 domain, of versican could enhance migration. Overexpression of G3 versican in astrocytoma cells enhances colony growth in soft agarose gel as well as tumor growth and blood vessel formation in nude mice. Both G1- and G3-overexpressing osteosarcoma cells exhibited enhanced *in vitro* growth when cultured on ECM substrates and in the absence of ECM anchorage [Ricciardelli

et al., 2009]. G1-overproducing sarcoma cells were more invasive than the corresponding G3 transfectants and, upon subcutaneously inoculation into nude mice, the G1 transfectants formed larger tumor masses than vector transfected cells [Ricciardelli et al., 2009].

Testicans play as proteinase inhibitors modulating cell motility and tumor invasion. Human testicans 1 and 3 bind and inhibit MT1-MMP in *in vitro* assays, so that glioma cells show a more metastatic phenotype in the absence of testican 3. On the contrary testican 2 seems to abrogate the MMP inhibitions, but much more needs to deeply understand the role of these PGs [Roll et al., 2006].

Via its extracellular domain, CD44 binds TGF β , HGF and VEGF, respectively activating ankyrin-CD44 interaction, that leads to Smad-dependent invasion, c-Met and VEGFR2, that activate endothelial cell migration, sprouting and tubule formation [Hertweck et al., 2011; Lounderbough and Schroeder, 2011]. *In vivo* studies on rat pancreatic carcinoma showed that transfection of CD44 variants into a nonmetastatic rat pancreatic carcinoma cell line conferred metastatic potential in these cells when injected into rats, which could be blocked by treatment with anti-CD44 v6 monoclonal antibody. The same results have been obtained from studies on breast cancer. It has been developed a tetracycline-inducible CD44s isoform in the weakly metastatic MCF7 breast cancer cell line and found that induction of CD44s in these cells promotes aggressive characteristics *in vitro* and metastasis to the liver when injected into immunodeficient mice, although it did not affect growth rate and local invasion [Lounderbough and Schroeder, 2011]. Moreover CD44 can modulate matrix remodeling influencing the expression of different proteases like MMP2, MMP8, MMP13. In particular in chronic lymphocytic leukemia cells CD44 binds gelatinase B/MMP9 and α 4 β 1 integrin, modulating the anchoring of B-CCL cells and mediating migration capacity and invasiveness [Hertweck et al., 2011]. Osteopontin interacts with the extracellular domain of CD44 and binds selectively the isoforms v6 and v7. This interaction promotes cell survival, migration and invasion, cancer growth and metastasis [Lounderbough and Schroeder, 2011]. The same effect is due to the interaction of CD44 extracellular portion with both high and low molecular weight Ha in *in vitro* cell culture. The binding activates the Rho family of GTPases and induces cell invasion and migration [Lounderbough and Schroeder, 2011]. The intracellular domain of CD44 may interact indirectly with the ERM proteins via the actin of cytoskeleton. This protein promote cytoskeletal remodeling and invasion. ERM compete with merlin for CD44 binding: merlin is an ERM-related protein that function as a tumor suppressor so the binding competition can lead to both tumor suppression and stimulation. High molecular weight Ha and an high cellular density promote merlin binding to CD44 and inhibit Ras-activated cell growth. Conversely the phosphorylation of merlin inhibits its binding to CD44 and leads ERM

proteins to bind it, promoting tumor growth and invasion [Lounderbough and Schroeder, 2011]. This is one of the antithetic effect showed by CD44 on cancer growth and invasion. For this reason it is important to investigate on the dual role of CD44 in tumor progression [Lounderbough and Schroeder, 2011]. Different studies have shown that variability in CD44 function may be due to the expression of its different isoforms. For example CD44v3 isoform interacts with Rac and Rho to promote cell migration and invasion whereas the standard isoform is upregulated and required for epithelial-mesenchymal transitions.

Consistent results were observed in cell migration and related assays about the involvement of collagens molecules in cell motility modulation. Experiments on umbilical vein endothelial cells through a collagen filter show that cell migration could be inhibited by low doses of endostatin-XVIII and NC1, two domains of collagen type XVIII core protein. Inhibiting invasion of the same cells into a basement membrane-like structure, required higher doses of endostatin and presumably interfered with MMP activation [Sasaki et al., 2002]. Migration inhibition by endostatin was also observed for endothelial cells under maximal growth in high serum conditions, and seems to be partly mediated through the early response of c-myc gene. Such high-serum conditions, however, abrogated endostatin's effects on apoptosis and growth [Sasaki et al., 2002].

Several informations suggest that NG2 plays a role in effective cell migration. Early work on NG2 showed that melanoma cell attachment and spreading could be inhibited by NG2 antibodies, and that NG2 was capable of triggering rearrangement of the actin cytoskeleton [Stallcup and Huang, 2008]. The first demonstration that NG2 can be important for cell motility came as a result of the finding that NG2 is a cell surface ligand for collagen type VI. Collagen type VI binds to the extended central D2 domain of NG2, as shown not only by solid phase binding assays with purified NG2 fragments, but also by studies in which recombinant deletion mutants of NG2 were expressed in rat B28 glioma cells [Stallcup and Huang, 2008]. NG2 transfectants lacking the D2 domain showed unchanged motility in the presence of collagen type VI, whereas full-length transfectants and transfectants that included D2 exhibited increased motility when exposed to collagen type VI (compared to parental B28 cells). Similar results were also obtained with human U251 glioma cells transfected with NG2. Moreover, oligodendrocyte progenitors from wild type mice migrate very well on collagen type VI-coated surfaces. In contrast, progenitors from NG2 null mice are much less motile on these same surfaces, emphasizing the importance of NG2 for cell motility in response to collagen type VI. Comparable results have been achieved on laminin 2-coated surfaces [Stallcup and Huang, 2008]. The significance of these experiments may be questioned on the grounds that collagen type VI and laminin-2 are not major components of the brain parenchyma. However, their association with brain vasculature and with axonal processes

could provide a means for migration of NG2-positive glioma cells along blood vessels and nerve fiber tracts [Stallcup and Huang, 2008].

In vitro studies on different tumor types show that lumican core protein is an inhibitor of cell motility affecting the interaction between cell and matrix. In particular melanoma A375 cells cultured on collagen type I and fibronectin matrices demonstrate reorganization of the actin fibers and a reduction in vinculin expression. This is due to a reduction in the $\beta 1$ integrin-vinculin link that is affected by the binding of lumican with $\beta 1$ integrin. In these cells it is possible also to observe a reduction in the ratio between focal adhesion kinases and the phosphorylated form pFAKs. Also in CHO cells transfected with the $\alpha 2$ integrin subunit it is possible to appreciate such a decrease, that is related with a decreased chemotactic migratory capacity of these cells. The use of siRNA directed against $\alpha 2\beta 1$ integrins on A375 cells determines an abrogation of the anti-migratory effect of lumican, suggesting that the binding of the PG with these integrins has a pivotal role in its biological function. When B16F1 melanoma cells stably transfected with lumican are injected syngeneically, number and size of lung metastasis nodules are decreased and there are an increasing in tumor cell apoptosis within metastasis. The nodules maintain a constant cell proliferation rate with a number of blood vessels decreased. This suggests that lumican acts also on the angiogenic aspect of tumorigenesis [Iozzo and Sanderson, 2011; Theocharis et al., 2010].

Brevican expression was seen to be upregulated in different invasive tumors of the brain, such as astrocytoma, oligodendroglioma or glioblastoma. In these tumors, the PG appears to be related with the migratory and invasive cell capacity. *In vitro* and *in vivo* studies on non-invasive 9L gliosarcoma cell line, that does not express brevican, underlain the important role of the molecule in tumor invasion. In particular transfection of these cells with the brevican gene determines an invasive cell phenotype and cells become able to clusters extending well beyond the main tumor mass.

A study demonstrated that proteins isolated from the culture medium of human hepatoma cells had the capacity to sustain human endothelial cells growth. The N-terminal of one of these proteins was discovered to have an amino sequence identical to that of bikunin, more deeply it corresponds to the truncated form of bikunin. This PG is suggested to be anti-inflammatory and anti metastatic both in animal and human, so that a bikunin therapy has been investigated in patients with sepsis, pancreatitis, lung injury and advanced cancer. Studies on bladder carcinomas demonstrated that bikunin may block tumor cell invasion by inhibiting tumor cell associated plasmin activity and u-PA. The plasminogen activator u-PA, is capable of catalyzing the conversion of the inactive zymogen plasminogen to the active proteinase plasmin, that can degrade most

extracellular proteins. Bikunin acts also inhibiting proteolytic enzymes, that are implicated in cancer metastasis.

ONLY GAG CHAINS

The GAG chains are essential for some of betaglycan's functions, in particular they are involved in the binding of FGFs, that reduces PG-mediated inhibition of cell migration [Bilandzic and Stenvers, 2011]. Silencing betaglycan gene expression in MCF10A breast epithelial and MDA-MB-231 breast cancer cells results in I κ B degradation and NF κ B mediated transcriptional activation by a β -arrestin2-dependent mechanism. Betaglycan can block NF κ B signaling in a direct way or by binding TGF β , that act on NF κ B signaling [Bilandzic and Stenvers, 2011]. Similarly, silencing betaglycan in nontumorigenic NMuMG mouse cells increased cell motility and proliferation in an *in vivo* xenograft mouse model, which was associated with increased NF κ B-mediated gene transcription and downregulation of E-cadherin [Bilandzic and Stenvers, 2011].

Syndecan 4 HS chains are responsible for the binding of fibronectin and the regulation of cell adhesion and spreading. *In vitro* experiments show that the overexpression of SDC4 in CHO cells promotes focal adhesion formation and decrease cell migration. On the other hand SDC4 null fibroblasts plated on fibronectin show enhanced lamellipodia formation and an increased level of Rac1 and low level of Rho. In vascular smooth muscle cells, shear stress causes SDC4 dissociation from the focal adhesions. Overexpression of SDC4 blocks this dissociations and also results in reduced mechanical stress-induced cell migration. It is suggested that SDC4 is involved in the same way in the regulation of smooth muscle migration during arteriogenesis [Tkachenko et al., 2005]. Syndecans also modulate cytoskeletal organization. Expression of syndecan 2 or 3 induces filopodia formation in COS-1 and CHO-K1 cells. Moreover, syndecan 2, in cooperation with integrin α 5 β 1, regulates actin cytoskeletal organization in an expression level-dependent manner: Lewis lung carcinoma-derived P29 cells expressing high levels of syndecan 2 form stress fibers, whereas low-expressing LM66-H11 cells derived from the same tumor form cortical actin [Choi et al., 2011].

For its capacity of capturing and storing growth factors by entrapping them within both the basement membrane and the tumor stroma, perlecan is involved in promoting the growth and invasion of tumor cells. Its mRNA and protein levels are notably increased in the metastatic neoplasms [Iozzo, 1998]. Purified perlecan enhances invasiveness of human melanoma cells whereas contact with basement membrane perlecan augments the growth of transformed endothelial cells but suppresses that of their normal counterparts [Iozzo, 1998]. Stable overexpression of an antisense perlecan cDNA in NIH-3T3 cells as well as in human metastatic melanomas leads to reduced levels of perlecan and concurrent suppression of cellular responses to FGF2. The binding

of perlecan to FGF2 factor occurs via HS chains [Iozzo, 1998]. In contrast, in fibrosarcoma cells, antisense expression of perlecan cDNA causes enhanced tumorigenesis characterized by heightened growth *in vitro* and in soft agar, increased cellular invasion into a collagenous matrix, and faster appearance of tumor xenografts in nude mice. Thus the cellular context is important in mediating perlecan's function [Iozzo, 1998]. Large deposits of immunoreactive perlecan are present in the newly vascularized stroma of colon, breast and prostate carcinomas. In tumor xenografts induced by subcutaneous injection of human prostate carcinoma PC3 cells into nude mice, perlecan was actively synthesized by the human tumor cells and it was clearly deposited along the newly formed blood vessels of murine origin [Iozzo, 1998]. Another function of perlecan is the regulation of the permeability in the glomerular basement membrane. In fact removal of HS chains increases glomerular permeability to proteins and leads to proteinuria [Iozzo, 1998]. In various glomerulonephrities it was seen an alteration in both core protein and chains, indicating that perlecan is involved in several renal pathologies [Iozzo, 1998].

Nasopharyngeal carcinoma cells express high levels of serglycin and its expression is correlated with the metastatic potential of different tumor cell clones [Kolset and Pejler, 2011]. Serglycin's function of promoting cancer cell metastasis depends on glycosylation of its core protein. RNAi-mediated inhibition of serglycin expression blocked serglycin secretion and the invasive motility of highly metastatic cells, reducing metastatic capacity *in vivo*. Conversely, serglycin over expression in poorly metastatic cells increased their motile behaviour and metastatic capacity *in vivo*. Growth rate was not influenced by serglycin in either highly or poorly metastatic cells. Secreted but not bacterial recombinant serglycin promoted motile behaviour, suggesting a critical role for glycosylation in serglycin activity.

1.5. Neurite outgrowth

ONLY CORE PROTEIN

Agrin induces acetylcholine receptor aggregation in cultured myotubes and binds also the acetylcholine esterase that limits the action of acetylcholine. It is suggested also a role for agrin in postsynaptic cleft organization and it may also play a key role in the regeneration of synapses during reinnervation of damaged sites by providing a template of the location of the original synaptic site [Iozzo and Murdoch, 1996; Iozzo, 1998]. The C-terminal modules of agrin core protein binds and sequester locally the PDGF and TGF- β factors, perhaps contributing to motor neuron survival [Iozzo and Murdoch, 1996]. Agrin binds the coreceptor MASC and indirectly acts on the receptor MuSK. These binds are essential for agrin-dependent synaptogenesis. Agrin, alone

or in combination with MuSK, act as a stop signal for neurite outgrowth. It is important in neuromuscular junctions formation, in fact agrin binds AchRs throughout the LG3 region of core protein C-terminal domain [Bezakova et al., 2003; Iozzo, 1998]. In *in vivo* null models the absence of agrin has no effect on brain development, but in *in vitro* cultures of hippocampal neurons isolated from agrin null mice the synapse formation seems to be disrupted.

To investigate the role of NG2/CSPG4 in the neurite outgrowth, NG2 was purified in a native state from B49 cells, the neural tumour cell line in which NG2 was first identified. Neurons do not attach to NG2-coated surfaces unless provided with adhesive molecules such poly-L-lysine, laminin or the L1 cell adhesion molecule [Tan et al., 2005]. These cell adhesion molecules all promote the growth of neuritic processes; however, when NG2 is a component of the substrate, the extent of neurite outgrowth is reduced by 40–45%. Removal of the chondroitin sulphate GAG chains from the NG2 core protein by digestion with chondroitinase ABC did not alter the ability of substrate-bound NG2 to inhibit neurite extension. On the other hand, treatment of the substrate with polyclonal antibodies against NG2 reduces the extent of growth inhibition [Tan et al., 2005]. When neurons were grown on growth-promoting substrates with either stripes or spots of NG2, the axons avoided the NG2-coated regions but grew extensively on the permissive surfaces [Tan et al., 2005]. Same portions of NG2 core protein, when added to cultures of newborn rat dorsal root ganglion neurons, induce the collapse of growth cones; this demonstrates that NG2 has all the properties associated with repulsive axon guidance cues and suggests that the dense accumulation of NG2 at glial scars could contribute to the creation of a barrier against successful axon growth [Tan et al., 2005]. To study the NG2 domain involved in these functions, Tan et al. prepared a series of Fc and myc/his fusion proteins encoding individual domains of the NG2 core protein and combinations of adjacent domains. Each fusion protein was tested for its ability to induce growth cone collapse of newborn neurons and to inhibit the growth of axons from neonatal cerebellar granule neurons. The fusion proteins containing either domains 1 or 3 are inhibitory in both of these assays [Tan et al., 2005]. The domain 2, which contains the sites of GAG attachment, is modestly inhibitory only when the GAG chains were present. Removal of the chondroitin sulphate GAG chains with chondroitinase ABC renders domain 2 inactive [Tan et al., 2005]. Curiously, chondroitinase digestion has no effect on the activity of a domain 1 and 2 Fc-fusion protein that also contains chondroitin sulphate GAG chains. Clearly, the GAG chains are not required for the inhibitory activity of large fragments of NG2 containing either domains 1 or 3 in these *in vitro* assays. The presence of inhibitory chondroitin sulphate GAG chains at glial scars in association with chondroitin sulfate-PGs other than NG2 may be one reason why chondroitinase ABC is effective in stimulating axon regeneration [Tan et al., 2005]. When NG2 is present as an integral membrane

protein, domain 1, which extends away from the plasma membrane, may be available to interact with the growth cones of damaged and sprouting neurons. Domain 3 lies close to the plasma membrane and may be inaccessible. When cleaved from the membrane and incorporated into the ECM, domains 1 and 3 would both be accessible. Thus, secretion or shedding of NG2 at glial scars could amplify the inhibitory signals transmitted by NG2 [Tan et al., 2005].

In the adult mouse, testicans are detected only in the brain, instead the human expression is more broader, and they are found also in prostate, testicles, heart, blood and cartilage. They show an anti-adhesive function, in particular testican 1 can block substrate attachment and neurite outgrowth of neuronal cells. This function is due to its capacity of binding and inhibition of proteases via the core protein portion of testican 1 [Roll et al., 2006].

No specific ligands for phosphacan has been reported, but several binding partners have been described and can be grouped according to the portion of the extracellular domain that they recognize. The growth factor pleiotrophin and the Ig superfamily CAMs L1/Ng-CAM, N-CAM, Nr-CAM associate with the phosphacan spacer region and the IgCAM protein contactin 1 binds to the C-terminal domain. Importantly, the association between phosphacan on glia and contactin 1 on neurons promotes the outgrowth of neurites and induces bidirectional signaling between glia and neurons suggesting that this interaction plays a role in nervous system development [Bouyain and Watkins, 2010].

ONLY GAG CHAINS

Considerable evidence indicates that versican actively regulates neuronal differentiation, maturation, neurite outgrowth, and synaptic transmission. Due to the difference in CS domains, versican V1 or V2 show distinct roles in cell function. It was demonstrated that V1 could induce mature neuronal differentiation. In contrast, V2, which is the predominant form of versican in the mature brain, exerts an inhibitory effect on neurite outgrowth. Through activating EGFR expression and modulating the downstream ERK signaling pathway, V1 could enhance cell proliferation and protect cells from apoptosis.

Agrin plays an important role also in brain diseases like Alzheimer. The PG augment the rate of formation of fibrillar β amyloid in the diseased brain and protects the proteolytic degradation of the β amyloid fibrils by binding them via its GAG chains. This means that agrin plays a crucial role in the formation of senile plaques and together with other extracellular matrix components which are known to bind to agrin such as laminin and thrombospondin, stimulate the bundling of fibrillar β amyloid into larger aggregates.

COOPERATION

The neurocan C-terminal domain may mediate the binding of neurocan to a variety of neural cell adhesion molecules including Ng-CAM, N-CAM and TAG-1/axonin-1, inhibiting their hemophilic interaction, and blocks neurite outgrowth [Iozzo, 1998]. Different studies show that also if both CS chains and core protein are involved in N-CAM binding with neurocan, the core protein retains binding activity also in absence of GAG chains. Similar binding characteristic are observed for Ng-CAM [Rauch, 2001]. Moreover neurocan interacts with tenascin and axonin-1 [Iozzo, 1998]. It may also bind heparin through the C terminal globular domain and this interaction has the important function of stabilizing the interaction of neurocan with its ligands [Rauch et al., 2001]. For example heparin stabilizes the binding of neurocan with FGF2, the heparin binding growth associated molecule HB-GAM and amphoterin. HB-GAM is a neurite-promoting matrix-associated protein lining growing axons in the brain. Amphoterin is a protein found in the leading edge and in substrate-attached material of growth axon cones and migrating cells. Not only the neurocan core protein but also CS chains bind FGF2 and the treatment of the PG with chondroitinase reduce the interaction by 35% [Rauch et al., 2001]. In contrast to the interaction with FGF2, the interaction of neurocan with HB-GAM and amphoterin appears to occur in a mainly CS chain-dependent manner. In fact chondroitinase treatment of neurocan reduces its binding capacity by 80%. It is interesting to note that HB-GAM-induced migration of neurons could be inhibited by addition of CS-6 sulfated chains but not by addition of CS-4 sulfated [Rauch et al., 2001].

1.6. Matrix assembly

ONLY CORE PROTEIN

Decorin binds collagen type I and II in *in vitro* and *in vivo* assays and it has an important role in organizing the extracellular matrix. The interaction is due to the LRR region of the core protein [Hardingham and Fosang, 1992; Iozzo and Murdoch, 1996]. *In vivo* experiments with decorin null animals models give the opportunity of studying the genetic evidence for a role of decorin in maintaining collagen fibrillogenesis. Mice carrying a homozygous disruption of the decorin gene grow normally to adulthood; however, they manifest a phenotype characterized by increased skin fragility. When sample of skin from the wild type and decorin null animals were subjected to biochemical testing, the latter samples exhibited a markedly reduced tensile strength that could be associated with an abnormal collagen fiber formation. Ultrastructural analysis of skin revealed bizarre and irregular collagen morphology with coarser and irregular fiber outlines in the decorin null specimens [Iozzo, 1998]. The comparison of matrix production wild type and decorin-

null Dcn $-/-$ mouse livers, shows strong evidence about the role of decorin in protection against fibrogenesis. The chemical induction of matrix deposition was higher in the liver from Dcn $-/-$ mice. This response correlated well with the enhancement of collagen type I, III and IV proteins in the decorin deficient mice. Moreover the relative decrease in two major matrix metalloproteases, MMP2 and MMP9, and the concurrent increase in the hepatic levels of two major MMP inhibitors, TIMP-1 and PAI-1, indicated an involvement of decorin in the matrix regulation and remodelling [Baghy et al., 2012]. The functions of the decorin core protein as a matrix proteoglycan are well studied. It binds to collagen fibrils at the “d” or “e” bands and “decorates” the fibrils. One consequence of this interaction is a delay in triple helix formation and a reduction in the final diameter of the collagen fibrils *in vitro* [Seidler and Dreier, 2008]. The effect of irregular and heterogeneous diameter of collagen fibrils could be reproduced *in vitro* using decorin deficient fibroblasts and this phenotype could be rescued by exogenous decorin. However, *in vivo*, decorin was detected preferentially associated with a population of thicker fibrils in the interterritorial regions of articular cartilage, and was absent on the thinner fibrils in the territorial matrix around the chondrocytes, where collagen type IX was detected in greater amounts [Seidler and Dreier, 2008]. The decorin core protein was described to function as a signaling mediator. Decorin acts as a ligand for both the EGFR and the insulin-like growth factor receptor [Seidler and Dreier, 2008]. The importance of decorin role in matrix assembly process is highlighted in different pathological situation. For example in Marfan Syndrome there is a reduction in decorin gene transcription in fibroblasts and this is related with the connective tissue disorder that is characteristic of this syndrome [Hardingham and Fosang, 1992]. In Lyme disease, decorin binds *Borrelia burgdorferi* spirochete, that is the responsible of the tick-borne disease. The spirochete is not able to bind collagens type I and III directly, but it contains two decorin-binding proteins that act as adherins mediating the attachment of the organism to derman collagen via decorin. Decorin is involved not only in the initial colonization of the dermis, but it binds and inactivate the complement component C1q and it is involved in he further steps involving cytokine-controlled mediators of inflammation and immunological response [Iozzo and Murdoch, 1996]. Decorin is involved in the formation of atherosclerotic plaques and this is confermed also by different *in vivo* studies. For example systemic decorin overexpression resulted in a significant decrease in atherosclerotic plaque formation in Apo-E null mice. This was associated with a decrease in macrophage and collagen accumulation and decrease in gelatinase activity. In addition, serum triglyceride levels were also decreased suggesting a possible role for systemic decorin expression in the modulation of lipid profile [Singla et al., 2011].

The LRR region of fibromodulin core protein contains the sequences for the binding of fibril like collagens type I and II and for this reason, fibromodulin has an important role in organizing the extracellular matrix [Hardingham and Fosang, 1992; Iozzo and Murdoch, 1996]. Different *in vivo* studies on fibromodulin null mice *Fmod*^{-/-} show that in absence of this PG there is a significant reduction in tendon stiffness and the ECM show particular characteristics like irregular contour of fibrils and a higher concentration of small fibrils [Chakravarti, 2002]. It is possible to conclude that in particular tissues like tendon, fibromodulin is essential early in collagen fibrillogenesis to stabilize small-diameter fibrils.

The C-terminal domain of neurocan core protein binds tenascin C and R, two related oligomeric extracellular matrix proteins. In particular tenascin C is the perfect partner of neurocan for the formation of the fundamental system of matrix organization: the complex glycoprotein/proteoglycan/hyaluronan, while tenascin R show a different behaviour. This protein expression seems to be inversely related to the neurocan one, in fact while the first increases during development, neurocan expression declines postnatal [Rauch et al., 2001].

Brevican is present in two different isoforms, one secreted and one anchored. The secreted isoform contains a C-terminal region that binds tenascin and other ECM molecules such as fibulin 2, hyaluronan and the link protein Bral2. The GPI-anchored isoform lacks this domain [Gary et al., 1998]. The secreted isoform is expressed only by neurons instead the GPI-anchored one is expressed only by glial cells [Gary et al., 1998]. It is also present at the axonal initial segment and takes place prior to the formation of the mature form of the ECM. The link between brevican and AIS occurs via neurofascin 186, a glycoprotein from the Ig superfamily that is enriched at the AIS.

The core protein of different syndecans is directly involved in the matrix assembly. For example deglycosylated syndecan 1 core protein, but not the glycosylated form, is able to bind anti-elastase and $\alpha 1$ antitrypsin [Choi et al., 2011]. The core protein of syndecan 2 is able to bind TGF β directly and a truncated syndecan 2 cytoplasmic domain results in a decreased TGF-response and in an inability of cells to assemble laminin or fibronectin into a fibril matrix [Tkachenko et al., 2005]. Moreover, syndecan 2 core protein appears to directly bind the pro form of matrix MMP7 independent of GAG chains [Choi et al., 2011]. *In vitro* studies on different engineered cell types, like syndecan 2 knockdown HT1080 or CHO transfected with syndecan 2 lacking the C-terminal 14 aminoacids of the cytoplasmic domain, show that these cells can not assemble laminin and fibronectin ECMs. The same effects are shown in *Zebrafish* models. *In vivo* studies on syndecan 4 knockout mice demonstrate that also syndecan 4 core protein is essential for the formation of a correct matrix, especially during the fibrin-fibronectin matrix contraction, in fact in these mutant mice fibroblasts have defects in this particular process of the matrix assembly [Choi et al., 2011].

Asporin directly binds to TGF β 1 and inhibits Smad signaling in chondrocytes; this lead to the suppression of TGF β -mediated expression of different PGs like aggrecan that accumulate in the matrix. Also if the asporin-TGF β binding is not yet well known, competition assays suggest that amino acids 159-205 of aspirin mediate its interaction with TGF- β 1 and effectively repress TGF- β 1-induced cartilage matrix gene expressions. Asporin also bind and decreases the concentration of BMP2 via its LRR domain, becoming a negative regulator of osteoblasts differentiation [Duval et al., 2011]. Throughout the same domain, asporin can bind also collagen type II, competing with decorin and playing an important role in osteoblast-driven collagen biomineralization activity. It is abundant in osteoarthritis articular cartilage and its expression is regulated by different cytokines such TGF β , IL-1 β , TNF α . *In vitro* experiments on cells treated with cytokines to reproduce the increased levels of proinflammatory stimuli observed in osteoarthritis synovial fluid, show a decreased asporin expression [Duval et al., 2011]. Moreover it was demonstrated that osteoarthritis susceptibility is affected by the number of aspartic acid residues in the aminoterminal extremity of the asporin protein.

Mimecan/osteoglycin is essential in bone matrix formation because it can bind directly via its core protein different growth factors such as BMP2 and 3 and TGF β 1 and β 2. Osteoglycin knockout mice show reduced tensile strength of the skin, caused by alterations in the diameters of collagen fibrils, thereby supporting a role for this proteoglycan in determining elasticity and tensile strength [Kampmann et al., 2009].

The core protein plays the major role in the interaction between biglycan and collagen type VI and treatment with chondroitinase ABC does not affect the binding. This was supported by experiments demonstrating that the isolated chains were not able to inhibit the interaction *in vitro*. Collagen type VI have a role in the development of the matrix supramolecular structure as well as in tissue homeostasis by mediating interactions of cells with the extracellular matrix and its closely interaction with biglycan suggests that PG also may be of crucial importance in the matrix assembly and interaction with cells.

ONLY GAG CHAINS

Interestingly, the GAG chain of decorin had a reducing effect on collagen fibril diameter at early stages of fibrillogenesis [Seidler and Dreier, 2008]. In patients with a variant of Ehlers Danlos Syndrome, about half of the secreted decorin lack the GAG chain. These patients show a β 4 galactosyltransferase I deficiency resulting in a reduced amount of L-IdoA in decorin. Notably, some of these patients have a skin fragility phenotype that resembles that of the decorin null mice [Seidler and Dreier, 2008]. Decorin not only regulates collagen fibril formation, but it also acts as a

bridging molecule between type I and type VI collagen. Decorin interacts with both collagens via different binding sites [Seidler and Dreier, 2008]. Although banded fibril-forming and filamentous beaded collagens form independent networks, they intermingle with each other *in vivo*, providing mechanical stabilization of tissues [Seidler and Dreier, 2008]. More recently, a complex formation between the globular domains of collagen type VI and a decorin/matrilin-1 complex has been described which can act as a bridge between collagen type VI and type II in cartilage, where decorin binds to the globular N-terminal domain of type VI collagen.

Lumican play a pivotal role in the organization and maturation of a particular type of structure, that is the cornea. It is shown that in developing cornea, during the acquisition of cornea transparency, there is a marked upregulation of lumican mRNA and a concurrent switch from the nonsulfated to the KS sulfated isoform. This seems to underly the importance of KS GAG chains in the lumican biological function. [Iozzo and Murdoch, 1996] This conclusion is supported also from *in vivo* studies on lumican null-mice models Lum *-/-*. Lum *-/-* mice show a reduced cornea transparency and a marked skin fragility. In these animals skin, cornea and tendon show irregular collagen fibrils contours and the fibers show an increased diameter. Lumican seems to be fundamental in the binding of collagen fibers, in limiting lateral growth of fibrils during the later stage of fibril formation [Chakravarti, 2002]. Lumican expression is increased in breast cancer, especially in the tumour stroma, and this correlates with higher tumour grade. Lumican expression has also been reported to be altered in various types of human malignancies, including melanomas, osteosarcomas, pulmonary, pancreatic and colorectal carcinomas. However, there are a lot of contrastant opinions regarding the role of this PG as pro- or anti-tumorigenic molecule and regarding its role as a prognostic tumor marker. For example, lumican overexpression correlates with poor prognosis in advanced colorectal, pancreatic cancers, in lung adenocarcinomas and squamous cell carcinomas [Iozzo and Sanderson, 2011; Theocharis et al., 2010].

Opticin is present expecially in the ECM of vitreous humors where it play an important role in binding different matrix component. The presence of the GAG chains allow it to bind the CS chains of collagen type IX, stabilizing vitreous gel structure and mantaining vitreous adhesion to the retina. The GAG chains also bind the HSPGs like the collagen type XVIII and in this way it link vitreous collagen fibrils to the inner limiting lamina. Opticin functions as an adhesive at the vitreoretinal interface [Le Goff and Bishop, 2006].

The chondrodysplasia observed in the perlecan null mice is due to the fact that perlecan is involved in matrix assembly through its CS chains. In particular in cartilage matrix, CS perlecan chains binds and inhibits FGF2 binding to its receptor FGFR3 [Whiterlock et al., 2008].

COOPERATION

Changes in the expression of aggrecan CS epitopes are detected in mature canine articular cartilage after the experimental induction of joint instability leading to osteoarthritis. The aggrecan expressed in the experimental osteoarthritic cartilage contained CS that consistently had a longer chain and contained more of at least three different CS-epitopes detected by mAb [Hardingham and Fosang, 1992]. It is suggested that the altered CS chains may contain special properties, such as an increased affinity for GFs or other cytokines that may facilitate matrix repair by the chondrocytes [Hardingham and Fosang, 1992]. Different studies underline that also the core protein may play an essential role in matrix assembly and composition. In particular, the function of aggrecan in matrix structure like cartilage is demonstrated by the phenotype of two different mutant animals: the nanomelic chicken, a useful model to elucidate intracellular trafficking of proteoglycans, and the cartilage matrix-deficient (cmd) mouse [Iozzo, 1998]. In nanomelic chicken a single base mutation leads to a premature truncation of the aggrecan protein core, which lacks the C terminal globular G3 domain. This gene mutation determines a recessively inherited connective tissue disorder. In the cmd mice phenotype is due to a deletion in exon 5 of the aggrecan gene. The deletion occurs in the G1 domain, resulting in a truncated polypeptide. Although heterozygous cmd mice appear normal, the homozygous mice die soon after birth due to respiratory failure [Iozzo, 1998]. These data highlight the importance of aggrecan in destructive diseases such as osteoarthritis and underline its pivotal role in skeletal formation and maturation.

Different control systems are involved in syndecan matrix assembly properties, and it is proposed that the cooperation between GAG chains and core protein may favour syndecan capacity of matrix modulation. Syndecan-2, for example, interacts with MMP7 via its core protein and this binding potentiates the enzyme activation with subsequent cleavage and shedding of the syndecan 2 itself. Probably heparin and HS are also involved in the binding and activation of MMP7 [Couchman, 2010]. Another syndecan capable to bind and modulate proteases is the syndecan 1 and in the case of the interaction between syndecan 1 and MMP2, HS chains are involved and the interaction inhibits the catalytic activity of the MMP [Couchman, 2010]. *In vivo* experiments show that syndecan 4 can bind ADAMTS5, a member of the peptidase family ADAM, and it regulates its activity in a HS-mediated way [Couchman, 2010]. Syndecan 4 may interact also with ADAM12 via HS chains [Couchman, 2010].

1.7. Apoptosis

ONLY CORE PROTEIN

Within the glypicans family, glypican-3 is an important apoptosis regulator: its loss determines the overgrowth characteristic of SGBS. For this function, GAG chains are not required. In fact GPC3 core protein is able to directly binds bFGF and inducing apoptosis.

The binding of endostatin-XVIII to the surface of endothelial cells may lead to its rapid internalization and subsequent degradation. Intracellular forms, as well as signals transduced after engagement of specific endostatin receptors, could be responsible for the modulation of cell apoptosis and gene expression [Sasaki et al., 2002]. An increase in apoptosis was particularly prominent in FGF2 treated exponentially growing cells and was accompanied by the downregulation of anti-apoptotic proteins such as Bcl-2 and increased caspase-3 activity. Promotion of apoptosis was accompanied by the induction of tyrosine kinase signalling through the Shb adaptor protein and could be prevented by mutation of the heparin binding site of endostatin [Sasaki et al., 2002].

Chemoresistance is an important and problematic characteristic of many gliomas. Interestingly, in addition to its effects on cell proliferation and migration, NG2-dependent activation of $\alpha 3\beta 1$ integrin also has effects on cell survival due to increased signaling through the PI3K/AKT pathway [Stallcup and Huang, 2008]. NG2-transfected U251 glioma cells are resistant to treatment with TNF α and chemotherapeutic drugs such as doxorubicin, vincristine and etoposide that effectively trigger apoptosis in parental U251 cells. siRNA-mediated knockdown of NG2 expression effectively restores apoptosis sensitivity in U251/NG2 cells, further demonstrating the cause and effect relationship between NG2 expression and apoptosis resistance [Stallcup and Huang, 2008]. NG2 knockdown is also effective in increasing apoptosis sensitivity in endogenous NG2 expressing glioma lines such as U87 and A172, as well as in the A375 melanoma line, demonstrating that NG2-dependent apoptosis resistance is a widespread phenomenon in several tumor types. In all cases, there was a direct correlation of NG2 expression level with both $\beta 1$ integrin activation and the level of AKT phosphorylation. Two types of evidence indicate that the phenomenon operates *in vivo* as well as *in vitro* [Stallcup and Huang, 2008]. First, U87 cells produce significantly larger, faster growing tumors in NOD-SCID mice than U87 cells treated with NG2 siRNA to knock down expression of the proteoglycan *in vivo*. Growth of the siRNA-treated tumors is further inhibited by administration of TNF α , a phenomenon not seen in U87 tumors without siRNA treatment [Stallcup and Huang, 2008]. This demonstrates the increased apoptosis sensitivity provided by NG2 knockdown. The TNF α -independent decrease in tumor growth

provided by NG2 knockdown is likely due to the effects of NG2 on other parameters such as cell proliferation, reinforcing the idea that NG2 affects multiple aspects of glioma progression. Human glioma biopsy samples grown in spheroid cultures were tested for sensitivity to the chemotherapy drugs doxorubicin, etoposide and carboplatin. There was an excellent correlation between apoptosis resistance and the level of NG2 expression in these tumor samples [Stallcup and Huang, 2008].

1.8. Cell differentiation

ONLY CORE PROTEIN

CD44 mediate the binding of hematopoietic progenitor cells with Ha via its extracellular portion. In this way progenitor cells may interact with their respective niche in the bone marrow, proliferate and differentiate by regulation of local cytokine secretion [Hertweck et al. 2011]. CD44 play an important role also in T cell maturation. The v6 isoform mediates homing of progenitor cells from the bone marrow to the thymus where T-cells differentiation and selection takes place [Hertweck et al., 2011].

ONLY GAG CHAINS

In the family of syndecans, syndecans 3 plays an important role in the skeletal muscle cell differentiation. Syndecan 3 is able to bind and control FGF2, the HGF/scatter factor and the TGF β factor, controlling all these signal pathways via its GAG chains. When the syndecans 3 expression is suppressed, the myogenin is expressed. Myogenin is a transcription factor for muscle differentiation and its expression accelerates skeletal muscle differentiation and myoblast fusion [Tkachenko et al., 2005]. Also several BMPs may bind the syndecans GAG chains, stimulating chondrogenesis and chondrogenic differentiation of limb mesenchymal cells. Pretreatment of micromasses culture with heparinases, enhances the chondrogenic activity of BMP2, and reduces the concentration of BMP2 needed to promote chondrogenesis.

In vivo studies suggest that also biglycan GAG chains may play a pivotal role in the formation of bone matrix and in controlling skeletal cell differentiation by binding BMPs 2 and 4. Knockout mice for biglycan show diminished bone mass progressively with age and they are defective in their capacity to form bone. The osteoporosis-like phenotype that is characteristic of this mouse model, is due to defects in cells critical to the process of bone formation. These data shows that biglycan deficient mice have diminished capacity to produce marrow stromal cells, the bone cell precursors, and that this deficiency increases with age. The cells also have reduced response to TGF β , reduced collagen synthesis and relatively more apoptosis than cells from normal

littermates. In addition, calvaria cells isolated from biglycan deficient mice have reduced expression of late differentiation markers such as bone sialoprotein and osteocalcin and diminished ability to accumulate calcium judged by alizerin red staining. We propose that any one of these defects in osteogenic cells alone, or in combination, could contribute to the osteoporosis observed in the biglycan knockout mice [Young et al., 2002]. C2C12 myogenic cells were treated or untreated with BMP2 alone or in combination with glycanated, partially glycanated or de-glycanated BGN and it is shown that BMP signaling and function were increased when BMP2 was combined with de-glycanated BGN among the groups tested.

1.9. Angiogenesis

ONLY CORE PROTEIN

The C-terminal fragment of collagens type XVIII core protein is suggested to play a key role in angiogenesis. Angiogenesis is dependent on several integrin receptors, the activation of proteases, in particular matrix MMPs, and cytoskeletal changes required for cellular migration. Several of these components have been examined as potential targets of endostatin XVIII [Sasaki et al., 2002]. Several *in vivo* studies have consistently demonstrated that endostatin reduces the growth of various primary tumors as well as metastases because selectively decreases blood flow and size of tumor vessels and enhances apoptosis of tumor cells [Sasaki et al., 2002]. Endostatin treatment did not interfere with vessel density in the granulation tissue, wound contraction, or the final stage of repair. During the peak of angiogenesis, however, endostatin interferes with vessel maturation, as indicated by massive hemorrhages and pathological changes in the ultrastructure of vessel walls [Sasaki et al., 2002]. These findings are consistent with a higher sensitivity of tumor vessels, which are known to have a chaotic and leaky architecture and also integrate tumor cells into their endothelial lining [Sasaki et al., 2002]. Different studies underline the capacity of endostatin to bind and inhibit MMP2 and MT1-MMP, reducing endothelial cell invasion into a basement membrane matrix [Sasaki et al., 2002]. Endostatin was also found to bind $\alpha 5\beta 1$ and some other RGD-dependent integrins, modulating cell spreading, focal adhesions formation and cell migration, in particular cell types like the endothelial cells. Endostatins do not have a cell adhesive RGD sequence, however the binding of these integrins may involve other sites similar to those also involved in the binding of MMP2 [Sasaki et al., 2002] There is also some evidence that endostatin binds weakly to tropomyosin and to disassemble focal cell adhesion plaques containing plasminogen activator. Whether endostatin can directly bind to cytoskeletal proteins remains an open question and would require its uptake by cells, for which phenomenon there are some

evidence exists [Sasaki et al., 2002]. Endostatin-XVIII and -XV are also present in the circulation, as shown by their isolation from large volumes of human plasma hemofiltrate and in immunological studies [Sasaki et al., 2002]. Endostatin-XVIII concentrations comparable with that present in mouse and human serum, were shown in *in vitro* assays to inhibit migration and other properties of cultured endothelial cells suggesting that circulating endostatin is involved in the control of vessel stability by counteracting local angiogenic stimuli [Sasaki et al., 2002]. Besides being involved in the early stages of the angiogenesis, endostatin is involved also in the mature vessel. In fact endothelial cells grown in contact with collagen fibrils readily form tube-like structures similar to vessels during early angiogenesis and these tubes were apparently stabilized by endostatin-XVIII. A core protein domain of collagen type XVIII, different from endostatin and called NC1, show a different function in angiogenesis. A more comprehensive study demonstrated that trimeric NC1-XVIII caused a disassembly of these tubes into scattered cells, a process that was antagonized by monomeric endostatin [Sasaki et al., 2002]. Vascularization of embryonic chick chorioallantoic membranes is one of the standard models to study collagens involvement in angiogenesis *in situ*. Microgram amounts of endostatin-XVIII were shown to inhibit chick chorioallantoic membranes angiogenesis prior to or after stimulation with FGF2 or VEGF [Sasaki et al., 2002]. The major effect was a reduced capillary sprouting that in most studies was evaluated by a non quantitative scoring of vessel branching. Mutations of endostatin indicated that heparin, is essential for the inhibitory activity [Sasaki et al., 2002].

Endocan mainly expressed by endothelial cells and its expression is regulated *in vivo* by different inflammatory cytokines such VEGF, FGF2, TNF α . A marked expression of endocan is shown in breast, brain, lung, liver, kidney, suggesting that this PG may perhaps be important in the angiogenesis and endothelial-mesenchymal transition processes, modulating the presence of different growth factors like FGF2, TGF β , IGF2 via its N-terminal and EGF-like domains [Carrillo et al., 2011]. Endocan is also associated with filopodia of angiogenic endothelial tip cells in invasive bladder cancer. Notably, endocan expression on tumor vessels correlated strongly with staging and invasiveness, predicting a shorter recurrence-free survival time in non-invasive bladder cancers. Both endocan and VEGF-A levels were higher in plasma of patients with invasive bladder cancer than in healthy individuals. Investigations in cultured blood vascular endothelial cells or transgenic mice revealed that endocan expression was stimulated by VEGF-A through the phosphorylation and activation of VEGFR-2, which was required to promote cell migration and tube formation by VEGF-A. Taken together, these data suggest that endocan interaction with VEGFR-2 or VEGF-A could stimulate tumor angiogenesis.

Syndecan core protein may play an important role in the angiogenesis process. For example, the core protein ectodomain is involved in the binding of different pro-angiogenic factors. Syndecan 1 ectodomain is seen to bind integrins, VEGF and their respective receptors, stimulating endothelial cells to initiate endothelial invasion and budding. Short inhibitory peptide that mimic syndecan 1 ectodomain, called synstatin, abrogate PG interactions and inhibits endothelial cell invasion and tumor growth *in vivo* [Morgan et al., 2007; Teng et al., 2012]. An *in vivo* model provided the use of anti-syndecan 2 morpholino oligonucleotides in *Zebrafish* shows that this syndecans may modulate VEGF signalling. Syndecan 2 knockout *Zebrafish* have the suppression of intersegmental vessels, whereas dorsal vessel formation is not affected. The overexpression of VEGF 165aa in syndecans 2-morphans was not able to induce ectopic vessel formation whereas coexpression of syndecans 2 and VEGF 165aa resulted in an increase of vessel formation compared with VEGF alone [Tkachenko et al., 2005].

It was shown that domain V of the perlecan core protein, renamed endorepellin, harbored a powerful angiostatic activity as demonstrated by various *in vitro* and *in vivo* angiogenic assays [Whiterlock et al., 2008]. Endorepellin is composed of three laminin-like globular domains (LG1–LG3) interspersed by four EGF-like modules, and interacts specifically with the $\alpha 2\beta 1$ integrin, an established receptor for collagen type I, in platelets and endothelial cells. In the latter, endorepellin triggers a signaling cascade that leads to disruption of the endothelial actin cytoskeleton and thus to cytostasis [Whiterlock et al., 2008]. Importantly, systemic delivery of human recombinant endorepellin to tumor xenograft-bearing mice causes a marked suppression of tumor growth and metabolic rate mediated by a sustained down-regulation of the tumor angiogenic network [Whiterlock et al., 2008]. Genetic analysis using siRNA-mediated block of endogenous $\alpha 2\beta 1$ integrin or animals lacking the $\alpha 2\beta 1$ integrin receptor have definitively shown that this is a key receptor for endorepellin and have further demonstrated that endorepellin targets the tumor xenograft vasculature in an $\alpha 2\beta 1$ integrin-dependent manner [Whiterlock et al., 2008]. The last laminin-like globular domain, LG3, possesses most of the biological activity and can be released from the parent molecule by BMP1/Tolloid-like metalloproteinases which recognize a dipeptide that is highly conserved across species including human, mouse, *Drosophila* and *Zebrafish* [Whiterlock et al., 2008]. This highly conserved region within the perlecan core protein together with the high conservation of BMP1/Tolloid-like metalloproteinases suggests that liberation of LG3 might be of physiological importance. Mutations in LG3 molecules displaying lower or no affinity for calcium disrupt LG3 angiostatic activity [Whiterlock et al., 2008]. LG3 fragments with identical N-terminal residues (i.e., cleaved by BMP1/Tolloid-like metalloproteinases) have been found in the urine of patients with end-stage renal failure and chronic allograft nephropathy, and in the amniotic

fluid of pregnant women with a marked increase in women with symptoms of premature rupture of fetal membranes and those carrying trisomy 21, Down Syndrome, fetuses. In addition, endorepellin fragments have been found in the media conditioned by apoptotic endothelial cells. In this case, the secreted LG3 interacts with the $\alpha 2\beta 1$ integrin receptor of fibroblasts and triggers a signaling cascade that leads to activation of an anti-apoptotic pathway and potentially to a fibrogenic response [Whiterlock et al., 2008].

CD44 promotes angiogenesis in tumor environment by binding TGF β and promoting MMP9 activity. CD44 v6 isoform has been shown to activate endothelial cell migration, sprouting and tubule formation through activation of c-Met and VEGFR-2 in response to HGF and VEGF-A binding to the extracellular domain of CD44 [Louferbough and Schroeder, 2011].

NG2 may be an important linker between endothelial cells and pericytes. Vascular endothelial cells do not express NG2 proteoglycan, but exposure to NG2 stimulates the motility of glioma cells. This *trans* effect is due to the interaction of the proteoglycan with the galectin-3/ $\alpha 3\beta 1$ integrin complex on the endothelial cell surface, resulting in enhanced $\beta 1$ integrin signaling, greater endothelial cell motility and enhanced endothelial tube formation *in vitro*, and dramatically increased blood vessel development *in vivo* [Xu et al., 2011]. These phenomena are significant because of the intimate interaction that exists in blood vessels between endothelial cells and NG2-positive pericytes. NG2 may be important as one element of the crosstalk that occurs between endothelial cells and pericytes. The significance of this will become more apparent when we discuss on neovascularization [Stallcup and Huang, 2008]. The role of NG2 in blood vessel development is extremely relevant in glioma progression. While the majority of vascularization studies focus on the endothelial component of blood vessels, it is now clear that pericytes are also an early and critical component of microvascular development [Stallcup and Huang, 2008]. NG2 also has an important role in pericyte development and function, as demonstrated by the decreased post-natal neovascularization observed in the NG2 null mouse. In ischemic retinal vascularization and in corneal vascularization induced by FGF2, blood vessels development is decreased more than 2-fold by genetic ablation of NG2 [Stallcup and Huang, 2008]. The NG2-deficient vasculature that forms in these pathological eye models is characterized by a diminished pericyte:endothelial cell ratio (dropping from 1:1 to as low as 1:4). The most obvious cause of this change is the reduced proliferation of pericytes in the absence of NG2, as detected by BrdU incorporation [Stallcup and Huang, 2008].

ONLY GAG CHAINS

Syndecans GAG chains composition is directly involved in the PGs control of angiogenesis. In mouse mammary cells the treatment with TGF β determines an increased expression of syndecans chondroitin sulfate chains with the synthesis of longer chains as well as the increase in CS number attached to the core protein. CS-rich syndecan binds specifically to thrombospondin, an antiangiogenic protein which fails to bind syndecan with a regular complement of CS and HS [Hardingham and Fosang, 1992].

Some families of growth factors different from the FGF one, have been shown to demonstrate differential binding to perlecan HS with one such example being the VEGFs [Whiterlock et al., 2008]. One of the longer isoforms, VEGF₁₈₉, which contains exon 6 that encodes a basic stretch of amino acids and which has been shown to be responsible for matrix localization, binds to perlecan HS derived from endothelial cells whereas the shorter and more highly expressed VEGF₁₆₅ does not. Interestingly, a fraction that included both the secreted and cell surface HSPGs from fibroblasts was shown to bind VEGF₁₆₅. This would support the idea that perlecan localizes the larger forms of VEGF to the matrix but does not sequester the shorter forms, enabling them to diffuse through the pericellular matrix and bind to the cell surface HSPGs where they can activate the signal cascade. An elegant study in *Zebrafish* conducted by Whiterlock et al., shows that the localization of VEGF in the matrix was disturbed by the knockdown of the expression of the enzyme 6-*O*-sulfotransferase which affects the levels of sulfation present within HSPGs. Cell proliferation occurs satisfactorily but the process of branching morphogenesis is severely retarded. It is possible that the perlecan produced by endothelial cells undergoing angiogenesis would have low amounts of 6-*O*-sulfate and if it produced a perlecan that had a high proportion of these sulfate groups, it would prevent angiogenesis by hindering the diffusion of VEGF: this may be a process that cells use to modulate the response of the endothelial cells to VEGFs produced in the pericellular environment [Whiterlock et al., 2008]. Perlecan is largely expressed in the stroma of different type of tumors and it might directly contribute to the scaffolding of angiogenic blood vessels binding bFGF via the GAG chains and functioning as a low-affinity coreceptor for this factor, and for this reason perlecan become an important component in the process of bFGF-tumor angiogenesis [Iozzo and Murdoch, 1996]. The knockdown of perlecan in metastatic prostate cancer cells reduces the responses to FGF2 and VEGF and *in vivo* tumor growth. This PG colocalizes with sonic hedgehog in aggressive prostate carcinomas and its knockdown in these cells leads to an attenuation of cell proliferation and Shh signaling [Bix and Iozzo, 2008]. Increased perlecan in breast and colon carcinomas correlates with enhanced metastatic potential [Bix and Iozzo, 2008].

Collectively, by binding and protecting these various growth factors from degradation and misfolding, perlecan could modulate angiogenesis and tumor growth [Bix and Iozzo, 2008]. Notably, antisense targeting of endogenous perlecan in a variety of transformed cells including colon carcinoma and melanoma cells causes a significant inhibition of tumor growth and angiogenesis [Whiterlock et al., 2008]. Seemingly, colon carcinoma cells with a somatic cell mutation leading to a perlecan null phenotype show growth retardation and minimal angiogenesis in tumor xenografts. The central role of perlecan in angiogenesis is further confirmed by genetic manipulation leading to complete ablation of the perlecan gene [Whiterlock et al., 2008]. A significant proportion of perlecan-null mice develop numerous vascular anomalies including transposition of the great arteries and abnormal coronary arteries. In an animal model expressing a mutated form of perlecan lacking the glycosaminoglycan attachment site, and thus lacking HS side chains, there is impaired angiogenesis and retarded tumor growth [Whiterlock et al., 2008].

Using a murine oxygen induced retinopathy model, it was discovered that opticin possesses anti-angiogenic activity. Using an *ex vivo* chick chorioallantoic membrane assay, it was shown that opticin inhibits angiogenesis when stimulated by a range of growth factors. It suppresses capillary morphogenesis, inhibits endothelial invasion, and promotes capillary network regression in three-dimensional matrices of collagen and Matrigel. It is then shown that opticin binds to collagen and thereby competitively inhibits endothelial cell interactions with collagen via $\alpha1\beta1$ and $\alpha2\beta1$ integrins, thereby preventing the strong adhesion that is required for proangiogenic signaling via these integrins.

1.10. Coagulation

ONLY CORE PROTEIN

Bikunin is a proteinases inhibitor present in plasma and urine. It can inhibit trypsin, chymotrypsin, granulocyte elastase, plasmin, cathepsin G and acrosin. However, bikunin binds these enzymes less avidly than other, more abundant proteinase inhibitors in plasma, making the physiological function of bikunin unclear. The amino acid residue in the binding site of the C-terminal domain (domain II) is Arginine, a residue which seems to be conserved among mammals. The construction of different modified bikunin molecule makes possible to assign the binding capacity of this PG to its core protein domain II. Domain I is involved only in some of the total activity against cathepsin G and granulocyte elastase [Fries and Blom, 2000].

COOPERATION

Thrombomodulin inhibits thrombin-induced fibrinogen clotting and promotes inactivation of thrombin by binding antithrombin through both the CS chains and one of the EGF- like region (EGF 5-6) of the core protein [Hardingham and Fosang, 1992; Koutsi et al., 2007]. Thrombomodulin may also bind and activate zymogen form of the anticoagulant protein C and this function is not related to the chains but it depends only on core protein. For this reason if it is possible to say that the major anticoagulant activity of thrombomodulin is due to its core protein, however GAG chains are important for the modulation of this function [Hardingham and Fosang, 1992]. Thrombomodulin is present on the surface of endothelial cells and its EGF-like domain (EGF 4-6) bind with high affinity to thrombin that is generated close to intact endothelium. This binding determines the loss of the procoagulant activity of thrombin and the gain of the ability to activate protein C [Anastasiou et al., 2012]. The high concentration of circulating thrombomodulin in the microcirculation is crucial for local protein C activation and blood anticoagulation [Anastasiou et al., 2012]. Despite the binding is due to one of the PG core protein domain, once modified with the CS, thrombomodulin enhances the PC activity, accelerates the neutralization of thrombin by heparin-antithrombin and by the PC inhibitor and facilitates binding of platelet factor-4 to PC to accelerate its activation [Anastasiou et al., 2012; Koutsi et al., 2007]. Different *in vivo* experiments confirm the important function of thrombomodulin in the coagulation process. Transgenic mice with single nucleotide modification leading to Glu387Pro substitution (TMPro) in the thrombomodulin gene, show a mild hypercoagulable state associated with vascular bed-specific fibrin deposition, moderately accelerated platelet thrombus formation and a strong predilection for stasis-induced thrombosis. TMPro animals do not develop spontaneous thrombosis [Anastasiou et al., 2012]. Moreover, in the thrombomodulin-deficient TM *-/-* chimeric mice, the fibrin deposits were largely restricted to pulmonary vessels, suggesting that localized thrombomodulin deficiency, as it occurs for example in atherosclerosis lesions or iatrogenic endothelial cell damage, triggers localized coagulation and thrombosis [Anastasiou et al., 2012].

1.11. Immune response

ONLY CORE PROTEIN

Thrombomodulin controls the complement arm of the innate immune system in a thrombin-dependent manner through activation of the TAFI that binds the EGF-like repeats 3-6 domains of thrombomodulin core protein. An intact thrombin-thrombomodulin complex is required for TAFI to suppress complement activation [Anastasiou et al., 2012; Koutsi et al., 2007]. When associated with

thrombomodulin, the pro-inflammatory properties of thrombin are abrogated and in this way thrombomodulin become an indirect anti-inflammatory molecule. Instead the N-terminal C-type lectin-like domain of thrombomodulin has direct anti-inflammatory properties by mediating signals that interfere with MAPK and NFκB pathway [Anastasiou et al., 2012; Koutsi et al., 2007]. The complement control may happen also in a thrombin-independent constitutive manner via thrombomodulin lectin-like extracellular domain [Anastasiou et al., 2012].

PRELP play a fundamental role in immunological disease as modulator of the immune response. For example in rheumatoid arthritis, the cartilage tissue is destroyed and fragmented molecules, including PRELP, are released into the synovial fluid where they may interact with components of the complement system. In different studies PRELP is found to interact with the complement inhibitor C4-BP, which is suggested to locally down-regulate complement activation in joints during rheumatoid arthritis. It is shown that PRELP directly inhibits all pathways of complement by binding C9 and thereby prevents the formation of the membrane attack complex. PRELP does not interfere with the interaction between C9 and already formed C5-8, but inhibits C9 polymerization thereby preventing formation of the lytic pore. The alternative pathway is moreover inhibited already at the level of C3-convertase formation due to an interaction between PRELP and C3. This suggests that PRELP may downregulate complement attack at basement membranes and on damaged cartilage and it therefore limit pathological complement activation in inflammatory disease such as rheumatoid arthritis.

ONLY GAG CHAINS

After the generation of serglycin knockout mouse models it become easy to study the role of this PG in immune system and, in particular, in the process of granulopoiesis. In the knockout model, the generation of secretory granules in mast cells shows to be compromised and there is a reduction of several important proteases, histamine and serotonin [Kolset and Tveit, 2008, Kolset and Pejler, 2011]. It is clear that also secretory granules of cytotoxic T lymphocytes, mast cells, neutrophils and platelets are compromised in knockout mice [Kolset and Tveit, 2008]. It is important to underline that granzyme A and B are not affected by the lack of serglycin, more precisely the storage of granzyme B but not A is affected rather than protease mRNA expression. The same effect showed in serglycin knockout mice is seen also in NDST-2 knockout mice that lack the enzymes involved in GAG chains production. For this reason is possible to conclude that all the effect of serglycin on the granule storage may be attributed to GAG chains presence and binding [Kolset and Tveit, 2008; Kolset and Pejler, 2011]. In neutrophils only one type of granules, the azurophil ones, is affected in knockout models. Studies on Gram-negative bacteria infection of

serglycin knockout mice and control mice, show that the first one model seems to be more susceptible to the infection, because the lack of serglycin may affect immune defence [Kolset et Tveit, 2008]. Serglycin is shown to bind some proteases, like tryptases, forming tetramers complex, and it covalently binds also MMP9 as it is demonstrated in monocyte-like THP-1 cells [Kolset and Tveit, 2008]. Interacting with them, serglycin is involved in the retention of proteases in storage granules in mast cells. Not all the granule components depend on serglycin presence, in fact granzyme A and cathepsin G are not affected by the lack of this PG [Kolset and Tveit, 2008]. Complexes of serglycin and proteases are released from mast cells and serglycin is implicated in the secretion of different granule molecules, like TNF- α from macrophages, MMP9 from monocytes or chemokines from HIV-infected T cells. So it is possible to conclude that serglycin is essential for the regulation of the secretion of an impressive repertoire of molecules important in inflammatory reactions [Kolset and Tveit, 2008]. The secretion of the serglycin-ligand complexes is linked to the cell activation. After secretion, the change in microenvironment pH conditions causes the release of serglycin partner molecules [Kolset and Tveit, 2008; Kolset and Pejler, 2011]. So it is clear that serglycin has also important roles after immune cell secretion. In particular its heparin chains are important for the protection of enzymes inactivation because protease inhibitors are not able to bind heparin. Moreover heparin chains may mediate encounter between proteases and their substrates and are involved in activation and processing of proteases. Serglycin is also necessary to protect its partner molecules during their transport, for example proteases are only released to perform its function when the complex has reached its final destination [Kolset and Tveit, 2008; Kolset and Pejler, 2011]. Thanks to studies on serglycin knockout mice and NDST-2 knockout mice, it is clear that GAG chains linked to serglycin core protein are cell type-dependent. In particular in connective tissue-type mast cells serglycin bind prevalently heparin chains and this is the only cell type capable to synthesize the highly sulfated GAG heparin whereas a multitude of other cells like macrophages synthesize HS. The mucosal mast cells subtype produce serglycin binding CS chains, carrying *O*-sulfate groups at the 4- and 6-position. In cell type other than mast cells, for example in T lymphocytes, lower sulphated GAG species of CS type are predominantly attached to serglycin [Kolset and Pejler, 2011]. The composition of serglycin structure and the GAG chain type attached may depend on immunological signals. In fact it is shown that in eosinophils serglycin carries prevalently CS-4 sulfated chains after stimulation of cells with IL-3 or GM-CSF [Kolset and Pejler, 2011]. Serglycin is involved in granules control in most hematopoietic malignancies where its aggregation with the partner molecules may prevent extensive diffusion outside inflamed tissues. In human multiple myeloma is demonstrated an high cell surface localization of serglycin that binds cell surface by its GAG chains [Kolset and Tveit, 2008; Kolset and Pejler, 2011]. Myeloma-derived

serglycin interfered with bone mineralization providing a possible explanation for osteoporosis commonly in multiple myeloma patients. Serglycin is highly produced in acute myeloid leukemia but not in acute lymphoblastic leukemia [Kolset and Pejler, 2011].

Syndecans are able to bind most chemokines and participate in immune responses. In particular syndecan 1 is directly involved in inflammation as suggested by increased leukocyte-endothelial interactions in syndecan 1 null mice. It also has an important role in forming complex with IL-8, that control syndecan 1 shedding, and in chemokine gradient formation for trans-endothelial and trans-epithelial migration of neutrophils [Tkachenko et al., 2005]. For example, syndecan-1 binds through its heparan sulfate chains to the CC chemokines CCL7, CCL11, and CCL17 implicated in allergic diseases, resulting in inhibition of CC chemokine mediated T cell migration and suppression of allergen induced accumulation of Th2 cells in the lung [Choi et al., 2011]. Syndecan 1 and syndecan 4 bind the chemokine RANTES on monocyte derived macrophages, facilitating the subsequent interaction of RANTES with its receptor CCR5. The interaction of syndecans with chemokines play a pivotal role in cell survival. For example SDF-1 associates with chemokine (C-X-C motif) receptor 4 (CXCR4) and syndecan 4 at the plasma membrane of Huh7 cells, inducing the growth of Huh7 cells by promoting their entry into the cell cycle and inhibiting tumor necrosis factor- α -mediated apoptosis [Choi et al., 2011]. Syndecans possess the unique ability to interact with pathogens. All members of the syndecan family possess similar capacities to interact with HIV-1. Enzymatic removal of the heparan sulfate chains abrogates the ability of syndecans to capture HIV-1, indicating the importance of the linear anionic heparan sulfate chains for HIV-1 binding [Choi et al., 2011]. Like HIV-1, a great number of other pathogens use syndecans as attachment receptors to facilitate either entry into host cells or persistence in the hostile host environment [Choi et al., 2011].

COOPERATION

T-cell activation during immune response not only requires the recognition of antigen-loaded major histocompatibility complex by the T-cell receptor, but also the interaction of additional surface receptors expressed by T-cells with their corresponding counter-receptors on APC cells. Agrin is one of these important additional receptors and it takes part in the T-cell-APC cells interaction, inducing the cluster of the surface receptors [Bezakova et al., 2003; Jury and Kabouridis, 2010]. Its splicing at the amino N-terminus produces either secreted or membrane-anchored proteins, whereas splicing at two additional sites closer to the carboxy C-terminal, named y and z in the mammalian system, produces proteins that either lack or include two small exons. On the T-cells only the transmembrane agrin isoform is expressed, it accumulates to distinct areas of

the cell membrane and T-cell activation causes its redistribution post-translationally modification to a form with an increased ability to aggregate receptors on T-cells. Although if the nature of this modification is unknown, it is shown that glycosylated agrin is dominant in resting lymphocytes and deglycosylation form is present in activated lymphocytes [Bezakova et al., 2003; Jury and Kabouridis, 2010].

Collagen type IX NC4 domain binds both C4-BP and factor H. C4-BP is the major soluble inhibitor of the classical and lectin pathway for the complement activation; factor H inhibits the alternative route. Binding these two molecules, collagen type IX play an important role in degrading C4b and C3b activating complement factors slowing down the complement activation process [Kalchishkova et al., 2011]; NC4 domain can inactivate complement directly inhibiting C9 polymerization and membrane attack complex formation [Kalchishkova et al., 2011].

2. MATERIAL AND METHODS

2.1. RNA extraction and reverse transcription-polymerase chain reaction (RT-PCR)

Total RNA from different sarcoma cells was prepared by using Trizol[®] (Life Technology Corporation, California, US) according to the manufacturer's instructions and RNA quality was checked by Biophotometer (Eppendorf AG, Germany) and 1% agarose RNase free TAE agarose gel electrophoresis. Total RNA (1µg) was reverse-transcribed with the QuantiTect[®] Reverse Transcription Kit (Qiagen, Netherlands) according to the manufacturer's instructions. Qualitative RT-PCR was performed at the beginning to check the presence of glypicans and syndecans (GPC1, GPC2, GPC3, GPC4, GPC5, GPC6, SDC1, SDC2, SDC3, and SDC4) mRNA in cells and it was amplified, as internal control, RLP41 housekeeping gene to test the integrity and functionality of cDNA from cells. To control the absence of DNA contamination it was performed a PCR with primers for RLP41 on reverse-transcribed without RNA as substrate. To quantify the exactly amount of each gene expressed in all the sample tested, it was performed a quantitative Real-Time PCR using TaqMan Low-Density Arrays (TLDA). Gene expression was normalized to endogenous housekeeping gene 18S rRNA and it was chosen cDNA of human mesenchymal stem cells (hMSC) as sample calibrator, because all sarcomas analyzed came from mesenchymal cells. An equal amount of input cDNA (100 ng) was used per reaction and loaded in one of the eight sample-loading port of the card. Results were analyzed using ABI PRISM 7900HT Sequence Detection System (ABI), and changes in gene expression levels were calculated using the "relative quantification method" based on the expression levels of a target gene versus a reference gene in each sample in comparison to a sample.

Total RNA from tumoral tissue biopsies were prepared by using alone or in combination Trizol[®] (Life Technology) and RNeasy Plus Mini Kit (Qiagen) according to the manufacturer's instructions and RNA quality was checked by Biophotometer (Eppendorf) and 1% agarose RNase free TAE agarose gel electrophoresis. Total RNA (1µg) was reverse-transcribed with the QuantiTect[®] Reverse Transcription Kit (Qiagen) according to the manufacturer's instructions. Qualitative RT-PCR was performed at the beginning to check the integrity and functionality of the cDNAs, and it was amplified human RLP41 (FWD: 5'-GGAGGCCACAGGAGCAGAAA-3'; REV: 5'-TGTCACAGGTCAGGGCAGA-3') and mouse RPL27 (FWD: 5'-CAAGAAGAAGATCGCCAAGC-3' and REV: 5'-TCGCTCCTCAAACCTTGACCT-3') housekeeping genes mRNA. To verify the presence of GPC5 gene transcript, it were used specific primers for human and mouse glypican 5 mRNA: (hFWD) 5'-TATCCGGTCGTTGGAAGAAC-3'; (hREV) 5'-GGTGGTCTTCATCCATGCT-3'; (msFWD) 5'-CCGAGGATGGATGCCCCGAC-3'; (msREV) 5'-CTTCGCAGCTCTCCACGCCC-3'. qPCR on 143B GPC5+ clones were done using the human RPL41 and human GPC5 primers previously mentioned and by

SYBR Green technology (Takara Bio Inc., Japan) and all samples were run on OpticonMJ Real-Time (Bio-Rad Laboratories Headquarters, California, US)

2.2. Purification of HSs

Bovine liver was homogenized in ice-cold acetone and lyophilized. The acetone powder was digested with actinase E, treated with 5% trichloroacetic acid, and the polysaccharides were precipitated with 80% ethanol as previously described [Yamada et al., 2002]. The resultant precipitate was subjected to DEAE-cellulose column chromatography using stepwise elution with a 0.05 M sodium acetate buffer, pH 4.0, containing 0.15, 1.0, and 2.0 M LiCl. Each fraction was desalted by ethanol precipitation and the precipitates were dissolved in water.

Bovine kidney HS, porcine intestine HS, and bovine liver GAG preparations were digested with a mixture of heparinases I and III [Ueno et al., 2001]. Each digestion was labeled with a fluorophore 2-aminobenzamide and subjected to anion exchange HPLC on an amino-bound silica PA-03 column (YMC Co., Japan) as previously reported [Kinoshita et al., 1999]. Identification and quantification of the resulting disaccharides were achieved by comparison with HS-derived authentic unsaturated disaccharides.

2.3. Cell culture and transfection

143B human osteosarcoma cells were transfected with pDisplay expression vector containing ORF cDNA of glypican 5 HA-tagged (Fig. 1) or glypican-6 HA-tagged and pDisplay empty expression vector as control (143B mock). The expression vector pDisplay containing ORF cDNA of GPC5 was gently provided by Guido David (University of Leuven-CME) and containing the box for G418 (Geneticin) resistance (Geneticin/Neomycin). The transfections were done using Metafectene™ Pro Reagent (Biontex, Germany) in condition predetermined to obtain maximum efficiency of transfection; briefly, Solution A (0.8 µg of vector DNA in 50 µl medium free of serum and antibiotics) and Solution B (8 µl of Metafectene™ Pro transfection reagent in 50 µl medium free of serum and antibiotics) were applied on 60-70% cell confluence and for 143B GPC5 transfected were performed an antibiotic monoclonal clones selection by G418 at concentration of 500 µg/ml, that is, after 48 h from the transfection, the cells were seeded at high dilution (6000 cells/100 mm dish) until formation of single clones, the individual clones were expanded and cells from each clones were screened by RT-PCR for presence of GPC5 mRNA. Positive clones were expanded and it was chosen the clone with the major level of glypican 5 expression revealed by quantitative Real-Time PCR.

143B cells were routinely grown in monolayer cultures and maintained at 37°C in an atmosphere of 5% CO₂, in DMEM (Sigma Aldrich, Missouri, US) with low Glucose (1.0 g/L), 25 mM HEPES Buffer supplemented with 100 U/ml penicillin, 100U/ml streptomycin, 2 mM L-Glutamine and 10% (v/v) FBS.

4D1 and 373 E1 mouse hybridoma cells, kindly provided by the National Cancer Institute of Aviano (Italy) were cultured at 6x10⁵ cells/ml DMEM culture medium with 4,5 g/L of glucose containing 20% FBS, 100 mg/ml of L-Glutamine, 100 U/ml of penicillin/streptomycin and 0,01 mg/ml of HybriMax (Sigma Aldrich) and incubated at 37 °C in a 5% CO₂ incubator. After 18 or 40 hours of cultivation, the culture supernatants were harvested. Cells and debris were removed by centrifugation at 550 g for 5 minutes. Ascites are provided from the National Cancer Institute of Aviano.

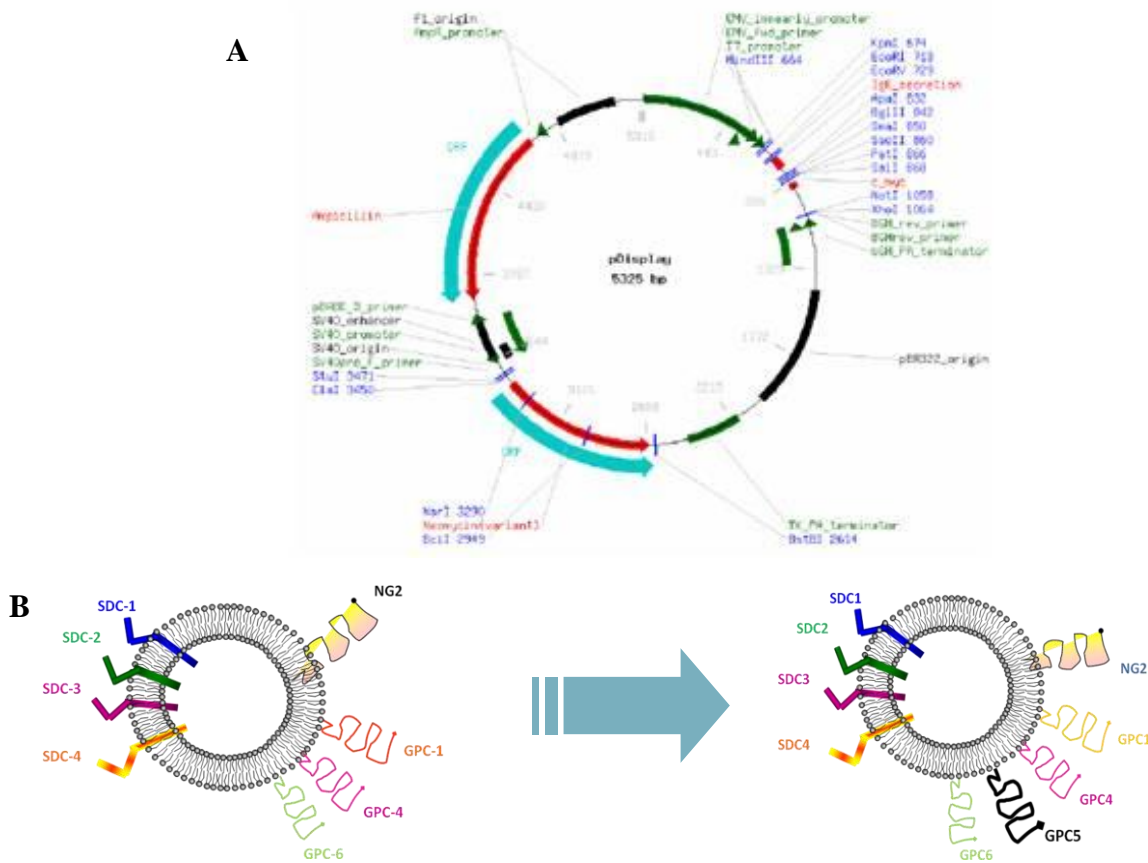


Fig.1: (A): schematic representation of the pDisplay vector used for 143B transfection; (B): 143B wild type (143B WT) compared with 143B transfected cells (143B 5+).

2.4. ECM molecules-cell adhesion

ECM molecules were diluted in bicarbonate buffer at the final concentration of 20 µg/ml and then distributed 50 µl per well in a 96 multiwell plate. In the control well 50 µl of 2% casein solution in PBS 1X were added. All wells were incubated at 4°C over night (O.N.) After the incubation, the excess solution were eliminated and wells were blocked with 100 µl per well of 2% casein solution in PBS 1X, for 30' at 37°C. 2% Casein blocking solution was eliminated and wells were gently washed. Both 143B WT and 5+ cells were grown in DMEM with 0,5% of FBS and seeded in quadruplicate at a density of $1,5 \times 10^5$ cells/well at 37°C with 5% of CO₂. After drying and gently washing the wells, 120 µl of MTS (Cell Titer 96 A Qu_{ieous} One Solution, Promega Corporation, Wisconsin, US) solution in DMEM with 0,5% of FBS were added to each well for 3 h. Wells were read with a microplate reader (Multiskan ex, Thermo Fisher Scientific Inc., California, US) To correlate the absorbance value with a cell number, a standard curve was prepared with the same protocol.

2.5. Flow cytometry

To confirm the GPC5 ectopic expression on 143B selected clones, 500.000 expressing GPC5 cells (143B 5+) and control cells (143B mock) were collected and incubated with 250 ng of direct PE-labeled monoclonal antibody anti-human/mouse GPC5 (clone 297716, R&D System, Minneapolis, US) on ice and then washed and resuspended in PBS1X (final concentration NaCl 137 mM, KCl 2.7 mM, Na₂HPO₄ 4.3 mM, KH₂PO₄ 1.47 mM, adjust to a final pH of 7.4) for the analysis. As a control, the same cells were treated with PE-labeled mouse IgG_{2A} isotype control (clone HOPC-1, SouthernBiotech, Birmingham, US) antibody in separate tube. All samples were analyzed on fluorescence activated cell sorter (Coulter EPICS XL-MCL Flow Cytometer).

2.6. Western blotting

Total protein cell extracts were prepared by lysing the cell for 10 min on ice in RIPA lysis buffer (final concentration Tris-HCl, pH 7.4, 50 mM, NaCl 150 mM, P-40 1%, Na-deoxycholate 0.5%, SDS 0.1%, EDTA 2 mM, leupeptin 50 µM, aprotinin 2 µg/ml, soybean trypsin inhibitor 2 µg/ml, pepstatin Na₃VO₄ 1 µg/ml, NaF 1 mM, Pefabloc SC 0.8 mM) after collection from a 100 mm dish and double washing with PBS1X. Protein concentration was measured by Bradford method. Supernatant of stable cell lines were collected after 24 hours of culture incubation in DMEM serum free and concentrated utilizing methanol protocol: 400 µl of supernatants were mixed with 2.5 volumes of cool 100% methanol, incubated overnight at -20°C, washed the precipitate with cool

100% acetone, the pellet recovered were dissolved in sterile water and 20µl of concentrated media were denatured with 2X sample buffer (final concentration Tris-HCl ,pH 7.4, 0.065 M, Glycerol 10.5%, SDS(10%) 21%, Bromophenol Blue (0.05%) 6.5%). Protein extract diluted in 2X sample buffer and concentrated media were resolved on 8% SDS-PAGE and transferred to Hybond-P membranes (GE Healthcare Life Science, Sweden) over day. Western blot analysis were performed using the following primary antibodies: anti-HA High Affinity (3F10, Roche Diagnostics, Switzerland) used 1:2000 in TBS with 0.1% Tween[®] and 5% skim milk, anti-human Glypican 5 (R&D) used 1:500 in TBS with 0.1% Tween[®], anti-actin (Sigma Aldrich) used 1:3000 in TBS with 0.1% Tween[®] and 1% skim milk as control. After incubation with the primary antibody, the blots were washed and incubated for 1 hour with the appropriate HRP-conjugated secondary antibody; labeled proteins were detected with an ECL-Plus detection system (GE Healthcare).

2.7. ELISA

ELISA 96-well plates (Nunc Maxisorp) were coated with the different purified PGs diluted to 10-20 mg/ml in 0.05 M bicarbonate buffer, pH 9.6, overnight at 4°C. Wells were extensively washed, saturated with 2% BSA in the same buffer for 1-2 hours at room temperature and incubated with primary antibodies as described below. GAG preparations, in their intact or chemically modified form, were biotinylated as previously described [Deepa et al., 2002] and 0.5 µg/well in PBS1X were added to streptavidin-coated 96-well Iduron plates which were then incubated overnight at 4°C. After extensive washing with PBS containing 0.05% Tween-20, blocking with 1% BSA in PBS1X at 37 °C for 1 hour, plates were incubated with mAb 4D1 (1:100 dilution), mAb 10E4 (1:1,000 dilution), or mAb HepSS1 (1:1,000 dilution), in PBS1X at 37° C for 2 hours. Wells were further extensively washed with 10 mM Tris-HCl buffer, pH 8.0, containing 0.05% Tween 20 and 0.15 M NaCl and incubated with polyvalent alkaline phosphatase-linked anti-mouse secondary antibodies (diluted 1:3,000) at 37° C for 2 hours. After washing the plates with the above indicated Tris-HCl buffer, antibody binding was detected by adding 50 µl of *p*-nitrophenyl phosphate in 0.1 M sodium carbonate buffer, pH 9.8 and adsorbance reading. Alternatively, non-biotinylated GAGs were coated onto Iduron plates (Iduron, UK) by overnight incubation at 4°C after saturation with 2% BSA, and processed for antibody binding as described above. Competition experiments were performed by pre-mixing for 15 min at room temperature mAb 4D1 with 3-10 µg each of HS oligosaccharides ranging from 4-18-mers or biotinylated heparin (4 µg) digested with 0.5 mU of heparinase I, II, or III in a total volume of 10 ul of 20 mM acetate buffer (pH 7.0) containing 2 mM calcium acetate at 37° C for 30 min. The reaction was terminated by boiling at 100°C for 1 min. Alternatively, an aliquot of the digest was directly immobilized onto streptavidin-coated plates in

PBS1X and plates were processed as above. In some cases heparinases I or III, or a mixture of the two enzymes, was added to wells with immobilized biotinylated heparin and incubated at 37° C for 1 hour to digest the GAG in situ.

2.8. Immunofluorescence and confocal microscopy

Immunocytochemistry was done on the transfected cells to confirm the presence of GPC5 protein expression and to determine its cellular localization. 30.000 cells seeded on each coverslips were fixed after 24 hours using 4% paraformaldehyde; coverslips were washed in PBS1X and if necessary permeabilized using 0.1% Triton; coverslips were then incubated with primary antibody diluted in a mixture that included 10% NGS and PBS1X. After overnight incubation at 4°C with the corresponding primary antibody, cells were incubated for 1 hour at room temperature with the secondary appropriate antibody as shown in the table below in a mix with 10% NGS and PBS1X. Nuclei were revealed with a 20 minute incubation of coverslips with Hoechst 33258 staining and then the coverslips were mounted and observed under epifluorescence Nikon eclipse E600 microscope connected with a Nikon DXM1200 camera. For confocal microscopy, cells were prepared with the same protocol shown previously and stained with the same primary and secondary antibodies. Samples were observed in confocal microscopy by LSM 510 meta (Zeiss) microscope and analyzed with dedicated software.

Primary antibody	Secondary antibody	Permeabilization
Ms anti-hu/ms GPC5 IgG2a (R&D System) dilution 1:200	Anti-ms IgG Alexa Fluor 488 (Life Technology) dilution 1:200	None
Rat anti-HA tag IgG1 (Roche) dilution 1:200	Anti-rat IgG Alexa Fluor 488 (Life Technology) dilution 1:200	None
Phalloidin-TRITC conjugated (Sigma Aldrich) diluted 1:1000	None	PBS+0,1% Triton X100, 30' RT*
Ms anti-ms FAK IgG1 (BD Bioscience) dilution 1:100	Anti-ms IgG1 FITC (Sigma Aldrich) dilution 1:50	PBS+0,1% Triton X100, 30' RT

Rb anti-rb P-Pax (Tyr118) (Cell Signaling) dilution 1:20	Anti-Rb FITC (Sigma Aldrich) dilution 1:50	PBS+0,3% Triton X100, 30' RT
---	--	---------------------------------

*RT: Room Temperature

2.9. *In vitro* proliferation assays

Viable cell were seeded in quadruplicate in 96-well culture plates at a density of 3×10^3 cells/well in DMEM with 10%, starvated overnight in 0,5% of FBS, if required, in three independent experiments. At different time points cells were stained with a DMEM solution containing Hoechst 33342 at final concentration of 10 μ M, incubated 1 hour at 37°C with 5% CO₂ and immediately scanned by a triple laser imaging cytometer Acumen® eX3 (TTP LabTech Ltd, UK). The number of viable cells were counted and analyzed by dedicated software and a growth curve (cell number) was established. To asses if cells were reactive to different growth factors, after starvation as previously described the cells were incubated with 10 ng/ml and 25 ng/ml of BMP2, BMP4 or BMP7 (Milteny Biotec, Germany), 5ng/ml, 10ng/ml or 50ng/ml of Wnt1A (Sigma-Aldrich), 5ng/ml, 10ng/ml or 50ng/ml of bFGF (Peprotech, New York, US), 50ng/ml and 100ng/ml of Shh (Sigma-Aldrich), 25 ng/ml, 50 ng/ml and 100 ng/ml of HGF (Sigma-Aldrich), 25 ng/ml, 50 ng/ml and 100 ng/ml of IGF (Sigma-Aldrich) and finally with 10 ng/ml and 25 ng/ml of VEGF_{165aa} (Milteny Biotec) in 0,5% of FBS cell culture medium. Data are expressed as mean \pm SE.

2.10. Anchorage-independent growth assay

Anchorage-independent growth assay was done using 35 mm Petri plates. Each plate contained 2 ml of 0.6% low-melting agarose in complete medium as the bottom layer and 5000 cells in complete medium containing 0.3% low-melting agarose were seeded as top layer. Cultures were maintained under standard culture conditions for 15 days and the number of colonies was determined with an inverted phase-contrast microscope at X100 magnification. A group of >10 cells was counted as a colony. The data are shown as mean number of colonies per field \pm SD. The assay was repeated thrice with 3 replicates each time.

2.11. *In vivo* tumorigenesis

Housing, treatment and sacrifice of animals followed national legislative provisions (Italian law No. 116 of 27 January, 1992) for the protection of animals used for scientific purposes. Athymic nude female mice (Harlan UK) were purchased at 5 weeks of age given at least 1 week to adapt to their new environment prior to the treatments. The mice were fed *ad libitum*. Animals were housed in animal care facility of the National Institute for Cancer Research, Genoa, Italy. All manipulations on the animals were performed under controlled conditions and all animals were subjected to regular health checks.

For the *in vivo* experiments, 10×10^6 143B cells, both 143B 5+ and 143B control, were resuspended in a matrigel solution with a 4:1 ratio and then injected subcutaneously into the flank of 8 to 10-week-old Hsd: Athymic Nude-nu mice. 22 and 37 mice were respectively inoculated with 143B mock and 143B 5+ cells. As control, 6 mice were injected with the same protocol with 143B 6+ cells.

The tumor dimensions were measured every 5 days and the volume (V) was calculated as $V = (d)^2 \times D \times 0.52$, where d and D are the short and long dimensions (centimetres) of the tumour, respectively, measured with a caliper. The mice were sacrificed by CO₂ inhalation when the tumors reached a volume of about 1.5 cm³. Primary tumors from the flank were excised and the tumors were weighed, fixed with 10% formalin and paraffin-embedded. Three tumor masses from three different mice representative of all the mice experimental groups were split and used for both immunostaining and RNA isolation.

The statistical significance of the results was determined using the non-parametric Mann–Whitney test. The tumor doubling time during the log phase of growth was calculated using the following equation: $t = (\log 2) / \text{slope of the log of tumor volume vs. days}$.

To analyze the ability of glypican 5 positive cells to form lung metastasis, 8 mice for cell clones were caudal intravenous injected with 2.5×10^5 , 5×10^5 or 1×10^6 in a physiological solution. 30 days after inoculation, mice were suppressed and a first evaluation of the formation of metastases in the lung was detected by gross observation and histopathological assessment. Briefly, visible tumor nodules (macrometastases) were counted immediately after *post-mortem* lungs explantation. After the animal suppression, lungs were explanted, fixed in 4% paraformaldehyde, processed and paraffin-embedded. The sample were then sectioned in 5 μm sections, every 10th section stained with hematoxylin and eosin (H&E), and analyzed for the presence of not visibly detectable micrometastases. Five sections of each tissue were examined. Each stained section was examined microscopically under low power (12.5X) to visualize approximately 50% of the lung section per

microscopic field. The total number of metastases per lung section was counted and the average was calculated.

2.12. Immunohistochemistry

Paraffin on tissue samples were dissolved incubating slides in xylene for 20 minutes; then the sections were rehydrated using a decreasing-graded ethanol series (Ethanol 100%, Ethanol 96%, Ethanol 80%, Ethanol 75% and Ethanol 50%, for 5 minutes each one). After washing with tap water, tissue slides were dipped in TBS1X with 1% Tween (TBST).

The immunohistochemistry protocols were set up to optimize each antibody staining, as shown in the table below, using appropriate Antigen Retrieval techniques for each antibody. TUNEL assay (DeadEnd Colorimetric Apoptosis Detection System, Promega) was made according to the manufacturer's instructions.

The slides were then incubated with 3% H₂O₂ for 10 minutes at room temperature (RT), washed with TBST1X, incubate for 30 minutes at room temperature (RT) with PBST1X with specific sera solutions to block unspecific antibody binding sites. Samples were incubated with primary antibodies appropriately diluted in PBS1X with 1% Triton X-100 (PBST). After a wash in PBST 1X for 30 minutes to remove any primary antibody nonspecific reaction, slides were treated for 1 hour at RT with secondary antibody conjugated with an enzyme-labeled polymer, according to manufacturer's recommended protocol (Ultra Vision LP Detection System-HRP Polymer, Thermo Scientific). The immunoreactivity was detected with 3,3'-diaminobenzidine solution (Liquid DAB Substrate, Chromogen System, DakoCytomation, DK). Samples were counterstained with Harris' haematoxylin solution (Sigma-Aldrich) for 15 seconds, washed with tap water and dipped in ammoniacal ethanol for 2 seconds. After several washes in deionized water, slides were mounted using an aqueous mounting medium. The detection of the immunolabeling was done using a light microscope ZENITH microscope with OPTIKAM 3 digital camera.

Specimen and human healthy tissues were kindly received from Dr. Gaetano Magro (Section of Anatomic Pathology, Department of G.F. Ingrassia, University of Catania, Italy). Deparaffinized TMAs were incubated with 3% H₂O₂ for 10 minutes at room temperature to quench endogenous peroxidase activity, further incubated with Ultra V Block according to manufacturer's instructions to block non-specific antibody binding sites and then incubated with anti-HS antibodies diluted in PBS1X for 1 hr at 37°C or overnight at 4°C: mAb 4D1 (ascites fluid, 1:75 dilution; supernatant, 1:50 dilution), 10E4 (USBiological, Massachusetts, US., 1:100 dilution); 3G10 (USBiological, 1:100 dilution) and HepSS1 (USBiological, 1:100 dilution). The same protocol was applied for

373E1 immunohistochemistry assays. MAbs 373E1 and BCD4 (Seikagaku, Japan) were diluted respectively 1:5 and 1:75 in PBS1X with 2% of BSA. After washing with PBS1X, the slides were incubated with the UltraVision LP Detection System, washed and developed for 1-5 minutes with Liquid DAB Substrate Chromogen System and counterstained with Harris' haematoxylin solution for 15 seconds. Slides were washed with tap water and dipped in ammoniacal ethanol for 2 seconds. For antigen retrieval, prior to the endogenous peroxidase blocking step, sections were dipped in citrate buffer, pH 6.0, and subsequently heated to 85°C for 60 minutes. After treatment with H₂O₂ to quench endogenous peroxidase activity, some sections were digested with the different heparinases (heparinases I-III, diluted in 50 mM of Tris-Acetate buffer, pH 7.0), used at the concentration of 0.05 mU/ml, for 60 min at room temperature. In some control experiments, mAb 4D1 was diluted at the optimal working dilution, pre-incubated with heparin (EPSOCLAR, used at the concentration of 5000 U/ml) for 30 minutes at room temperature and the mixture was then added to the tissue sections. In other cases, sections were treated with DNase I (Promega) at the dilution of 5 U/ml and incubated for 30 minutes at room temperature before addition of primary antibodies.

Primary antibody	Secondary antibody	Antigen retrieval	Serum block
Ms anti-hu/ms GPC5 IgG2a (R&D System) dilution 1:450	Anti-ms IgG HRP (Sigma Aldrich) dilution 1:500	Tris EDTA 10 mM buffer*, 30' 95°C	5%NGS+5%BSA 30' RT
Sh anti-HA tag IgG (AbCAM) dilution 1:1000	Anti-sh IgG HRP (Sigma Aldrich) dilution 1:500	none	5%ShS+5%BSA 30' RT
Rb anti-hu CENPA IgG (AbCAM) dilution 1:50	Anti-rb IgG HRP (Life Technology) dilution 1:600	Tris EDTA 10 mM buffer*, 30' 95°C	5%NGS+5%BSA 30' RT
Rb anti-hu Ki67 IgG (AbCAM) dilution 1:100	Anti-rb IgG HRP (Life Technology) dilution 1:600	Tris EDTA 10 mM buffer*, 30' 95°C	5%NGS+5%BSA 30' RT
Rat anti-ms Ki67 IgG2a (Dako) dilution 1:20	Anti-rat IgG HRP (Life Technology) dilution 1:500	Tris EDTA 10 Mm buffer, 30' RT	5%NGS+5%BSA 30' RT
Rb anti-ms NG2 IgG (AbCAM) dilution 1:3000	Anti-rb IgG HRP (Life Technology) dilution 1:600	Tris EDTA 10 mM buffer, 30' 95°C	5%NGS+5%BSA 30' RT
Rat anti-ms CD31 IgG2a (AbCAM)	Anti-rat IgG HRP (Life Technology)	Proteinase K solution in Tris EDTA 50 mM	5%NGS+5%BSA

dilution 1:100	dilution 1:500	buffer [#] , 30' RT	30' RT
----------------	----------------	------------------------------	--------

* Tris-EDTA Buffer (10mM Tris Base, 1mM EDTA Solution, 0.05% Tween 20, pH 9.0)

Proteinase K Solution: 20 µg/ml in TE Buffer (50mM Tris Base, 1mM EDTA, 0.5% Triton X-100, pH 8.0)

2.13. Vessel density and perfusion

To measure perfusion, mice were injected with Dextran 70kDa-FITC (Life Technology; 360 µmol/L, 50 µL/mouse) 3 min before sacrifice. Perfused vessels were visualized by fluorescent microscopy using DM LB2 microscope (Leica). Vascularization tumors was evaluated by anti-CD31 (Sigma Aldrich) staining. Microvessels vascular density (MVD) or percentage of perfusion was quantified by screening for the areas of highest vascularity or perfused vessels; for each sample, 10 representative fields at 200X magnification were counted. Confocal laser scanning microscopy was carried out with a Zeiss LSM 510 microscope using argon (488 nm) and helium-neon (543–633 nm) laser sources, depending on the size of tumor sections; images were collected at a magnification of 200X.

2.14. Data and statistical analysis

In all the experiments, if not differently specified, the results were expressed as the mean \pm SEM and Student's t-test was used for statistical analysis to determine the statistical significance. Significance was defined as a * = $P < 0.01$.

3. RESULTS

3.1. Glypican 5 control of cancer growth and dissemination

3.1.1. Proteoglycan surface pattern in sarcoma cells

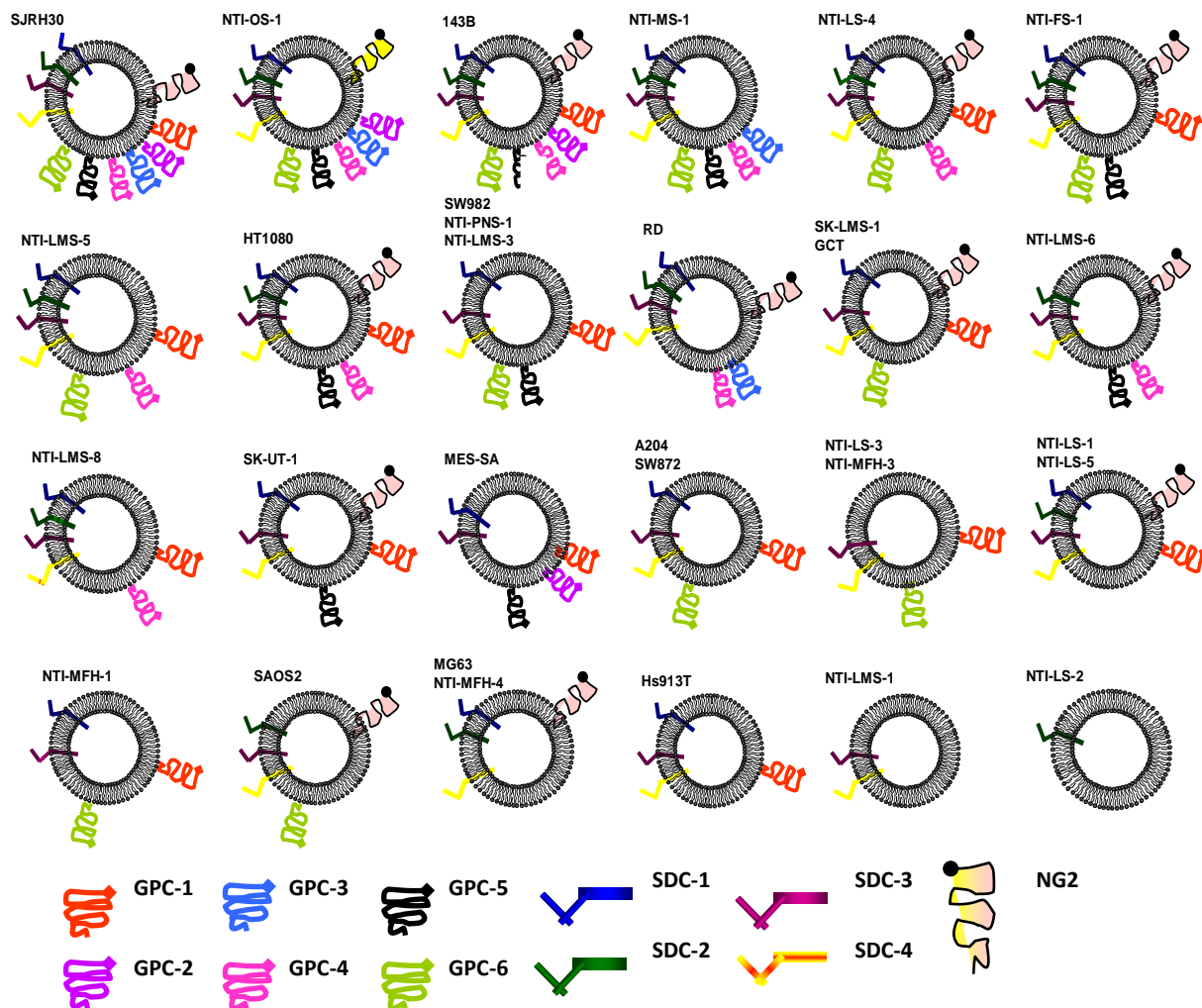


Fig.2. Surface PG expression pattern of different sarcoma models.

RT-PCR and TaqMan Low Density Array results allowed us to define a PG expression panel where it was possible to distinguish 24 different cellular PG models at the transcriptional level (Fig.2) with discrete surface PG pattern available for subsequent molecular manipulation, as gene transduction. Some sarcoma cells, even if belonging to different histotype, may present the same PGs pattern expression. On the base of these patterns, it was decided to use an osteosarcoma model, 143B cells, to *de novo* express GPC5 because these cells have a rather complex pattern of PGs expression. In particular this cell line express on its surface all the syndecans, the glypicans 1, 2 and 4, NG2 and a low expression of GPC6. This can allowed us to performe different *in vitro* and *in vivo* techniques,

analyzing also the possibility of a GPC interaction as mechanisms to compensate the different GPC5 expression.

These cells were subjected to the trasfection for the production of GPC5 and then tested for the cell surface PG expression. Wild type cells were used as control, in parallel with 143B cells trasfected with an empty vector (143B mock). There were generated more than one clone expressing GPC5 and we chose the higher expressing one, named 143B 5+, that was used for *in vitro* and *in vivo* assays. Flow cytometry (Fig.3,A), immunofluorescence staining with an antibody that specifically recognizes GPC5 (Fig.3,B) and western blot analysis (Fig.3,C) showed the *de novo* expression of GPC5 in about 90% of the transfected cells respect to 143B mock. 143B cells were also transfected with a pDisplay-GPC6 vector to obtain the clone 143B 6+ that overexpress this PG and that was used as an additional control to asses the specificity of GPC5 function.

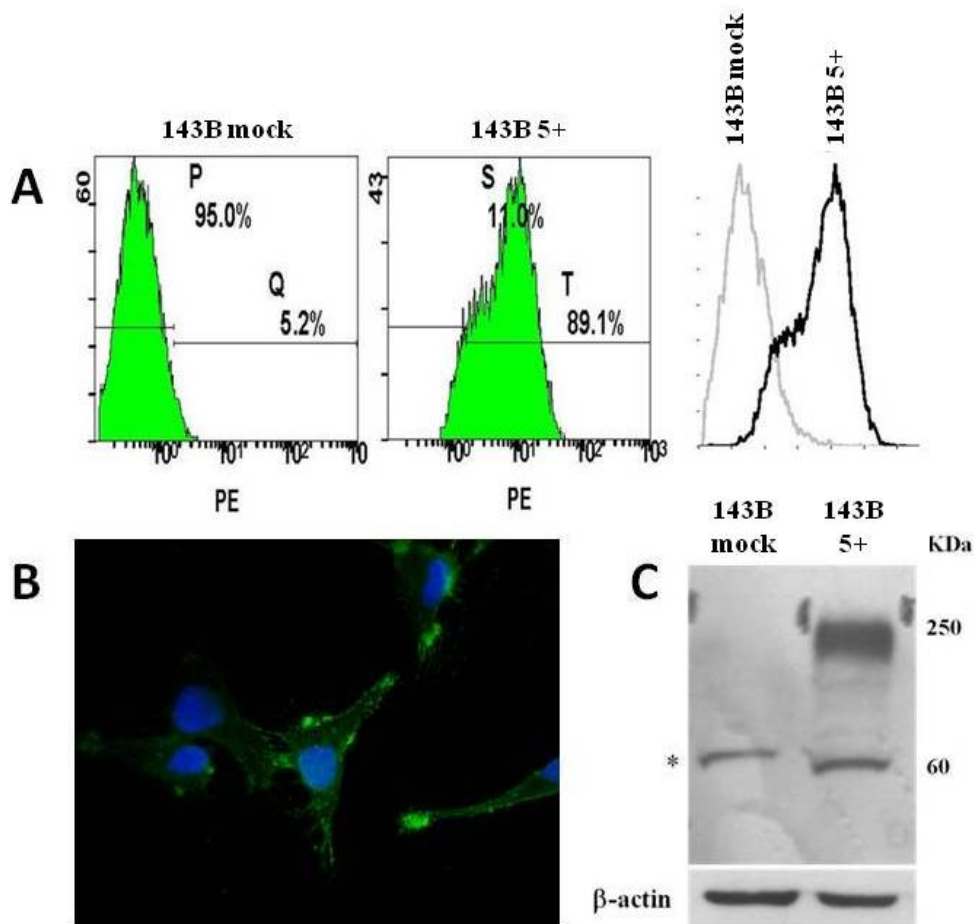


Fig. 3. (A): flow cytometry of 143B mock and transfected cells; (B): immunofluorescence staining of 143B 5+ cells. The GPC5 distribution on cell membrane corresponds to green spots and nuclei are stained with Hoechst (blu). Magnification 100X. (C) Western blot detection of GPC5 *de novo* expressed in 143B 5+ and control cells. It is present a nonspecific band of about 60 kDa (*)

3.1.2. GPC5 distribution on cell surface

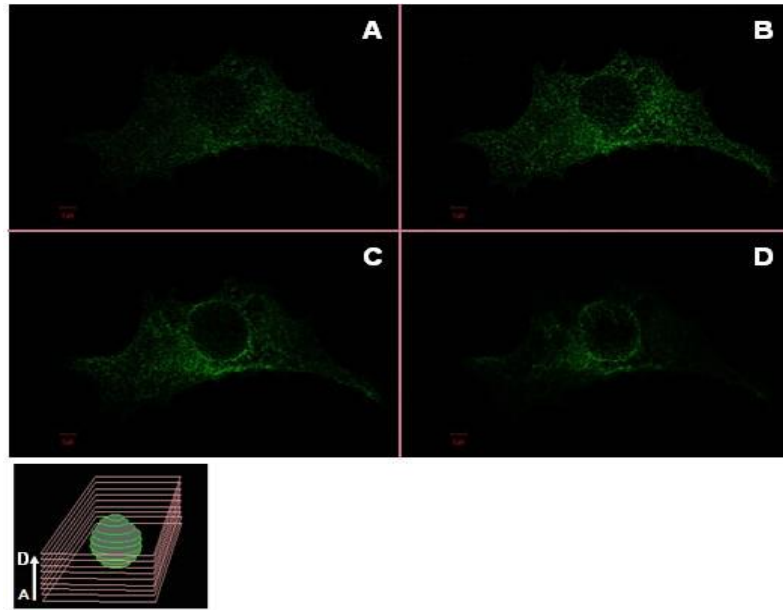


Fig. 4. Confocal sequences analysis of 143B mock immunolabeled with a human/mouse anti-GPC5 antibody (green). A little positivity may be due to the antibody crossreaction with cytoplasmic molecules. Microscope objective 63X.

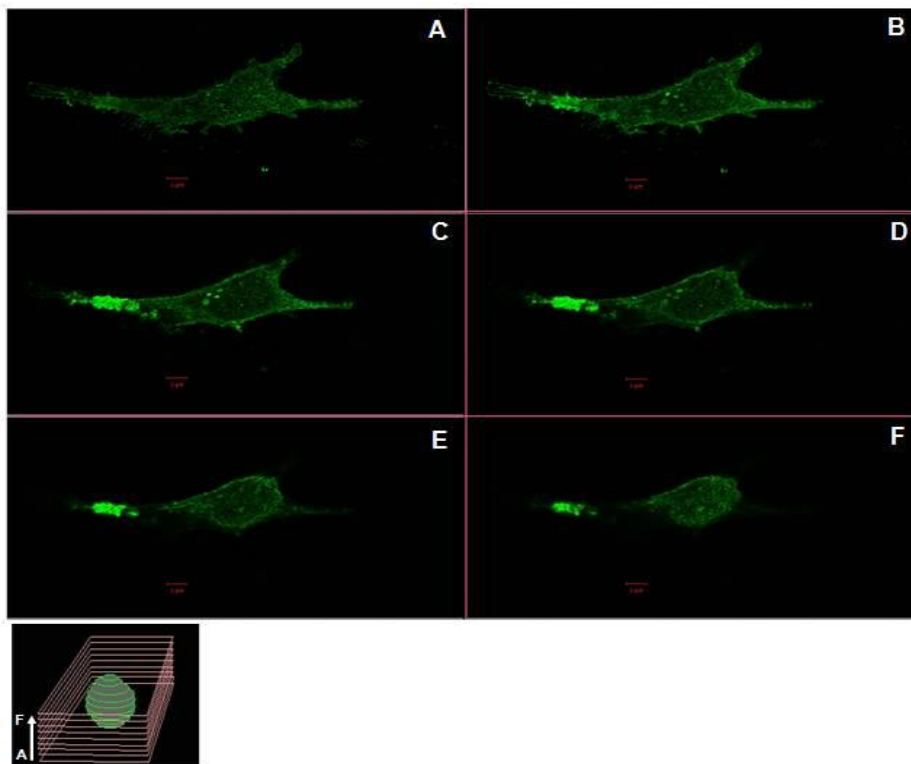


Fig. 5. Confocal sequences analysis of 143B 5+ immunolabeled with a human/mouse anti-GP5 antibody (green). Microscope objective 63X.

GPC5 expressing cells show a proteoglycan distribution that is different from that of control cells. More deeply, in 143B mock cells, GPC5-positivity seems to have a perinuclear distribution, probably related with an antibody cross reaction with endoplasmic reticulum and/or Golgi subcellular compartments molecules. In these cells GPC5 is completely absent from the cell surface (Fig. 4). Instead, 143B 5+ cells show a marked membrane distribution of GPC5 that appear to be concentrated in particular local areas of reinforcement probably corresponding with the lipid rafts (Fig.5). In particular GPC5 positive membrane domains seem to localize in particular cell extroflexions, the filopodia, produced by cell during its movement. There is a close relationship between plasma membrane domains like the lipid rafts and actin filaments. Immunostaining with phalloidin-TRITC conjugated allow us to relate GPC5 distribution and actin cytoskeletal conformation. Confocal analysis of double immunofluorescence staining suggest that in 143B 5+ cells, GPC5 colocalize with the membrane portion in which actin forms structural reinforcement (Fig.6, 7 and 8). These high positive membrane spots seems to correspond with the presence of focal adhesion molecules, such FAK or paxillin (Pax) in the activated phosphorylated form (P-Pax) (phosphorilation on Tyr118). Immunostaining shows that GPC5 may colocalize with these adhesion complexes, probably partecipating to their stability and biological functions (Fig.9).

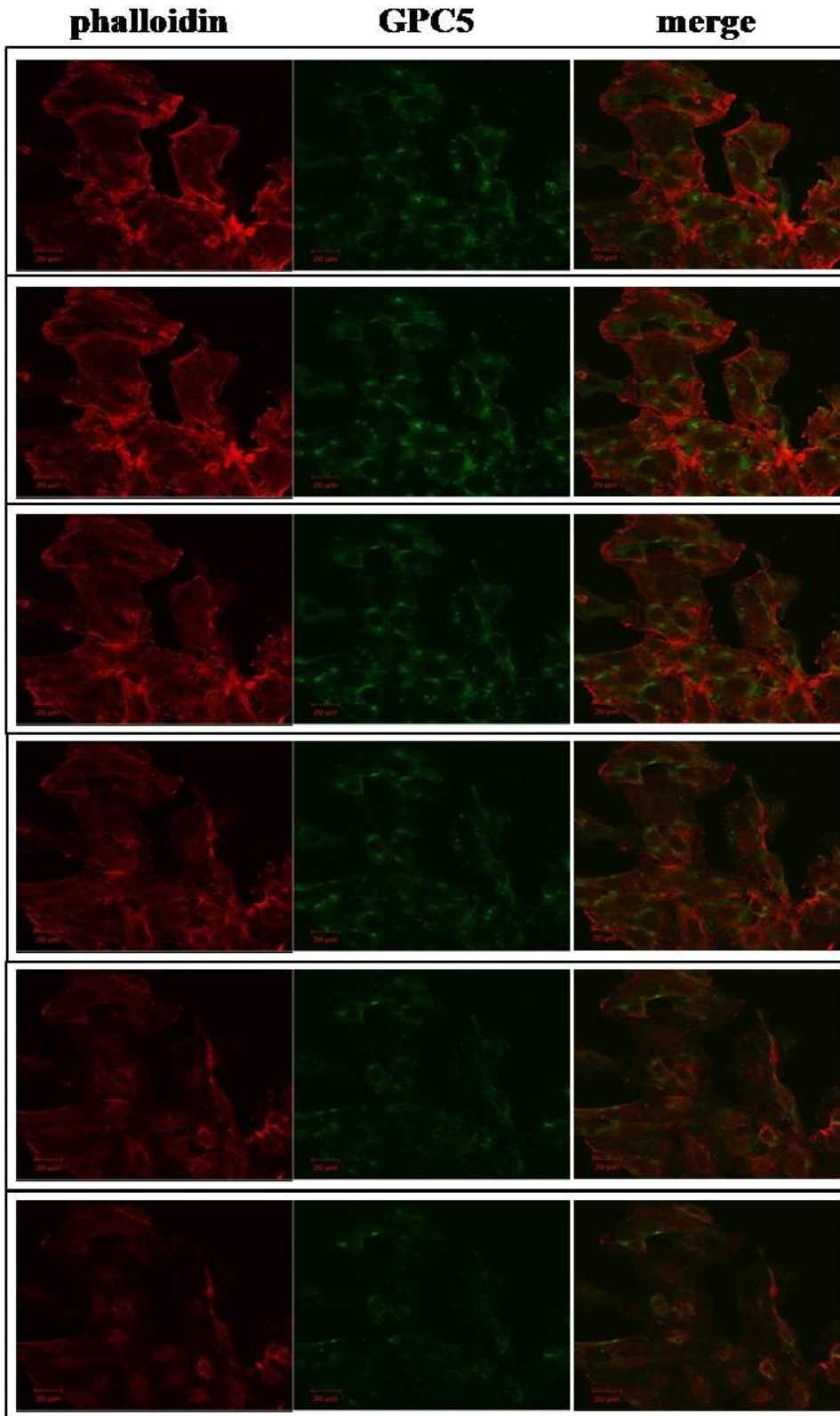


Fig. 6. Double immunofluorescence confocal analysis using phalloidin-TRITC conjugated (red) and the anti-human/mouse GPC5 antibody (green) on 143B WT fixed cells. The image sequence start from the basal cell surface. Microscope objective 40X.

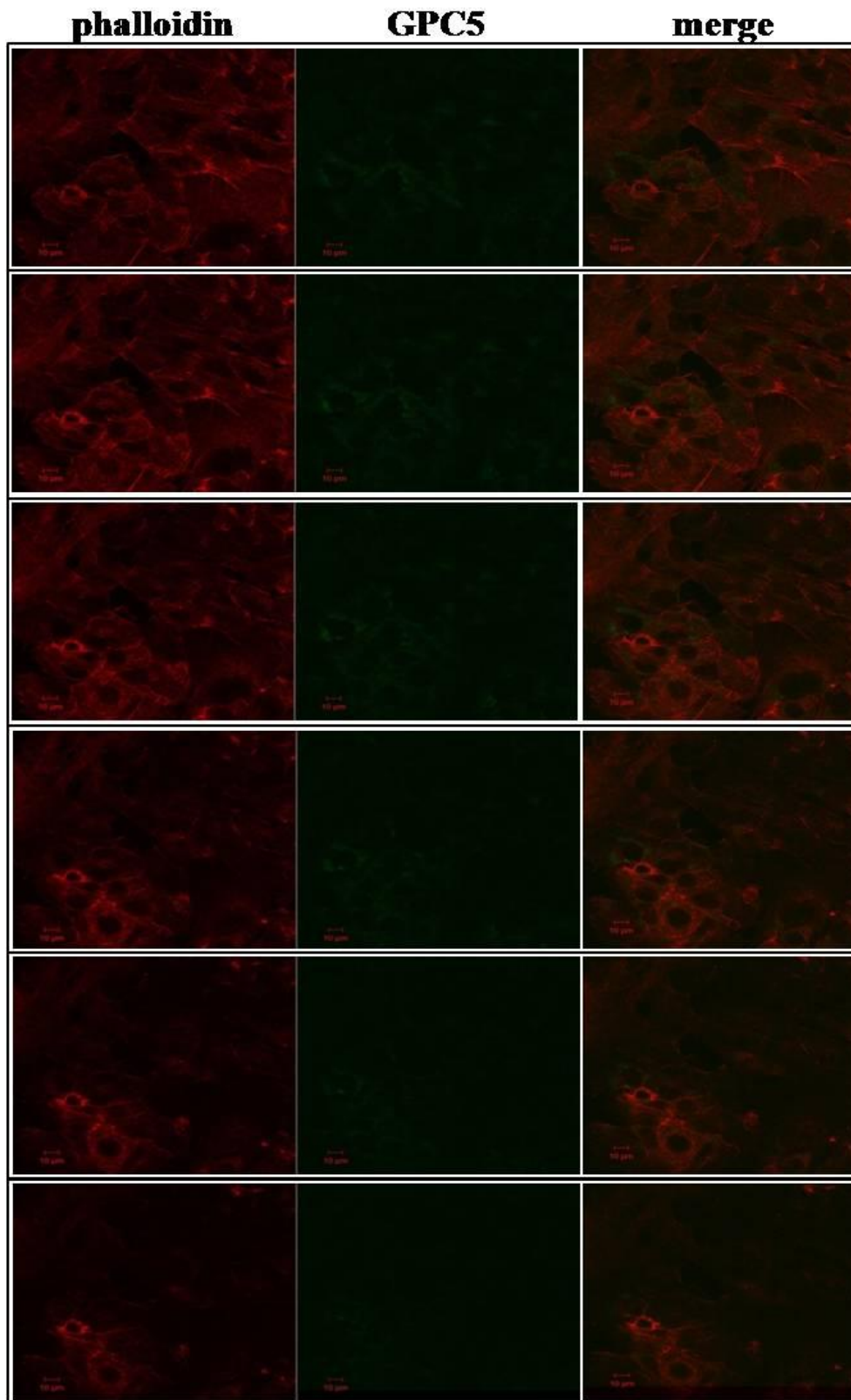


Fig. 7. Double immunofluorescence confocal analysis using phalloidin-TRITC conjugated (red) and the anti-human/mouse GPC5 antibody (green) on 143B mock fixed cells. The image sequence start from the basal cell surface. Microscope objective 40X.

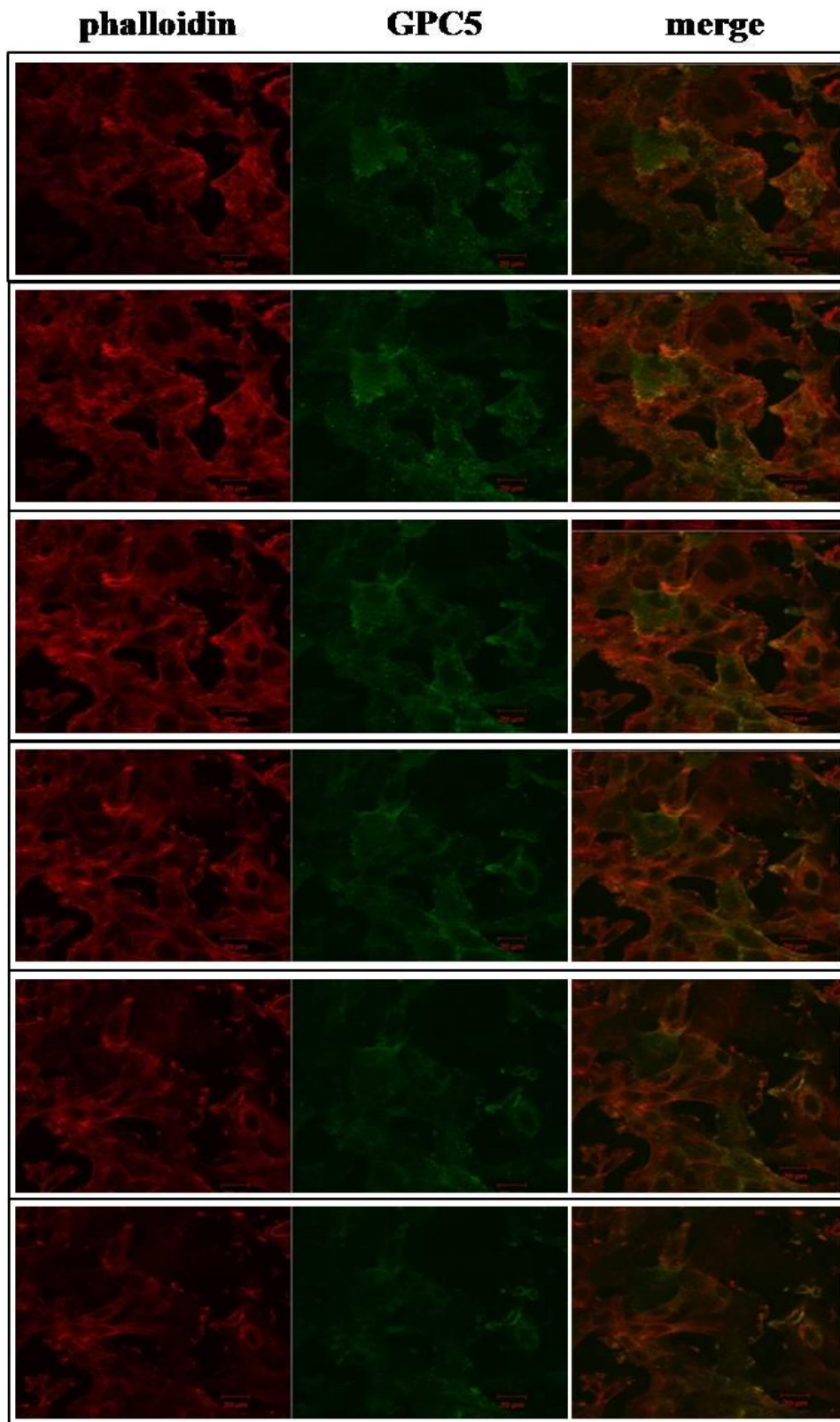


Fig. 8. Double immunofluorescence confocal analysis using phalloidin-TRITC conjugated (red) and the anti-human/mouse GPC5 antibody (green) on 143B 5+ fixed cells. The image sequence start from the basal cell surface. Microscope objective 40X.

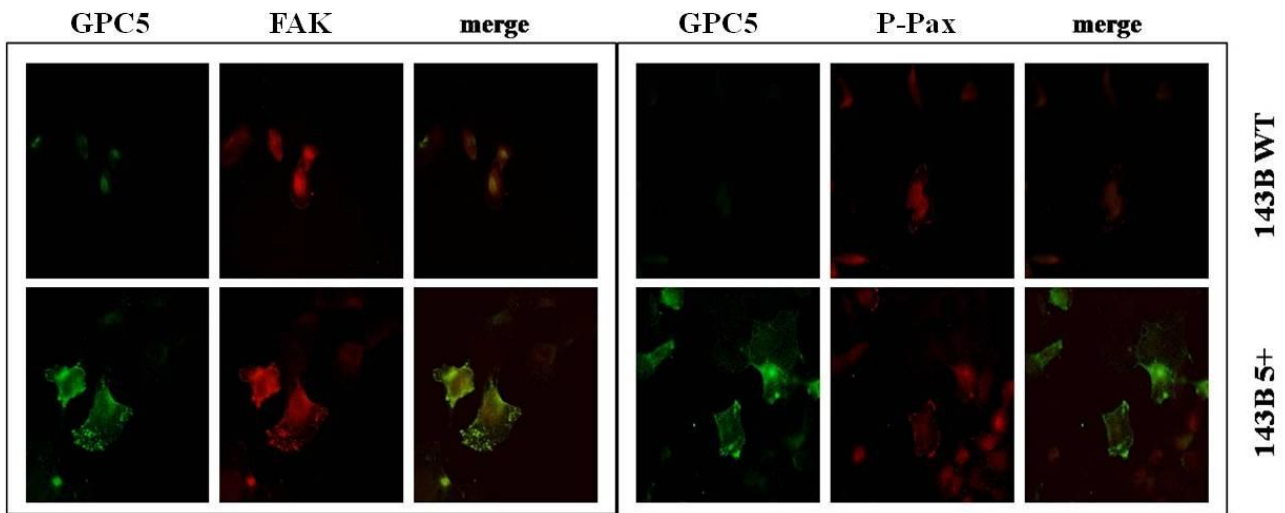


Fig. 9. double immunofluorescence staining on 143B WT and 5+ cells. In left panel, cells are stained with antibody anti-GPC5 (green) and anti-FAK (red). In the right panel the same cells are stained with antibody anti-GPC5 (green) and anti-P-Pax (red). In both immunostaining merges, the colocalization of GPC5 with the respective adhesion molecule is shown as yellow spots. Microscope objective 60X.

3.1.3. GPC5 influences cell adhesion and proliferation

The evaluation of the proliferation rate in a 0,3% FBS growth condition suggested us that 143B 5+ and mock cells have a comparable growth curve within the 24 hours after the seeding. These data allowed us to perform all the assays excluding the possibility that differences in the cell proliferation may affect the results. After 24 hours it is evident that both 143B 5+ and mock cells show a pushed growth rate in optimal growth conditions respect to nutrient deficiency conditions (Fig.10,A). Moreover it seems that the presence of GPC5 on the cell surface may negatively affect the cell proliferation capacity.

Cells expressing GPC5 demonstrate a different ability to adhere to different ECM molecules respect to wild type cells. In particular their adhesion capacity is suppressed on collagen type III-, collagen type VI-, fibronectin- and vitronectin-coated substrates (Fig.10,B). On un-coated plastic wells, both 143B 5+ and 143B wild type cells show the same anchorage ability, while no cell adhesion was seen on the casein block solution. The cell anchorage capacity is monitored after 1 hour after seeding.

We have also examined GPC5+ transfected cells capacity to growth in an anchorage-independent condition by a soft-agar assay. It is shown a significant decreased ability of GPC5 positive cells to growth without any adhesion to the substrate respect to wild-type control cells, while 143B 6+ ability to growth without any anchorage is comparable with that of control cells (Fig.10,C).

143B cell models were cultured in the presence of different growth factors. This assay suggest that the GPC5 expression on these cells may influence their response to some of these growth factors. In particular in fig. 11 A and D, are shown the most significant results obtained. In the graphs it is possible to see that in the presence of VEGF_{165aa} and HGF, 143B 5+ cells show a decreased proliferation rate respect to control cells, in particular 48 hours after the seeding. The same response, but not so evident extent, is obtained trainging cells with Wnt1 (Fig.11,C). In the graph B in fig.11, are reported the results of the same assay in presence of the IGF factor. In this case the presence of GPC5 on the cell surface seems to enanche the cell proliferation ability respect to control cells.

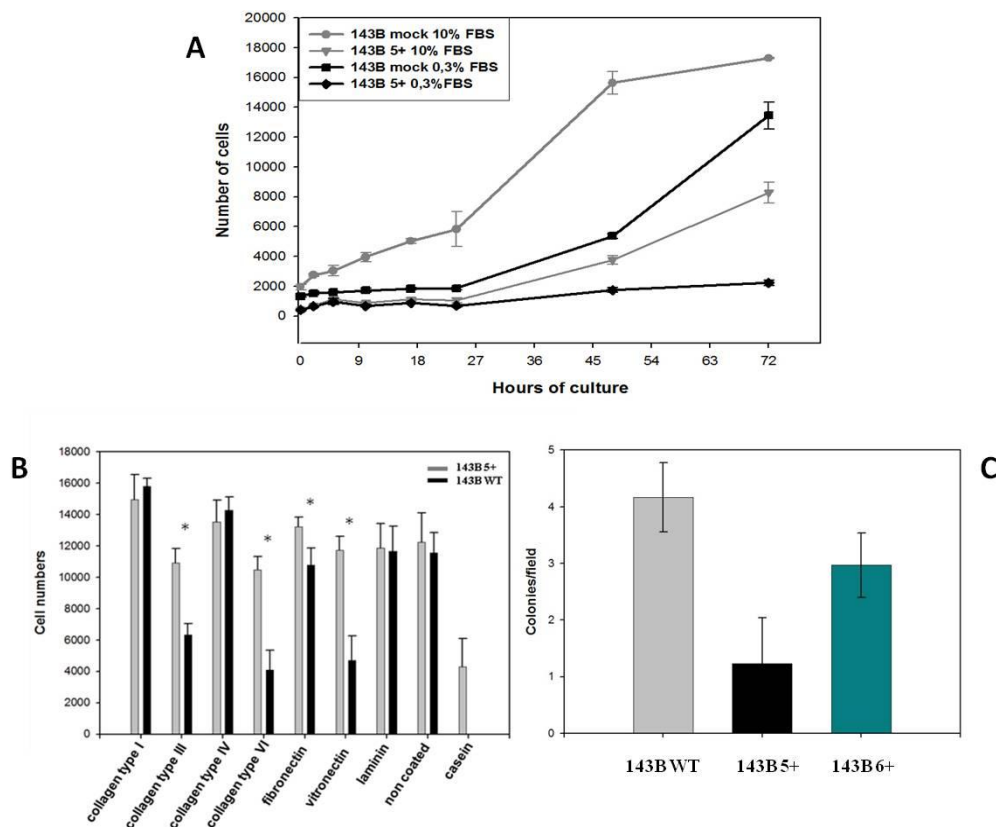


Fig 10. (A): growth curve of 143B mock and 143B 5+ cells in optimal (DMEM added with 10% of FBS) and wanting (DMEM added with 0,3% of FBS) growth conditions. Data are expressed as the means \pm SE. (B): trasfected 143B cells show a different ability to adhere to different ECM molecules respect to control cells. Cell number is calculated from values of MTS absorbance at 490 nm and interpolation on standard curve. Data are expressed as means \pm SD. (C): Anchorage-independent growth ability of 143B WT, 143B 5+ and 143B 6+ cells. It was considered a colony an aggregation of more than 10 cells and were counted 10 field in each replicate. Data are expressed as means \pm SD.

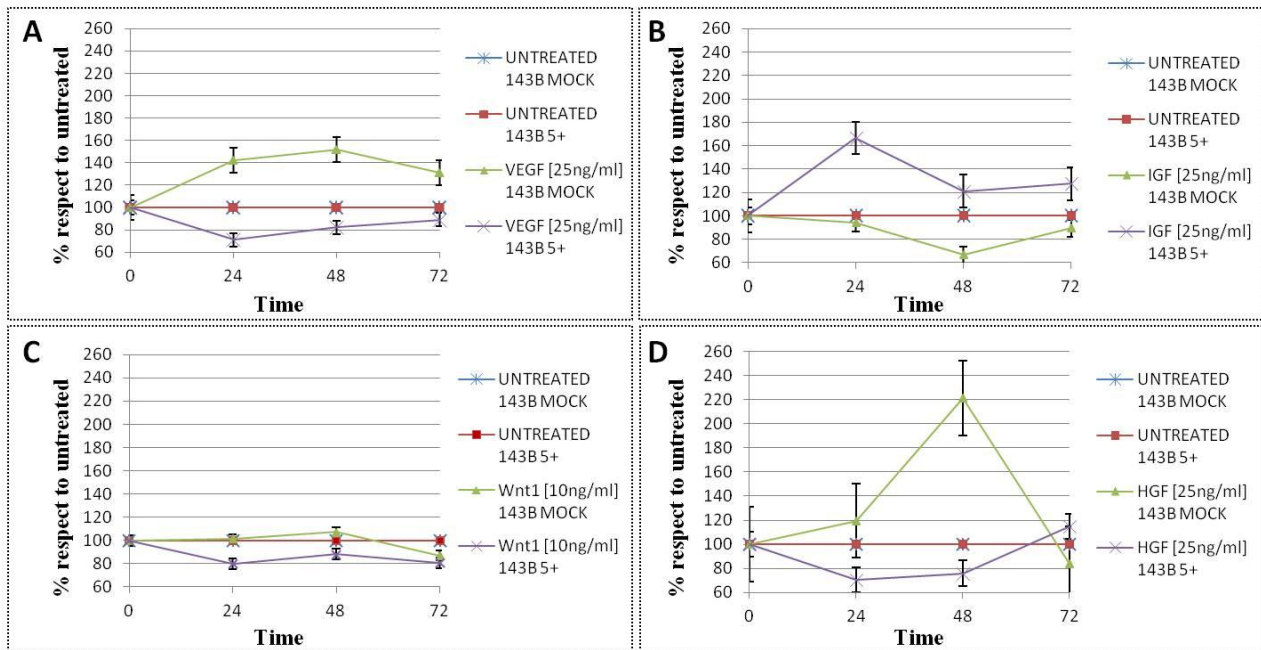


Fig. 11. Growth factor responsiveness: 143B 5+ and control cells were treated with (A): VEGF_{165aa} at the concentration of 25 ng/ml; (B): IGF at the concentration of 25 ng/ml; (C): Wnt1 at the concentration of 10 ng/ml and (D): HGF at the concentration of 25 ng/ml.

3.1.4. Inhibition of *in vivo* tumor formation

To investigate the role of GPC5 in *in vivo* tumour cell growth, nude mice were injected subcutaneously with respectively 143B WT, 143B 5+ and 143B 6+ cells. None of the mice showed any obvious clinical signs of tumor development during the first 12 days of observation following cancer cell injection. After this period, some mice showed small subcutaneous tumor masses (Fig.12) and they displayed morbidities such as hunched posture, inactivity, and shortness of breath; 33 days after the inoculation, all mice showed tumor masses and were suppressed. The analysis of tumor mass volumes, suggest that the presence of GPC5 on the surface of injected cells may reduce their capacity to induce tumor cell proliferation *in vivo* respect to controls (Fig.13,A). This ability may be specifically attributed to GPC5 expression because 143B 6+ control mice show a behaviour comparable to 143B WT.

In 143B 5+-induced tumors the number of vessels was significantly decrease more than 30% in comparison to CTRL tumors, while the percentage of vessel perfusion wasn't statistically different (Fig.13,B) suggesting a normal vessel structure and perfusion with a reduction in vascularization.



Fig. 12. Exemple of nude mice after the sacrifice; mice are injected respectively with 143B WT, 143B 5+ and 143B 6+ cell into subcutaneous space of the right flank

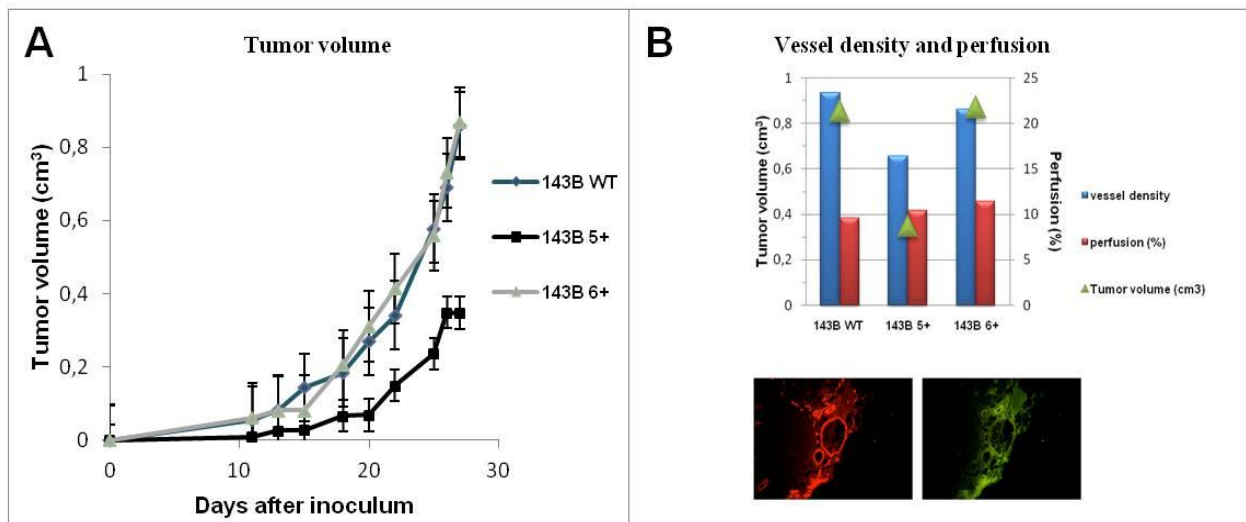
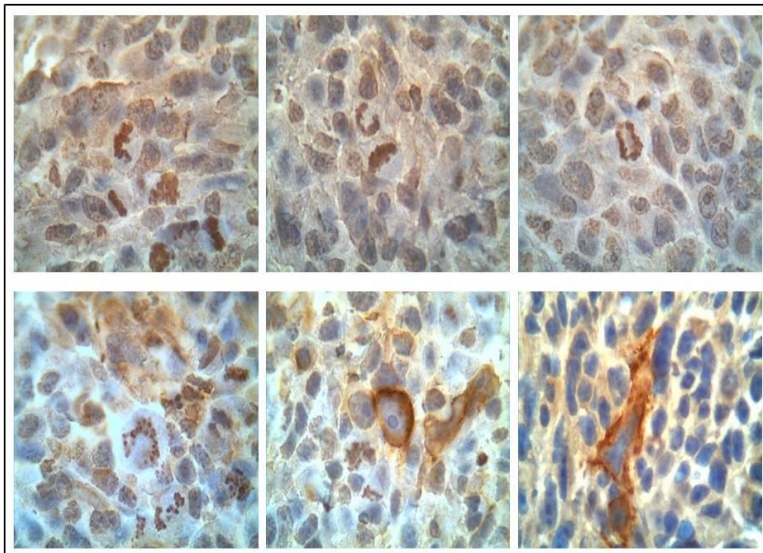


Fig.13. (A): growth curves of tumor volumes. The tumor dimensions were measured every 5 days, and the volume (V) was calculated as $V=(d)^2 \times D \times 0.52$, where d and D are respectively the short and long dimensions (centimetres) of the tumour, measured with a caliper.(B): Mann-Whitney statistical test was applied and values are mean \pm SE. In B panel is shown an immunofluorescence labelling example of anti-CD31 and Dextrane-FITC *in vivo* staining on 143B 5+ induced tumor mass OCT section by confocal microscopy; magnification 200X

After the explantation, tumor masses were treated and included in paraffin for the immunohistochemistry analysis. Immunostaining with the anti-human-GPC5 antibody (Fig.14) showed GPC5-positive cells in tumor obtained from the inoculation of 143B 5+ cells. These cells are characterized by a strong membrane positivity probably corresponding with the lipid rafts. It is also possible to recognize same positive cytosolic structure probably corresponding to the endocytic vesicles, containing GPC5 molecules. GPC5 negative masses do not present any membrane

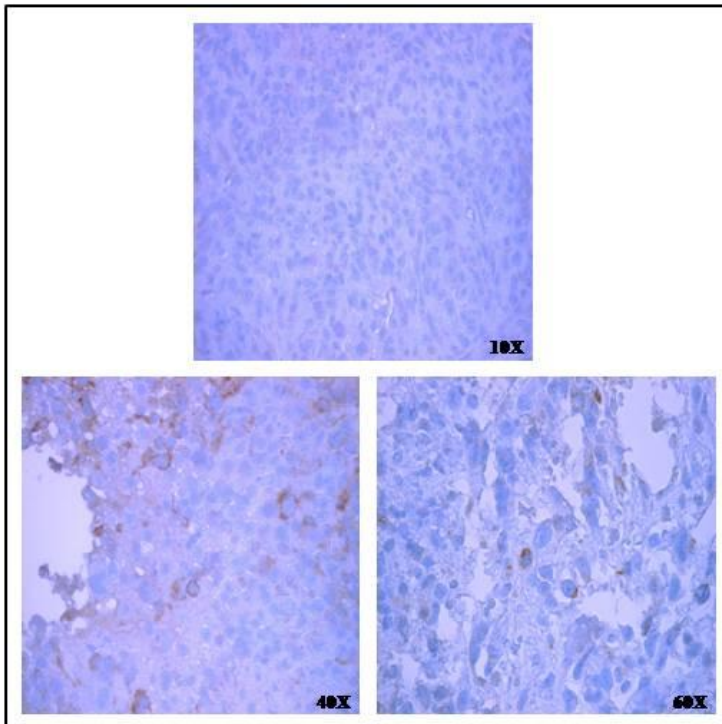
positivity but in these masses it is possible to see a nuclear positivity, probably due to atypical mitosis that are frequent in tumor cells. The presence of human GPC5+ cells is confirmed also by the staining of tumor masses with an anti-HA tag antibody. GPC5+ masses show single cell surface positive cells instead control masses are completely negative (Fig.15), confirming the anti-GPC5 staining. The presence of human cells within the tumor masses was investigated using an antibody that specifically recognizes a component of human nuclei, CENPA, that is a centromere protein component of nucleosomes. Both GPC5+ and control masses show a limited presence of human cells, without any particular difference between the two samples (Fig.16). We investigated more deeply the growth and apoptotic rate of cells within the tumors. In particular we started investigating the cell proliferation using two antibodies that specifically recognize human and murine Ki67. Ki67 is used as proliferation marker because it is a nuclear antigen present only in proliferating cells. In the second and third panels of figure 16 is possible to see that both samples show a low rate of proliferating cells (less than 10%), in either human and murine cells. To evaluate the apoptosis rate of tumors, it was used the TUNEL assay to measure the nuclear DNA fragmentation. Positive DNase treated and negative controls were used. As for proliferation marker, also in this case the immunostaining show single nuclear positive cells but no differences are detected between the GPC5+ and the control tumors (Fig.17). Another aspect that may influence the tumor development is the presence of a developed vascular network. For this reason we decided to evaluate the vessel organization using two different markers: CD31 and NG2 (Fig.18). CD31 is largely expressed on endothelial cells instead NG2 is expressed by pericytes and it may be considered a marker of the more mature vessels. For both the vascular immunostainings there were no particular structural differences between GPC5+ and control tumor masses.



143B WT

143B 5+

Fig.14. Light micrograph of mouse tumor tissues (DAB, brown): immunostaining with anti-hu/ms GPC5 antibody reveals the presence of nuclear crossreaction in control masses (first panel) and the presence of specific cytoplasmic and cell surface strong positivity in GPC5+ masses (second panel). Microscope objective 100X



143B WT

143B 5+

Fig.15. Light micrograph of mouse tumor tissues (DAB, brown): immunostaining with an anti-HA antibody confirms the presence of single positive cells in the GPC5+ tumors.. Control masses appears completely negative for the staining.

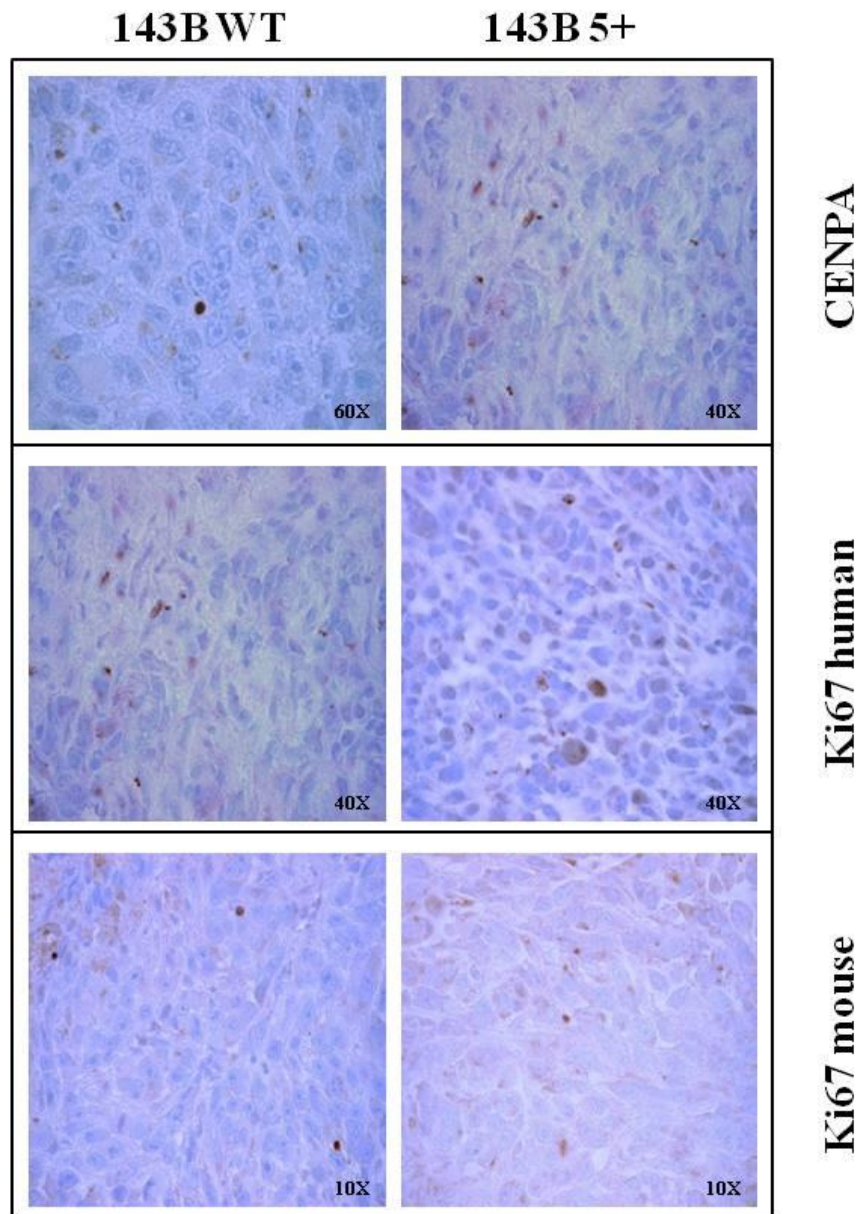


Fig.16. Light micrograph of mouse tumor tissues (DAB, brown): immunostainings with an anti-human CENPA (first panel), anti-human (second panel) and murine (third panel) Ki67 show no particular differences between tumor induced by 143B 5+ and 143B WT cells. 10 field per sample are analyzed

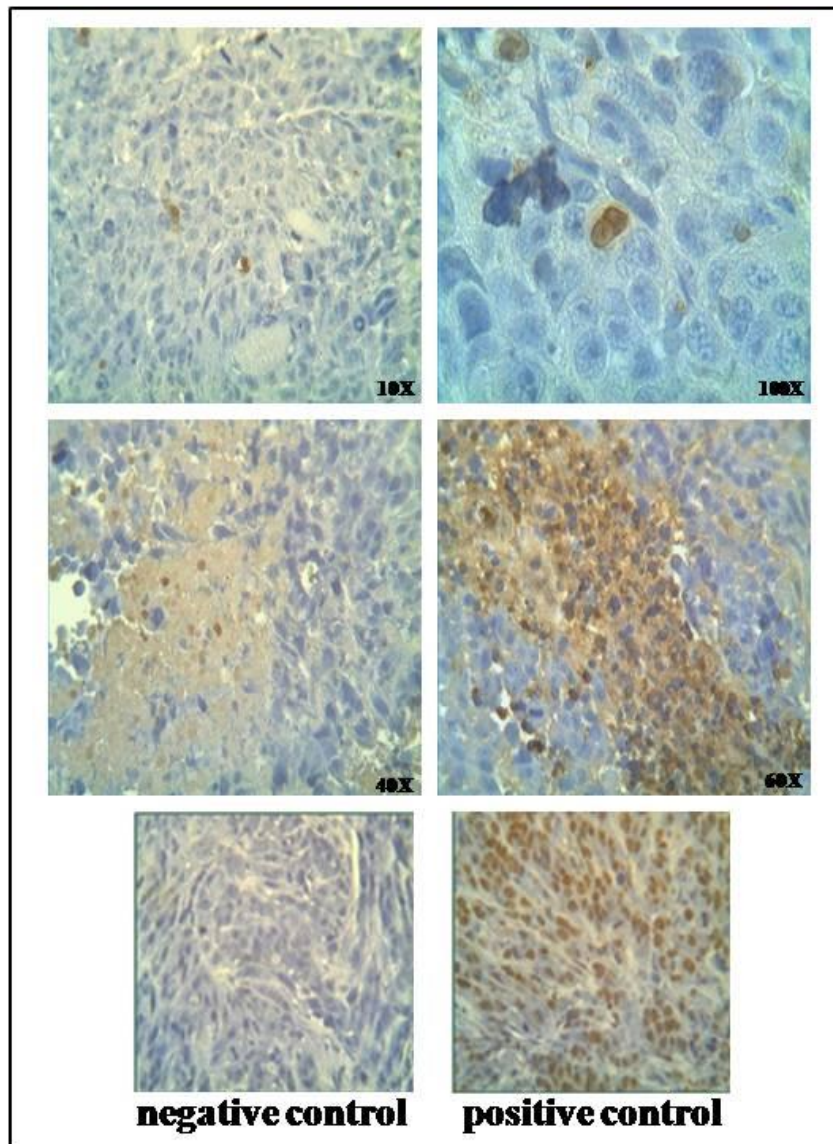


Fig.17. Light micrograph of mouse tumor tissues (DAB, brown): for the detection of apoptotic cells it is used the DeadEnd™ Colorimetric TUNEL System. In both GPC5+ and control masses it is possible to see positive cells but there are no differences between the two masses. For negative control no antibody is used and for positive control samples were treated with DNase before the antibody incubation. 10 field per sample are analyzed.

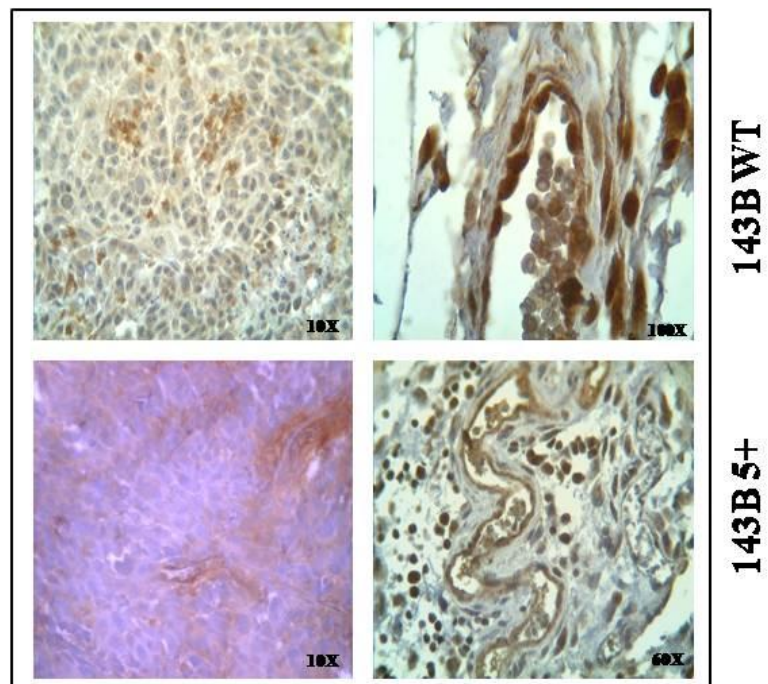
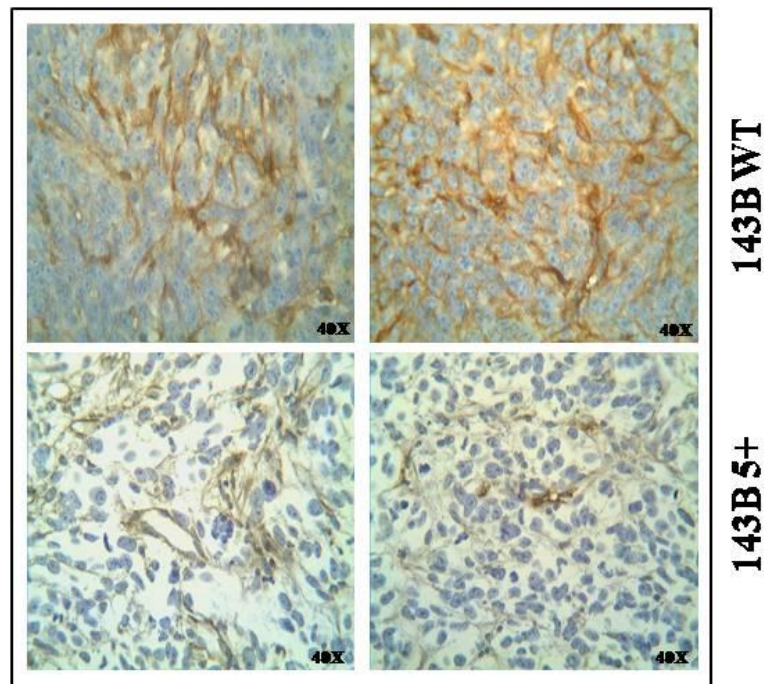


Fig.18. Light micrograph of mouse tumor tissues (DAB,brown): in the first panel it is shown the immunostaining of GPC5+ and control masses with anti-CD31 antibody. In the second panel it is shown the immunostaining with anti-NG2 antibody.

To evaluate the capacity of 143B 5+ cells to induce a distal metastasis, nude mice were subjected to intravenous inocula of 143B 5+. Three different experimental groups were inoculated with $2,5 \times 10^5$,

5×10^5 and 1×10^6 cells respectively. Mice lungs were analyzed for the detection of both macro and micro nodule formation. The simple observation of explanted lungs, showed no macronodules presence in both $2,5 \times 10^5$ and 5×10^5 inocula of 143B 5+ cells. The cellular organization of the lung of these mice seems to be not disturbed and the data were confirmed also by H&E staining of serial lung samples. As shown in figure 19, the immunostaining does not reveal any presence of metastatic formation. Differently, animals injected with 1×10^6 cells, show visible lung macronodules masses (not shown).

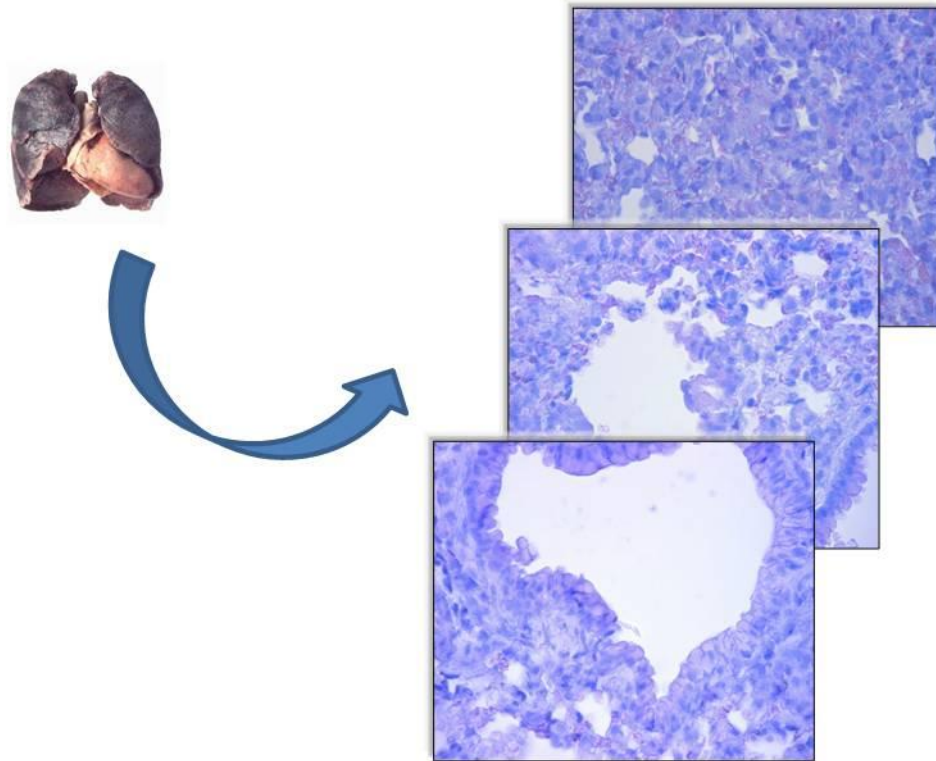


Fig.19. Example of H&E staining on a paraffin-embedded serie of sections of the lung from mice injected with $2,5 \times 10^5$ 143B 5+ cells. Microscope objective 10X

To detect the presence of human and murine GPC5 in tumor masses, RNA was extracted, retro-transcribed and amplified by PCR, using specific primers. Amplification products were visualized by 1% agarose gel electrophoresis. As controls, human RPL41 and murine rpl27bis housekeeping genes were amplified. In panels A and B of the figure 20 it is shown the detection of the two control genes. In panel C it is possible to see a weak presence of the transcript of human GPC5 amplification in all the three tumor masses analyzed; no amplifications are visible when it is used a

murine *gpc5* specific primer (Fig. 20, panel D). In all the amplifications, negative and positive controls are used.

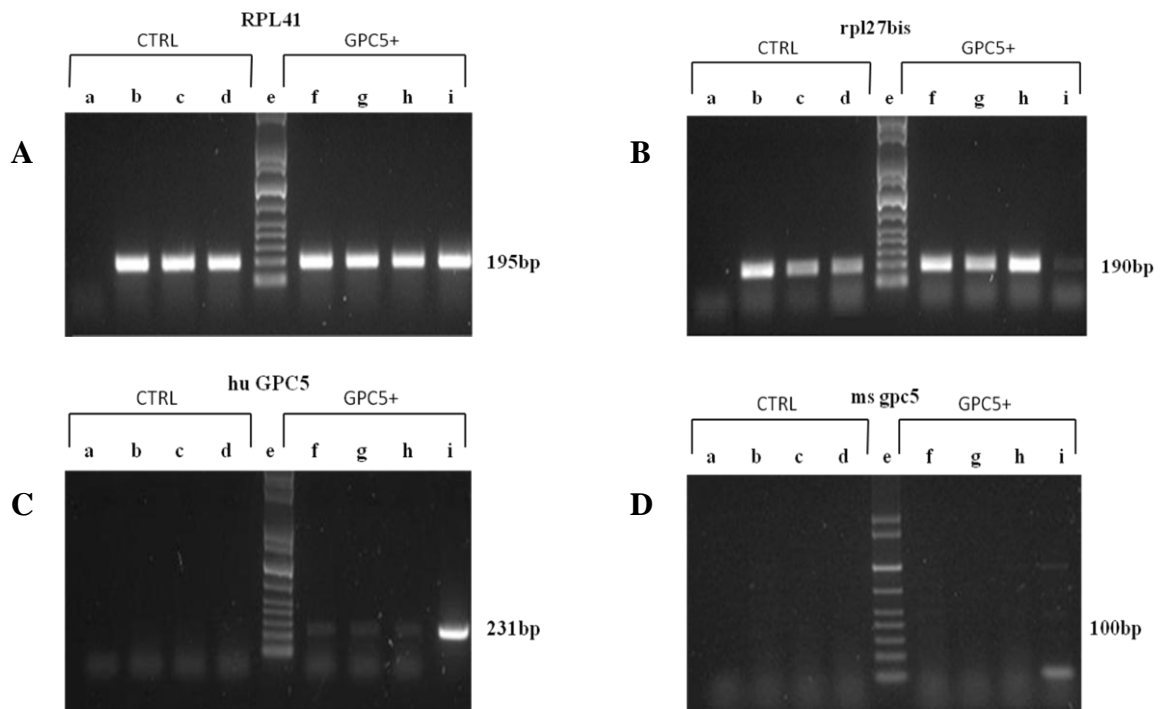


Fig. 20. Detection of GPC5 transcript in tumor masses. *a*: negative control lane; *b, c* and *d*: cDNA extracted from control masses; *e*: marker lane; *f, g* and *h*: cDNA extracted from 143B 5+ cell induced masses; *i*: positive control lane.

3.2. Immunomapping of highly sulfated heparan moieties in human tissues

3.2.1. Specificity of antibody 4D1

Antibody 4D1 was not found to react with CS-, DS- or KS-substituted PGs from a variety tissue sources and species (not shown), while combined ELISA and Western blotting indicated that it recognized a GAG chain-associated, rather than core protein-associated epitope. To ascertain this reactivity, mAb 4D1 was further screened against a panel of sulfated GAGs, including CS-A, chondroitin prepared by chemical desulfation of CS-A, DS, CS-C, CS-D, CS-E, a DS preparation particularly rich in IdoA α 1-3GalNAc (4,6-*O*-disulfate), one rich in IdoA(2-*O*-sulfate) α 1-3GalNAc(6-*O*-sulfate) and untreated low and high molecular weight and heparin treated with HNO₂ at pH 1,5 or at pH 3,9. MAb 4D1 was found to display a specific reactivity against HSs, with the highest affinity detected against intact heparin (Fig.21,A). A further comparison of the levels of reactivity of mAb 4D1 against HS variants with distinct sequences and sulfation degrees (Tab.6) showed that the antibody preferentially recognized HS chains containing highly sulfated domains (Fig.21,B) and accordingly failed to recognize both murine and human HSs perlecan (data not shown). This finding was confirmed by the loss of immunoreactivity seen against heparin digested with heparinase I or II (Fig.21,C) and partially or entirely desulfated heparin (Fig.21,D). Further hints about the structural requirements of epitope binding were provided by experiments with *N*-acetylated heparin (Fig.21,D). Comprehensively, these findings suggested that 2-*N*-, 2-*O*-, and 6-*O*-sulfate groups of the GAG were all indispensable for antigen binding and that the recognized epitope appeared to be a unique heparin/HS sequence composed of trisulfated disaccharide units of the HexUA(2S)-GlcN(NS, 6S) type.

3.2.2. The epitope of mAb 4D1 encompasses a highly sulfated tetrasaccharide repeat

To highlight its uniqueness, the specificity of mAb 4D1 was compared with that of the previously described anti-HS antibodies 10E4 and HepSS-1 using the set of diversely sulfated HS preparations. MAb 10E4 bound to all tested HS preparations and HepSS-1 preferentially reacted with HS preparations derived from the EHS tumour and characterized by a lower sulfation degree (Fig.21,B). The reactivity pattern of mAb 4D1 markedly differed from that of these mAbs since it only react with highly sulfated HS species (Fig.21,F). Interestingly, optimal recognition of such GAGs required their integrity, as shown by loss of reactivity upon heparinase fragmentation of high molecular weight heparin (Fig.21,C). Whereas HepSS-1 retained some ability to bind to completely

de-acetylated *N*-desulfated heparin and mAb 10E4 bound equally well to intact and 6-O-desulfated heparin, mAb 4D1 entirely failed to recognize de-acetylated/de-sulfated heparins. (Fig.21,D). We have comparatively assayed mAbs 4D1, 10E4 and HepSS-1 against chemically modified heparin preparations. Finally, to narrow down the mAb 4D1 epitope, we carried out competition ELISAs using immobilized heparin and a panel of HS oligosaccharide fragments of defined, progressively decreasing sizes as competitors (Fig.21,E). In agreement with the reactivity pattern observed following heparinase digestion of heparin, binding of mAb 4D1 to HS fragments was reduced by more than 50%. However, a certain inhibition of binding to intact high molecular weight heparin, could be seen with fragments encompassing a tetrasaccharide unit minimal, suggesting that the epitope required may be a tri- or tetrasaccharide and that optimal antibody recognition of HS/heparin requires a repeating highly sulfated unit of that size.

Table 6. Disaccharide composition of HS and heparin preparations (%)

Major disaccharide unit ¹	HS-BK	HS-PI	HS-BL (1M)	HS-BL (2M)	HS EHS	Human- perlecan HS	Murine- perlecan HS	Heparin PI	Heparin BL
ΔHexUA-GlcNAc	54	47	38	0	30	55	60	5	3
ΔHexUA-GlcNAc(6S)	12	12	9	2	0	6	10	4	4
ΔHexUA-GlcN(NS)	21	32	23	11	67	31	17	5	3
ΔHexUA-GlcN(NS,6S)	5	3	6	10	1	2	5	15	11
ΔHexUA(2S)-GlcN(NS)	4	2	3	4	2	4	3	4	10
ΔHexUA(2S)-GlcNAc(6S)	0	0	0	6	0	0	0	0	0
ΔHexUA(2S)-GlcN(NS,6S)	4	4	21	67	0	2	5	67	69

Abbreviations: ΔHexUA, unsaturated hexuronic acid; GlcNAc, *N*-acetyl-*D*-glucosamine; GlcN, *D*-glucosamine; 2S, 6S and NS,

2-*O*-sulfate, 6-*O*-sulfate and 2-*N*-sulfate; HS-BK, bovine kidney HS; HS-PI, porcine intestinal HS; HS-BL, bovine liver HS

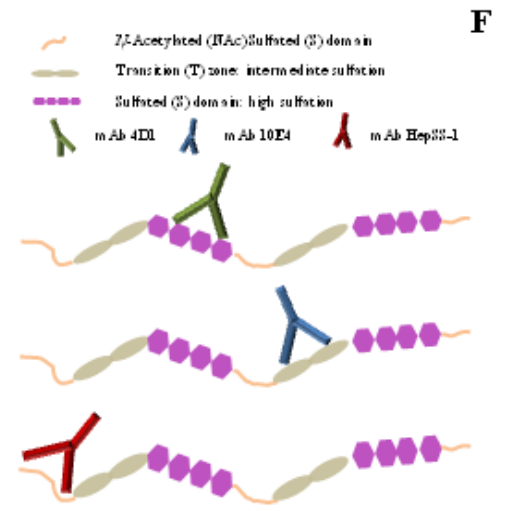
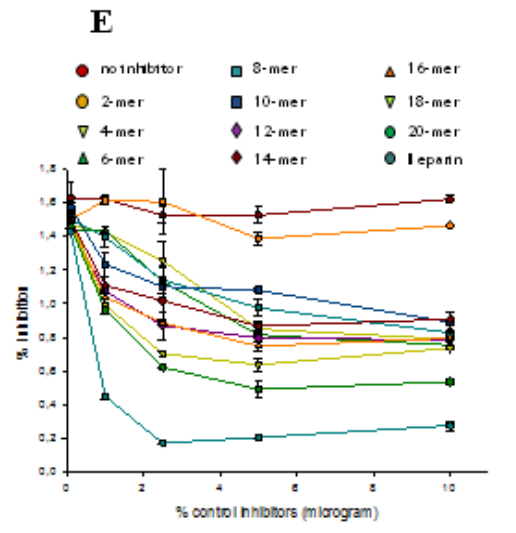
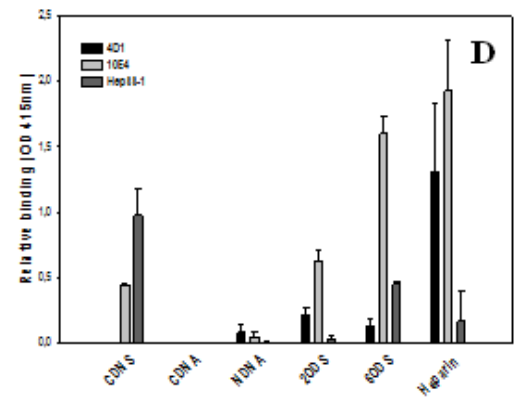
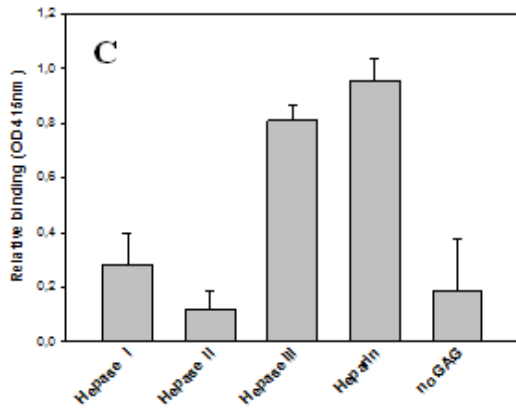
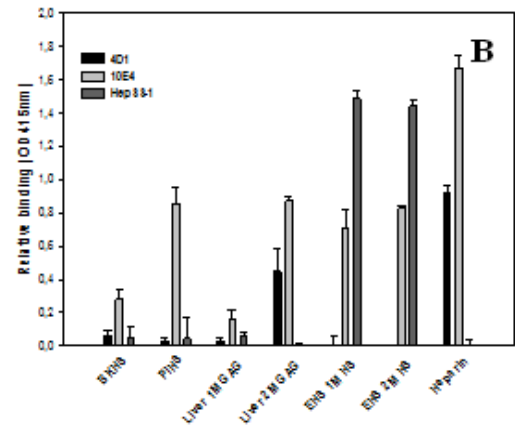
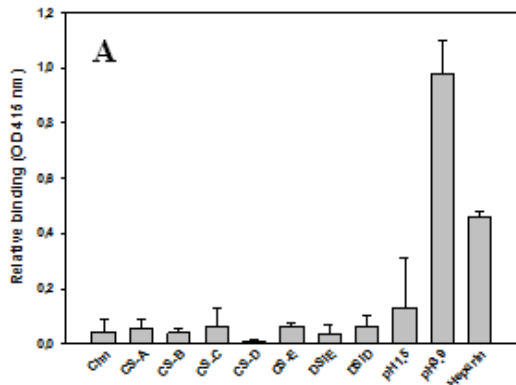


Fig.21. Reactivity of antibodies toward various GAG preparations.

Reactivity of mAb 4D1 toward various GAG preparations using an Iduron plate: chondroitin prepared by chemical desulfation of CS A (Chn); chondroitin sulphate A from whale cartilage (CS-A), dermatan sulphate from pig skin (CS-B), chondroitin sulphate C from shark cartilage (CS-C), chondroitin sulphate D from shark fin cartilage (CS-D), chondroitin sulphate E from squid cartilage (CS-E), dermatan sulphate from hag fish notochord rich in IdoA α 1-3GalNAc (4,6-*O*-disulfate) units (iE), dermatan sulfate from *Ascidia nigra* rich in IdoA(2-*O*-sulfate) α 1-3GalNAc(6-*O*-sulfate) units (iD), heparin treated with HNO₂ at pH 1,5 and at pH 3,9 (A); reactivity of the antibodies 4D1, 10E4, and HepSS1 toward HS/Hep preparations. Closed, open, and hatched columns show the reactivity of 4D1, 10E4, and HepSS-1, respectively. Bovine kidney heparan sulfate (BKHS), porcine intestine heparan sulfate (PIHS), bovine liver 1 M and 2 M HS was purified by an anion-exchange chromatography eluted with 1 M and 2 M LiCl, respectively, EHS 1 M HS and 2 M HS was purified from chondrosarcoma by an anion-exchange chromatography eluted with 1 M and 2 M LiCl, respectively (B); reactivity of mAb 4D1 toward the enzymatic digestion of heparin with Hep lyases (C); reactivity of the the antibodies 4D1, 10EA and HepSS-1 toward various chemically modified Hep preparations. CDNS, CDNA, and NDNA represent completely desulfated *N*-acetylated heparin, completely desulfated *N*-sulfated heparin, and *N*-desulfated *N*-acetylated heparin, respectively. 2ODS and 6ODS stand for 2-*O*-desulfated heparin and 6-*O*-desulfated heparin, respectively (D); inhibition of the reactivity of mAb 4D1 toward biotinylated heparin by heparin oligosaccharides at the concentration of 100 ug (E); binding site of different anti-HS antibodies (F). The results are expressed as means \pm SD.

3.2.3. Distribution of mAb 4D1-reactive HS chains in human adult tissues

To approach the tissue distribution of the HS species recognized by mAb 4D1 in the human body, we performed immunohistochemical stainings of TMAs encompassing a representation of more than 30 human tissues/organs (Fig.22) and compared these stainings with those obtained with the three previously described anti-HS antibodies, mAbs 10E4, HepSS1 and 3G10. The outcome of these mapping studies is summarized in tables 7 and 8.

Epithelia: stratified squamous epithelia of skin (Fig.22,A and 22,A), epithelia of esophagus (Fig.23,G) and cervix (data not shown) were intensely stained with mAb 4D1 and with immunoreactivity being particularly enriched in the luminal layers. The pseudo-stratified epithelium lining the bronchi (Fig.23,C) showed a prevalent positivity at the apical side, whereas glandular (secretory) elements of resting mammary glands (Fig.22,D), hepatocytes (Fig.23,E) and gastric mucosa shared a diffuse cytoplasmic staining. Absorptive cells of the colon had a prevalent luminal distribution of 4D1-reactive HS chains (Fig.22,G), whereas glandular epithelium of the uterus, the epithelium of the prostate, podocytes attached to glomerular capillaries of the kidney, and lung epithelium showed a weak immunoreactivity. Mucous cells and basement membranes were consistently negative in all tissues analyzed. The immunoreactive pattern of mAb 4D1 largely mirrored that of mAb 10E4 (Tab.9), which strongly labelled basement membranes, but failed to label the epithelial cells themselves (Fig.22,B).

Vascular structures: the endothelial cells of vascular structure resulted strongly positive (Fig.26) while they appeared no or weakly positive for the immunostaining with mAb 10E4 (data not shown).

Connective tissues: In dense connective tissues of both regular, such as that of the resting mammary gland (Fig.22,D), and irregular type, such as those of the skin, a marked positivity was noted for mAb 4D1, while mAb 10E4 more electively stained fibroblasts (Fig.22,E). In loose connective tissues, such as for example that surrounding mucous glands in the bronchus, there was similarly an intense expression of 4D1-reactive HS variants and a lack of 10E4-reactive ones.

Muscle tissues: In skeletal muscle and dermis mAbs 10E4 and HepSS1 gave weaker and less diffuse staining patterns than mAb 4D1 and the same applied to mAb HepSS1 in irregular dense connective tissues. Notable was also the weak (skeletal muscle) to absent staining (cardiac and smooth muscle) for mAb 4D1 of muscle fibers, whereas mAbs 10E4, and HepSS1 gave both positive reactions in these tissue structures. The smooth muscle of arteries showed a marked positivity for mAb 4D1 (Fig. 22,N) and a basal membrane positivity for mAb 10E4 (Fig. 22,O).

Nervous and endocrine tissues: In the CNS there was a very weak staining for mAb 4D1 in the grey and white matters (Fig.24,A) of the cortex and only a nuclear positivity in the granular layer of cerebellum was noted as exclusive of this antibody since it was not seen with other anti-HS mAbs. Purkinje fibers (Fig.24,B) and peripheral nerve (Fig.24,G). Endocrine cells, connective tissues of neuroendocrine glands, adrenal glands and thyroid, showed a weak positivity, whereas in the pancreas both exocrine and endocrine (Fig.24,D) components exhibited an intense immunolabelling. No such staining patterns were observed with mAbs 10E4 and HepSS-1. Finally, lymph nodes and spleen had many 4D1-positive cells showing a preferential nuclear staining. While connective tissue of the spleen showed some weak 4D1 positivity, it was much more intensely labeled by mAbs HepSS1 and 10E4.

Specificity of mAb 4D1 in situ staining: To ascertain the nuclear specificity of the staining (i.e. whether it was due to an unspecific binding of the antibody to DNA) we predigested sections with DNase I. No difference was observed with and without pre-digestion (Fig.24,A and B). Finally we used competition experiments to confirm the immunostaining data; for this purpose we preincubate samples with heparin. As expected there was no staining (Fig.24,C and D).

Consistently with the solid-phase binding data (Fig.21,C), all observed in situ staining patterns were strongly susceptible to pre-digestion of the sections with heparinase I and II, but were unaffected by heparinase III digestion (Fig.23)

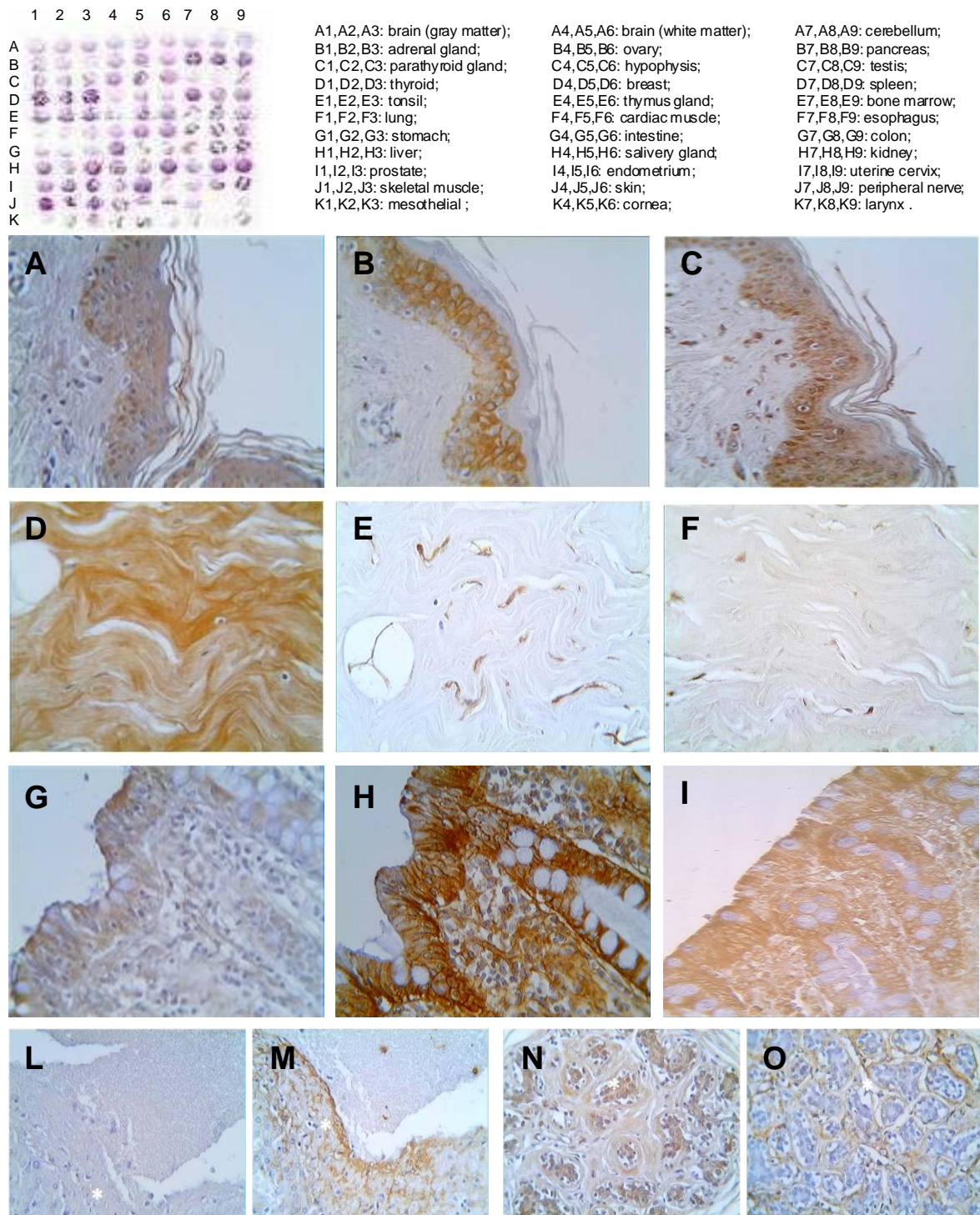


Fig.22. light micrographs of tissue microarray-Immunohistochemical assay (DAB, brown), X400. Human normal organ TMAs (Biomax, Inc., Rockville, US). (A): keratinized stratified squamous epithelia of the skin with mAb 4D1, (B) with mAb 10E4 and (C)with mAb HepSS1; (D): regular dense connective of resting mammary glands with mAb 4D1, (E) with mAb 10E4 and (F) with mAb HepSS1; (G): absorptive and goblet cells (arrow) of colon with mAb 4D1, (H) with mAb 10E4 and (I)with mAb 3G10; (L): smooth muscle cells under the vascular endothelium with 4D1 and (M)with 10E4; (N): glandular elements of resting mammary glands with mAb 4D1 and (O)with mAb 10E4.

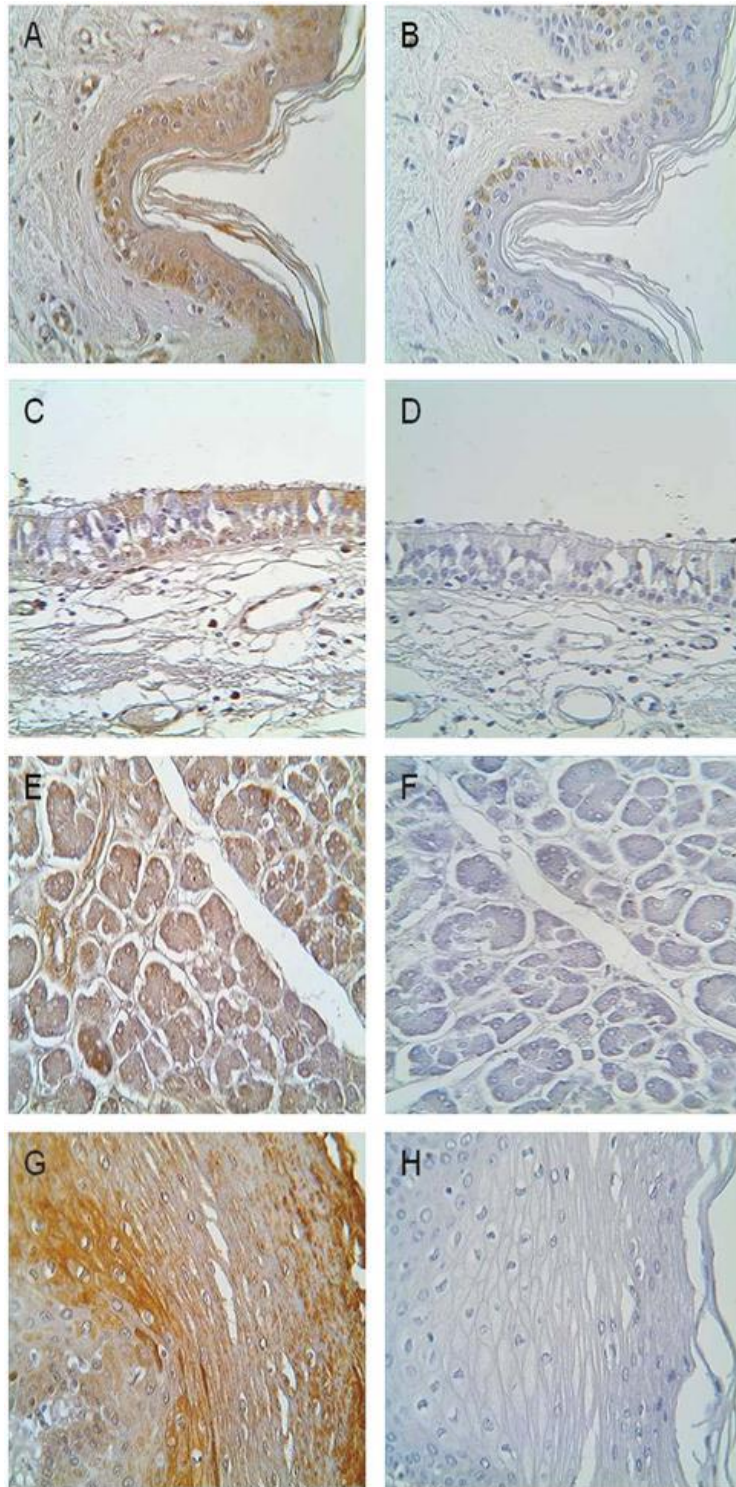


Fig.23. light micrographs of tumoral tissue microarray- Immunohistochemical assay with mAb 4D1(DAB, brown), X400.

(A): keratinized stratified squamous epithelia of the skin without any treatment and (B)after digestion with Heparinase III; (C): pseudo-stratified epithelium lining of bronchus without any treatment and (D)after digestion with Heparinase II; (E): hepatocytes of liver without any treatment and (F)after digestion with Heparinase I; (G): stratified squamous epithelium lining of esophagus without any treatment and (H)after digestion with Heparinase I

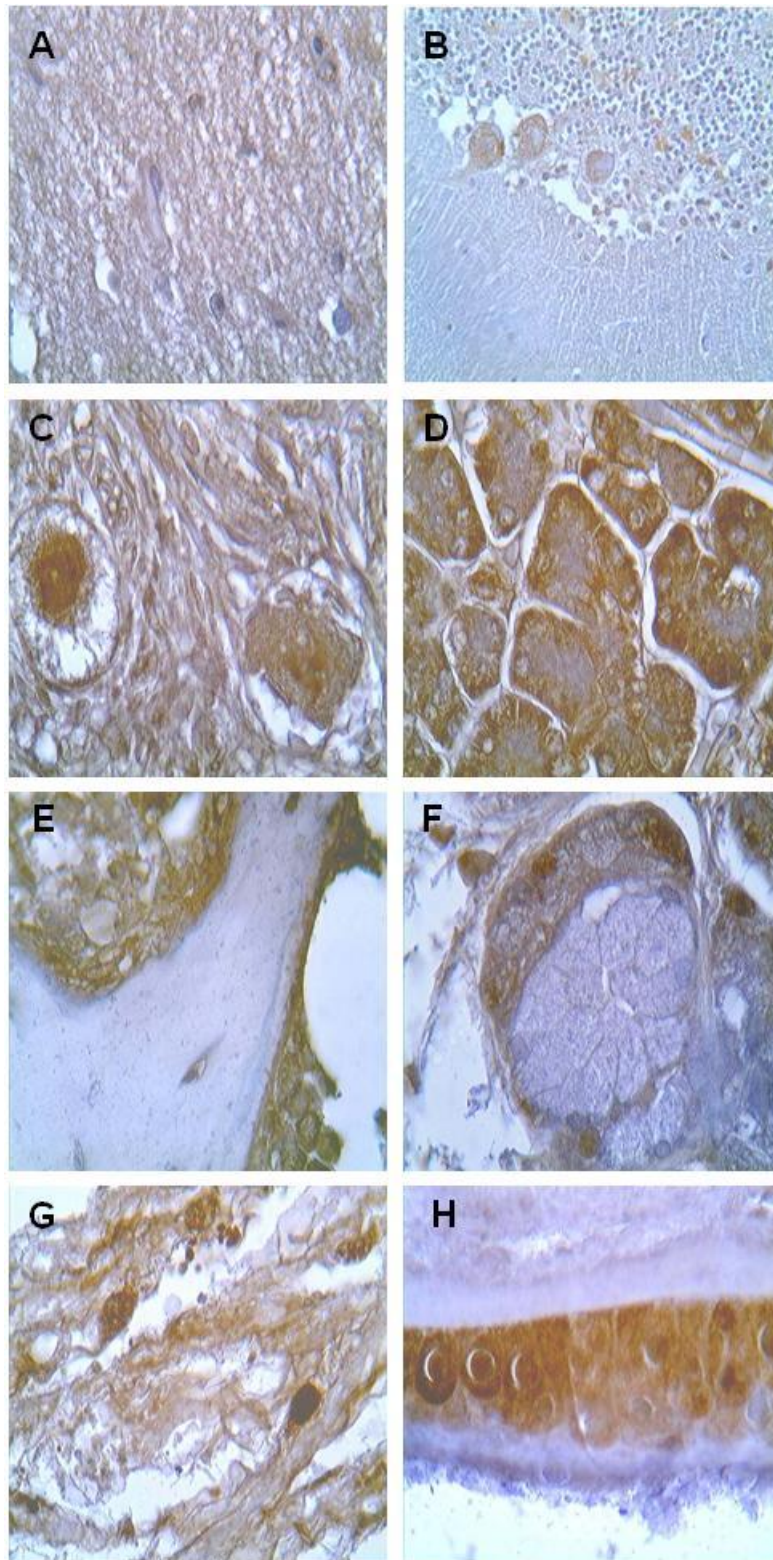


Fig. 24. light micrographs of tissue microarray - Immunohistochemical assay with mAb 4D1 (DAB, brown), X100.

(A): cerebral white matter; (B): purkinje fibers; (C): ovarian follicles; (D): endocrine cells of pancreas; (E): bone marrow; (F): salivary gland; (G): peripheral nerve; (H): cornea.

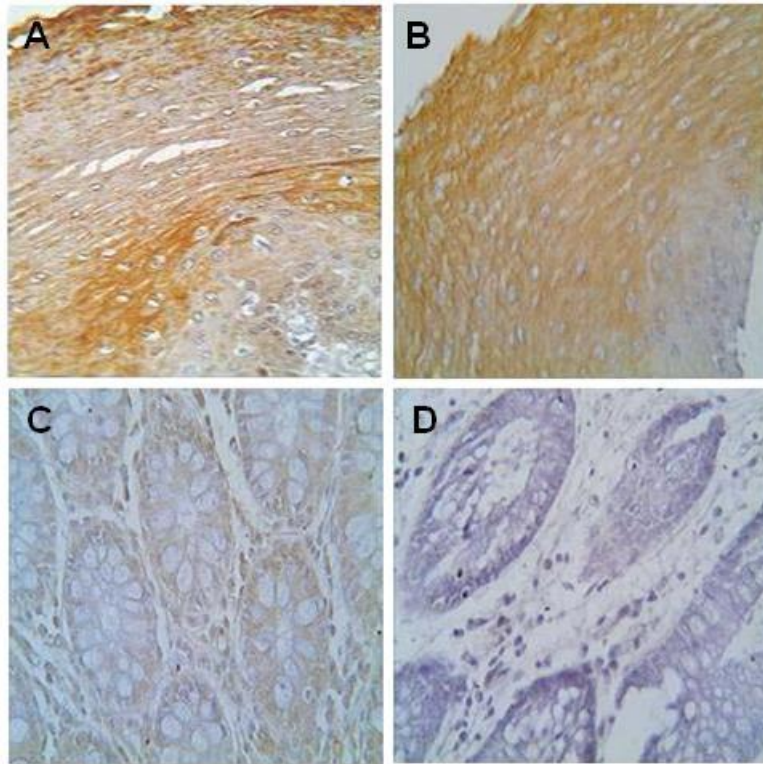


Fig.25. light micrographs of tissue microarray- immunohistochemical assay with mAb 4D1 (DAB, brown), X400.

(A): stratified squamous epithelium lining of esophagus without any treatment and (B) with DNase; (C): absorptive and goblet cells of colon with mAb 4D1 and (D)with mAb 4D1 diluted in presence of heparin.

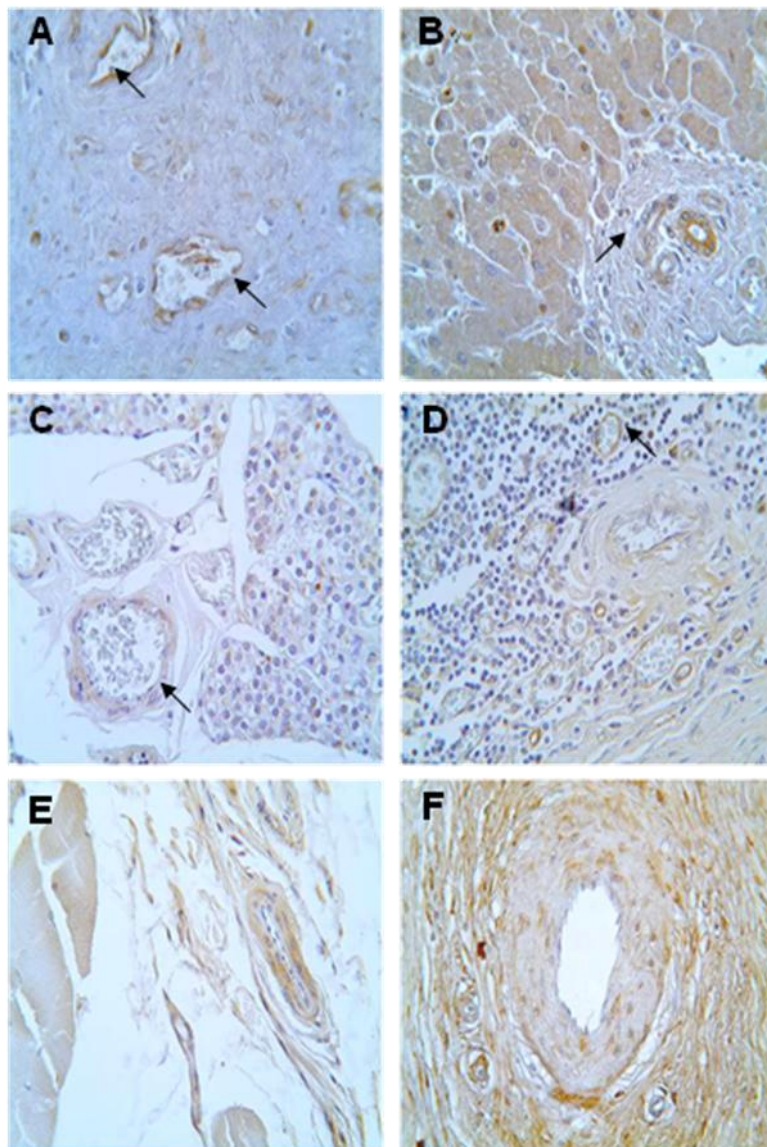


Fig.26. light micrographs of blood vessels- immunohistochemical assay with mAb 4D1 (DAB, brown),X400.

(A): capillaris of uterine cervix; (B): hepatic artery and portal vein of portal canal; (C): medium-size venules of parathyroid; (D): capillaries and a small arteriola of spleen; (E): arteriola of skeletal muscle; (F): a small artery.

Table 7. Comprehensive distribution map of HSs recognized by mAb 4D1 in healthy tissues

Organ	Number of elements*	Staining intensity [#]
Central nervous system	6	
Hematopoietic	4	
Liver and pancreas	3	
Digestive tract	13	
Respiratory system	5	
Cardiovascular system	2	
Female tissues	8	
Male tissues	5	
Urinary tract	4	
Skin and soft tissues	5	
Endocrine tissues	4	
Special senses	2	

*): number of cell types with expression/staining compared to the total number of analyzed cell types;

[#]): colour coding indicating staining intensity defined as:

- strong
- moderate
- weak
- negative

Table 8. Comparison of the immunoreactivity patterns of mAbs 4D1, 10E4, HepSS-1 and 3G10 on human normal tissues

Tissue/organ	Antibody							
	4D1		10E4		HepSS-1		3G10	
	Staining intensity	Cellular localization	Staining intensity	Cellular localization	Staining intensity	Cellular localization	Staining intensity	Cellular localization
Cerebral cortex:								
white matter	+	C	-	n.a.	n.a.	n.a.	n.a.	n.a.
gray matter	+	C	-	n.a.	n.a.	n.a.	n.a.	n.a.
Cerebellar cortex:								
granular layer	+ / ++	C	-	n.a.	n.a.	n.a.	n.a.	n.a.
Purkinje cell layer	+ / ++	C	-	n.a.	n.a.	n.a.	n.a.	n.a.
molecular layer	+	C	-	n.a.	n.a.	n.a.	n.a.	n.a.
Peripheral nerves	++ / +++	C/N	n.a.	n.a.	n.a.	n.a.	n.a.	n.a.
Cardiac muscle	++	C	- / ++	BM	n.a.	n.a.	n.a.	n.a.
Blood vessels	+++	C/N	+++	C	++	n.a.	++ / +++	C
Spleen	++ / +++	C	-	n.a.	+	C/N	n.a.	n.a.
Lung	+ / ++	C/N	-	n.a.	n.a.	n.a.	n.a.	n.a.
Larynx:								
mucous secreting cells	-	n.a.	n.a.	n.a.	n.a.	n.a.	n.a.	n.a.
epithelium	++ / +++	C/N	n.a.	n.a.	n.a.	n.a.	n.a.	n.a.

submucosa	++/+++	C	n.a.	n.a.	n.a.	n.a.	n.a.	n.a.
cartilage	-	n.a.	n.a.	n.a.	n.a.	n.a.	n.a.	n.a.
Salivary gland:								
mucous secretory unit	-	n.a.	-	n.a.	n.a.	n.a.	n.a.	n.a.
serous secretory unit	++	C/N	-	n.a.	n.a.	n.a.	n.a.	n.a.
Esophagus:								
epithelium	++	C	-	n.a.	n.a.	n.a.	+++	C
basal lamina	-	n.a.	+	BM	n.a.	n.a.	-	n.a.
muscularis mucosa	+ / ++	N	-	n.a.	n.a.	n.a.	++	C
Stomach:								
epithelium	++	C/N	-	n.a.	n.a.	n.a.	++	C
mucosa	- / +	C	++	BM	n.a.	n.a.	++	C
sub mucosa	++	C	++	BM	n.a.	n.a.	n.a.	n.a.
Small intestine:								
epithelium	++	C/N	-	n.a.	n.a.	n.a.	+++	C
sub mucosa	+	C	++	C	n.a.	n.a.	-	n.a.
muscularis mucosa	+	C	-	n.a.	n.a.	n.a.	-	n.a.
Colon:								
epithelium	++ / +++	C/N	+++	C	n.a.	n.a.	+++	C/N
lamina propria	+	C	+++	C	n.a.	n.a.	++ / +++	C/N
Liver:								
hepatocytes	+++	C/N	-	n.a.	n.a.	n.a.	++	C
intralobular structures	+++	C	-	n.a.	n.a.	n.a.	+++	C
Pancreas	+++	C	+++	BM	n.a.	n.a.	++ / +++	C
Kidney:								

renal glomeruli	-	n.a.	-	n.a.	++	C/N	n.a.	n.a.
podocytes	-/+	C/N	-	n.a.	+++	C/N	n.a.	n.a.
Bowman's capsule	-	n.a.	-	n.a.	+++	C/N	n.a.	n.a.
ducts	++	C	-	n.a.	+++	C/N	n.a.	n.a.
Testis:								
Leydig's cells	++/+++	C	++	C	n.a.	n.a.	n.a.	n.a.
seminiferous tubule	++	C	++	C	n.a.	n.a.	n.a.	n.a.
Prostate gland:								
mucosal gland	++	C	-	n.a.	n.a.	n.a.	n.a.	n.a.
mast cells	+++	C	-	n.a.	n.a.	n.a.	n.a.	n.a.
connective capsule	++	C	-	n.a.	n.a.	n.a.	n.a.	n.a.
Ovary:								
follicle	+++	N	-	n.a.	-	n.a.	n.a.	n.a.
stromal cells	++	N	-	n.a.	+	N	n.a.	n.a.
Uterus:								
endometrium	++/+++	C	-	n.a.	n.a.	n.a.	n.a.	n.a.
submucosa	++	C	++	BM	n.a.	n.a.	n.a.	n.a.
muscularis mucosa	++	C	+	BM	n.a.	n.a.	n.a.	n.a.
uterine cervix	++/+++	C	n.a.	n.a.	n.a.	n.a.	n.a.	n.a.
Breast:								
fibroblasts	+++	C	+++	C/N	+++	N	n.a.	n.a.
connective tissue	++/+++	C/N	+++	BM	-	n.a.	n.a.	n.a.
C-cells of thyroid gland	+++	N	n.a.	n.a.	++	N	n.a.	n.a.
Parathyroid gland	+++	C/N	n.a.	n.a.	n.a.	n.a.	n.a.	n.a.
Thymus	-/+++	C	n.a.	n.a.	n.a.	n.a.	n.a.	n.a.

Tonsil	-/+++	C/N	n.a.	n.a.	n.a.	n.a.	n.a.	n.a.
Hypophysis	-/++	C	n.a.	n.a.	n.a.	n.a.	n.a.	n.a.
Adrenal gland	+++	C	+++	C/N	n.a.	n.a.	n.a.	n.a.
Skin:								
epidermis	++	C	n.a.	n.a.	+++	C	n.a.	n.a.
dermis	-	n.a.	n.a.	n.a.	-	n.a.	n.a.	n.a.
fibroblasts	-	n.a.	-	n.a.	+++	N	n.a.	n.a.
Smooth muscle	+/++	C	n.a.	n.a.	n.a.	n.a.	n.a.	n.a.
Skeletal muscle	+/++	C/N	-	n.a.	+++	C/N	n.a.	n.a.
Bone marrow	++/+++	C	n.a.	n.a.	n.a.	n.a.	n.a.	n.a.
Eye:								
epithelium	+++	N	n.a.	n.a.	n.a.	n.a.	n.a.	n.a.
connective tissue	-	n.a.	n.a.	n.a.	n.a.	n.a.	n.a.	n.a.

3.3. Immunomapping of keratan sulphates

In collaboration with the group Seikagaku biobusiness corporation LAL & Biochemicals Marketing Department and Research we studied the characteristic of KS linked to aggrecan, through SDS techniques (Fig.27,A and B) and we evaluated the linkage of the monoclonal antibody 373E1 with KS through TEM photograph (Fig.27,C). Studies on this mAb was performed in comparison with those of another specific known antibody against intact keratan sulphate chains, mAb BCD4 (Seikagaku).

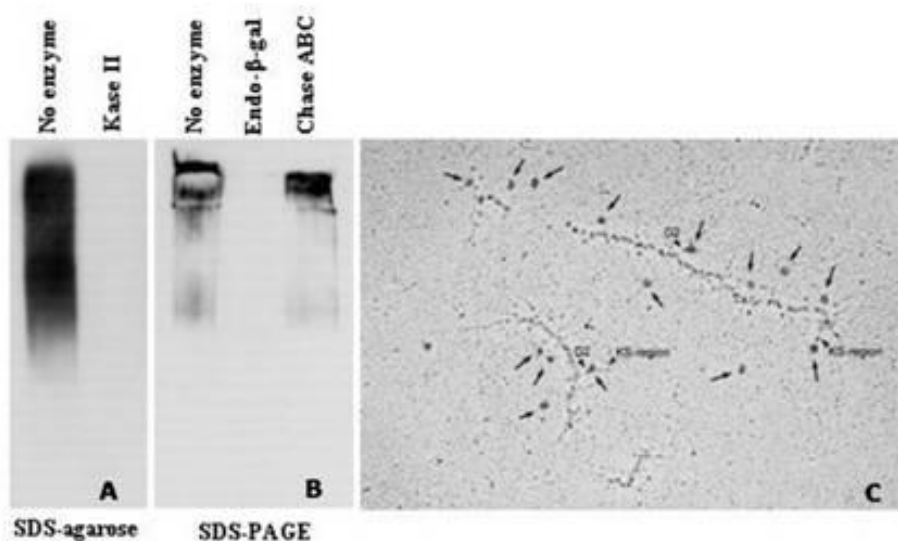


Fig.27. (A): run on a 5% agarose gel of KS moieties without digestion and after digestion with Keratanase II;enzimatic digestion degrades all KS moieties; (B): SDS-PAGE on gel with gradient of 3%-8% of KS moieties without digestion and after two different enzymatic digestion: with Endo- β .galactosidase and with Chondroitinase ABC. Gel gradient detain all big moieties like no-digested aggrecan, while Endo- β .galactosidase cut all moieties. Cheratanase ABC is used for a control digestion; (C): molecules of aggrecan showed by TEM. The core of aggrecan is compounded of uronic acid while KS-regions they are presents toward the outside of aggrecan. Arrows indicate the 373E1 moieties; part of them are linked to KS-regions while an other part of them are not-linked

3.3.1. Definition of the specificity of the anti-KS mAb 373E1

Characterization of mAb 373E1 was performed. Primarely 373E1 and BCD4 reactivity was tested on different GAG preparation, suggesting that both the antibodies specifically recognize KS moieties (Fig.28,A). The specificity of binding was examine by digestion of biotinylated-KS with Keratanase II (Fig.28,B). MAb 373E1 bound to non-treated biotinylated-KS and did not bind to digested-biotinylated-KS the same as mAb BCD4. These data confirmed that 373E1 specifically recognized KS. Reactivity of 373E1 and BCD4 to keratan sulphate from bovine cornea (KS(BC))

and keratan polysulphate from shark (KPS-1) were compared with inhibition assay. BCD4 reacted stronger with KPS-1 than KS(BC) (Fig.28,D). On the other hand, 373E1 reacted stronger with KS(BC) than KPS-1(Fig.28,C) and reactivity of 373E1 to KPS-1 was very weak. Reactivity of 373E1 and BCD4 to some NaCl-eluted fractions of anion-exchange column chromatography in KS(BC) and KPS-1 were compared in the same as above. BCD4 basically reacted stronger with higher NaCl fraction in KPS-1 and KS(BC). It is thought from these results that activity of BCD4 is mainly dependent on sulphation in KS. On the other hand, 373E1 did not react with any KPS fractions and react with higher salt fractions of KS(BC). It is presumed from these results that activity of 373E1 is dependent on not only sulphation but also structures in KS and 373E1 may strictly recognize any unique structures in KS.

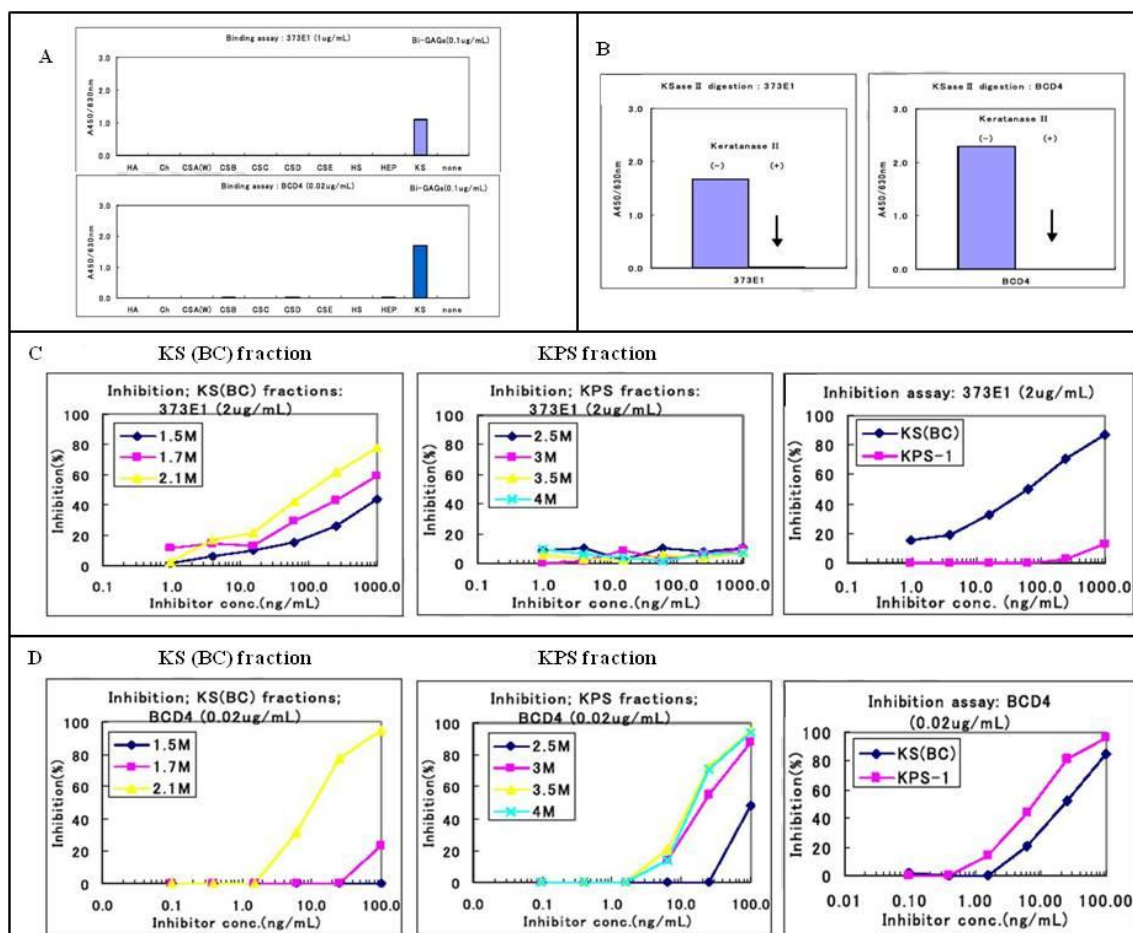


Fig.28. (A): binding test for 373E1 and BCD4 to various GAG preparations, HA: Hyarulonic acid Ch: Chondroitin CSA, (W): Chondroitin sulfate A from whale cartilage, CSC: Chondroitin sulfate C from shark cartilage, CSD: Chondroitin sulfate D from shark cartilage, CSE: Chondroitin sulfate E from squid cartilage, HS: Heparan sulfate from bovine kidney, HEP: Heparin from pig intestine. (B): specificity of the binding of 373E1 and BCD4 with and without digestion of Bi-KS with Keratanase III. (C): inhibition assays of NaCl-eluted fractions of KS(BC) and KPS in anion-exchange column chromatography for mAb 373E1. (D): inhibition assays of NaCl-eluted fractions of KS(BC) and KPS in anion-exchange column chromatography for mAb BCD4. KS(BC): keratan sulfate from bovine cornea; KPS-1: keratan polysulphate from shark.

3.3.2. Immunohistochemical staining patterns

MAb 373E1 may be used for both immunochemical and immunofluorescence staining (Fig. 29), but we performed the KS mapping through the classical immunohistochemical staining. The assays were performed to evaluate the distribution pattern of both mAbs 373E1 and BCD4. Tissue microarray were employed to evaluate the immunostaining of antibodies in many human normal tissues

Epithelial tissues: immunohistochemistry of epithelial tissues with mAb 373E1 (Fig.30) revealed that pseudo-stratified epithelium (Fig. 30,A) was negative instead a very weak positivity of the apical portion of the cells. Both absorptive and goblet cells of colon (Fig. 30,B) and the gastric mucosa (Fig. 30,C) showed a more intense cytoplasmatic expression for the epitope recognized by the mAb; mucus resulted always negative. Stratified squamous epithelia, for example those of the skin, of the esophagus or of the cervix (data not shown). and basal membrane (data not shown), were also negative. Epithelial cells of the liver (Fig. 30,E), lung (Fig. 30,F), prostatic and uterine glandular epithelium, and podocytes of kidney (Fig. 30,D), showed a weak immunoexpression.

The immunoexpression of mAb BCD4 (Fig. 31) was positive in stratified squamous epithelia of the skin (Fig. 30,A) and in absorptive and goblet cells of colon (Fig. 30,B). In colon mucus was negative while lumen of mucosal cells were positive. Glandular epithelium of uterus (Fig. 30,C) showed a strong coloration on the apical layer, and the same is for cuboidal cells that forms kidney proximal ducts (Fig. 30,D), while the rest resulted negative.

Connectival tissues: Both dense and loose connective (Fig.32) showed a weak diffuse positivity with mAb 373E1, as shown in of dense regular connective of resting mammary gland (Fig. 32,A) and loose connective surrounding mucous glands of the bronchus (Fig. 32,C).

Immunoexpression for BCD4 in connectival tissues was the same showed for 373E1 (Fig. 32.) with a weak diffuse positivity both in dense (Fig. 32,B) and loose (Fig. 32,D) connective.

Muscular tissues: In figure 32, microphotographs shows a very pale immunoexpression in a skeletal muscle (Fig. 32,E). All the other muscular tissues, smooth and cardiac, resulted completely negative for this antibody (data not shown).

Immunoexpression of muscle tissues was a little more intense for mAb BCD4 (Fig.32,F) compared to that for mAb 373E1. As for 373E1 this positivity is diffused and is the same for all types of muscle (in figure 32, F is shown the skeletal muscle while the cardiac and smooth muscle are not shown)

Nervous tissues: Both white matter (Fig.33,A) and grey matter (Fig.33,C) of cerebellum were negative for 373E1, while immunoeexpression of BCD4 in nervous tissues (Fig.33,B and D) was very strong.

Endocrine tissue: microphotographs in figure 33, E showed a pale immunoeexpression for mAb 373E1 in pancreatic cells, while the same cells resulted negative for mAb BCD4 (data not shown). The other neuro-endocrine tissues, such as thyroid and adrenal gland resulted negative with both antibodies (data not shown).

Enzimatic digestion: enzymatic digestion of different tissues with Endo- β -galactosidase and Keratanase II demonstrated different results. In some tissues the enzymatic digestion eliminated totally the immunoeexpression, while in other tissues the immunopositivity was not completely eliminated. The studies about this treatment will be continue to have more precise data.

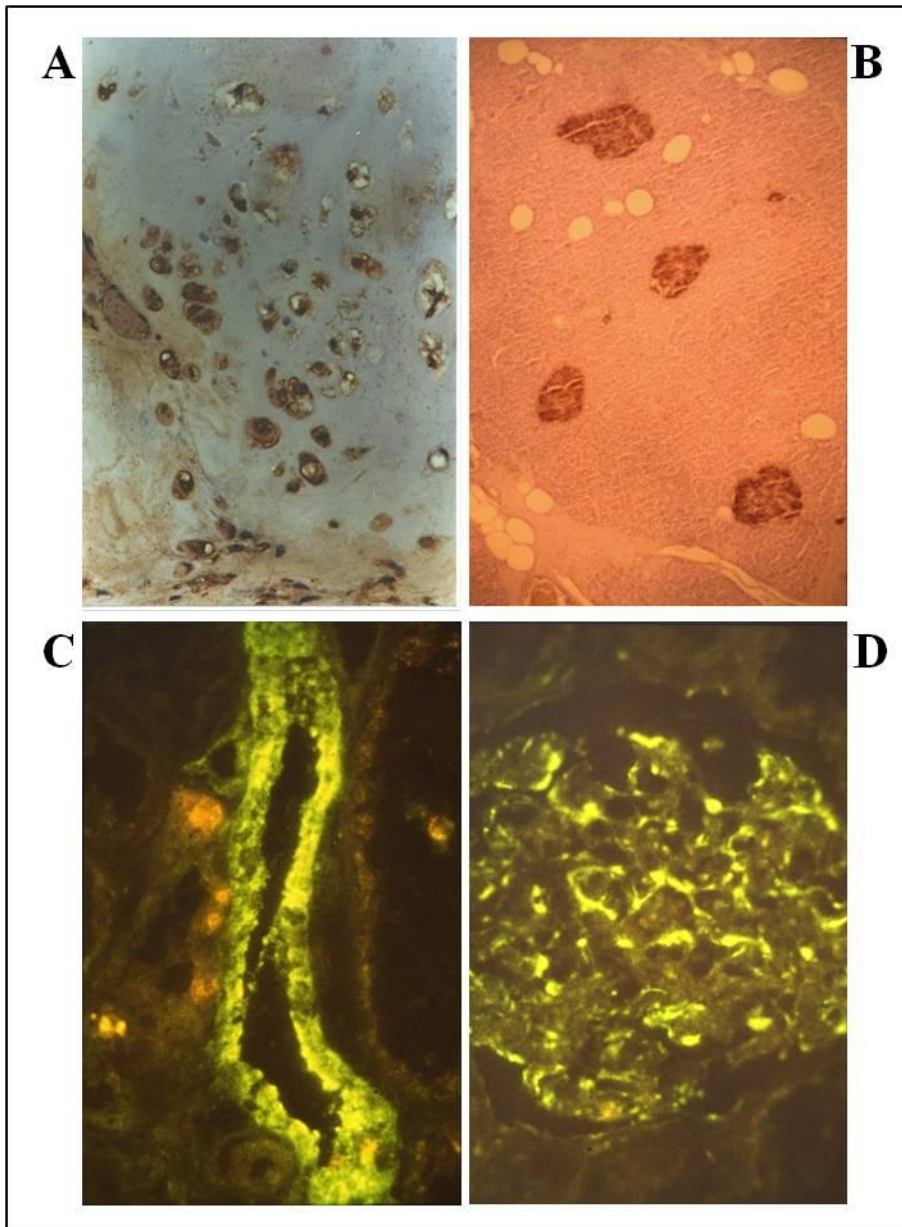


Fig. 29. light micrographs of tissue microarray with mAb 373E1. Immunohistochemical staining of (A) human adult cartilage and (B) fetal pancreas, immunofluorescence staining of (C) human adult duct of kidney and (D) a glomerulus.

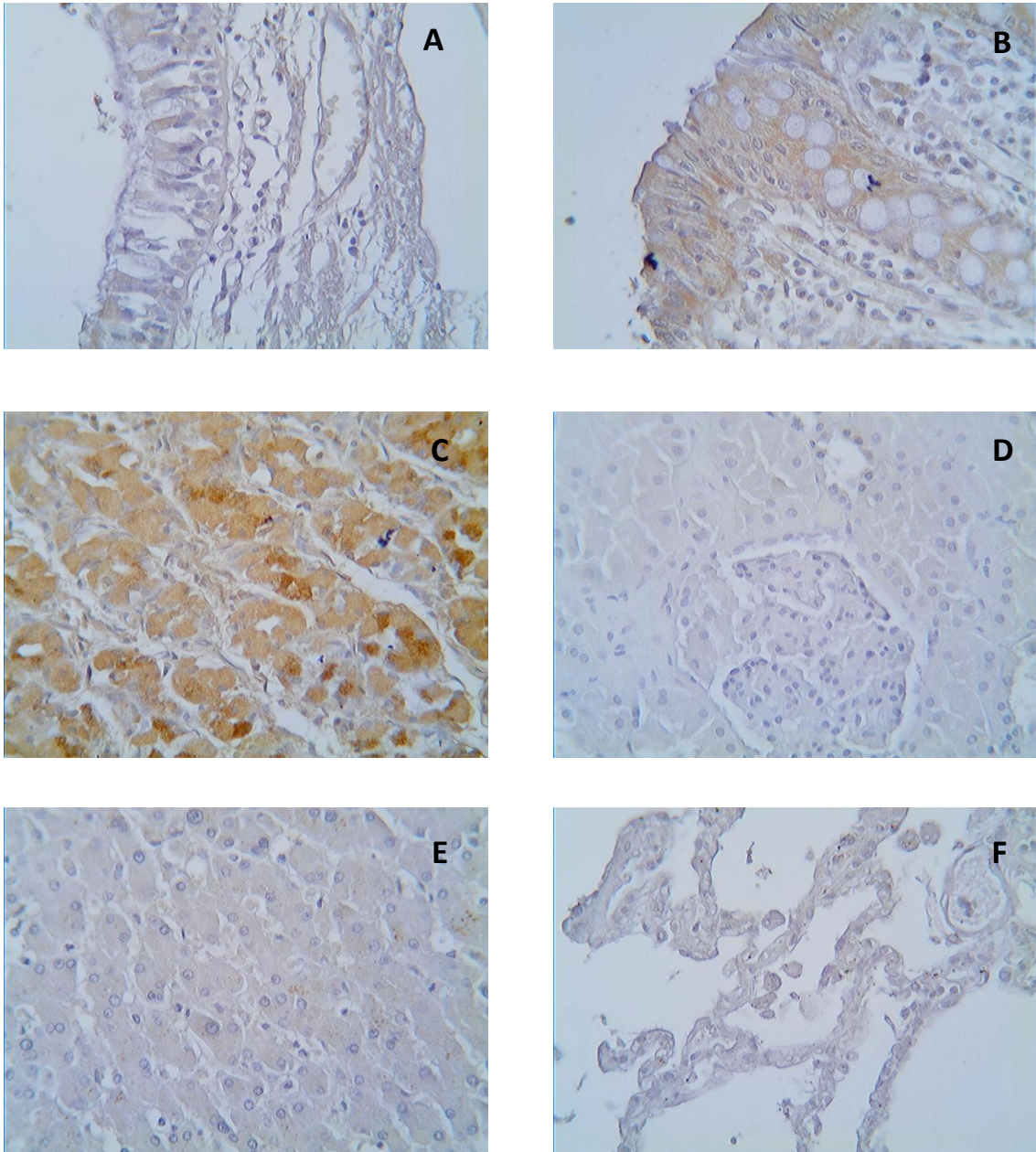


Fig.30. light micrographs of tissue microarray-Immunohistochemical assay with mAb 373E1 (DAB, brown), X400.

(A): pseudo-stratified epithelium lining of bronchus;(B): absorptive and goblet cells of colon;(C): gastric mucosa; (D):glomerulus and podocytes attached to glomerular capillaries;(E): hepatocytes separated by hepatic sinusoids: (F): cuboidal alveolar cells of lung.

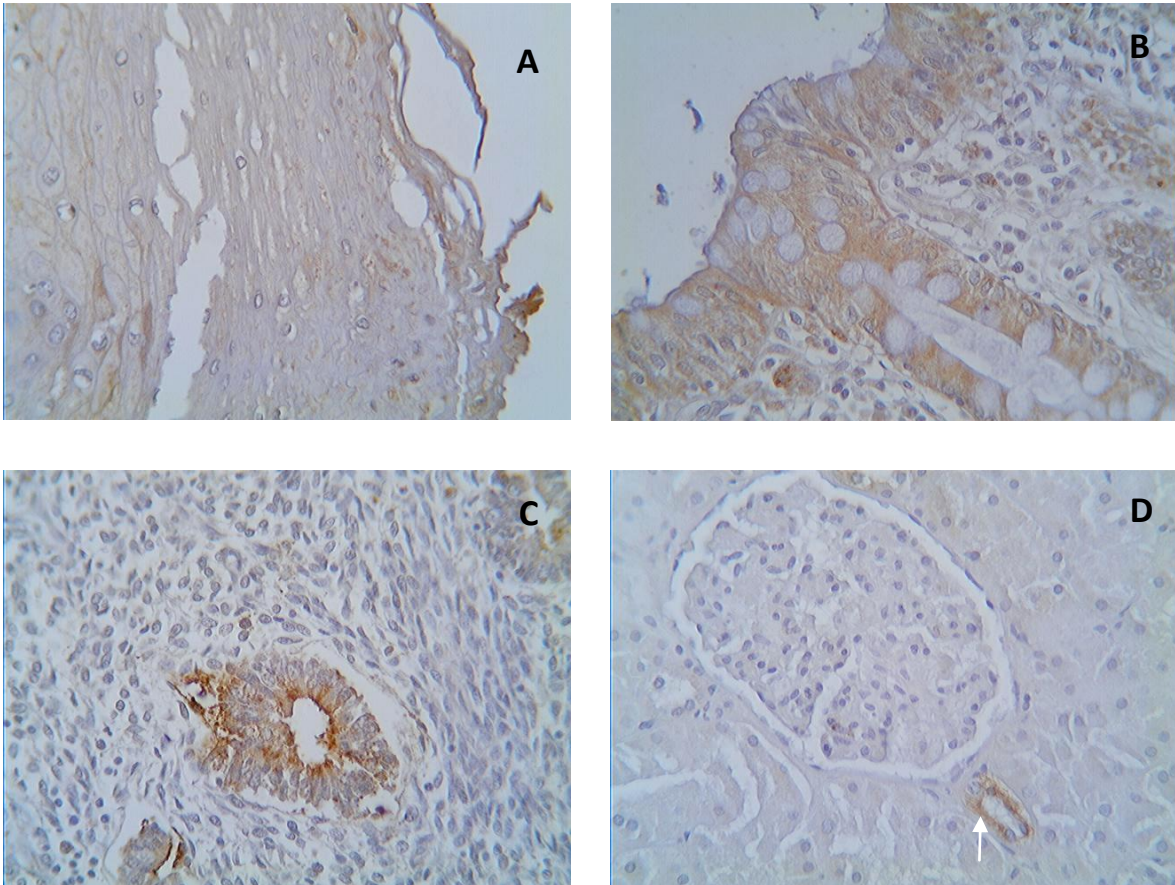


Fig.31. light micrographs of tissue microarray-Immunohistochemical assay with mAb BCD4 (DAB, brown), X400.
(A): keratinized stratified squamous epithelia of the skin; (B): absorptive and goblet cells of colon;(C): glandular epithelium of uterus;(D): glomerulus and podocytes attached to glomerular capillaries and cuboidal cell of kidney duct (arrow).

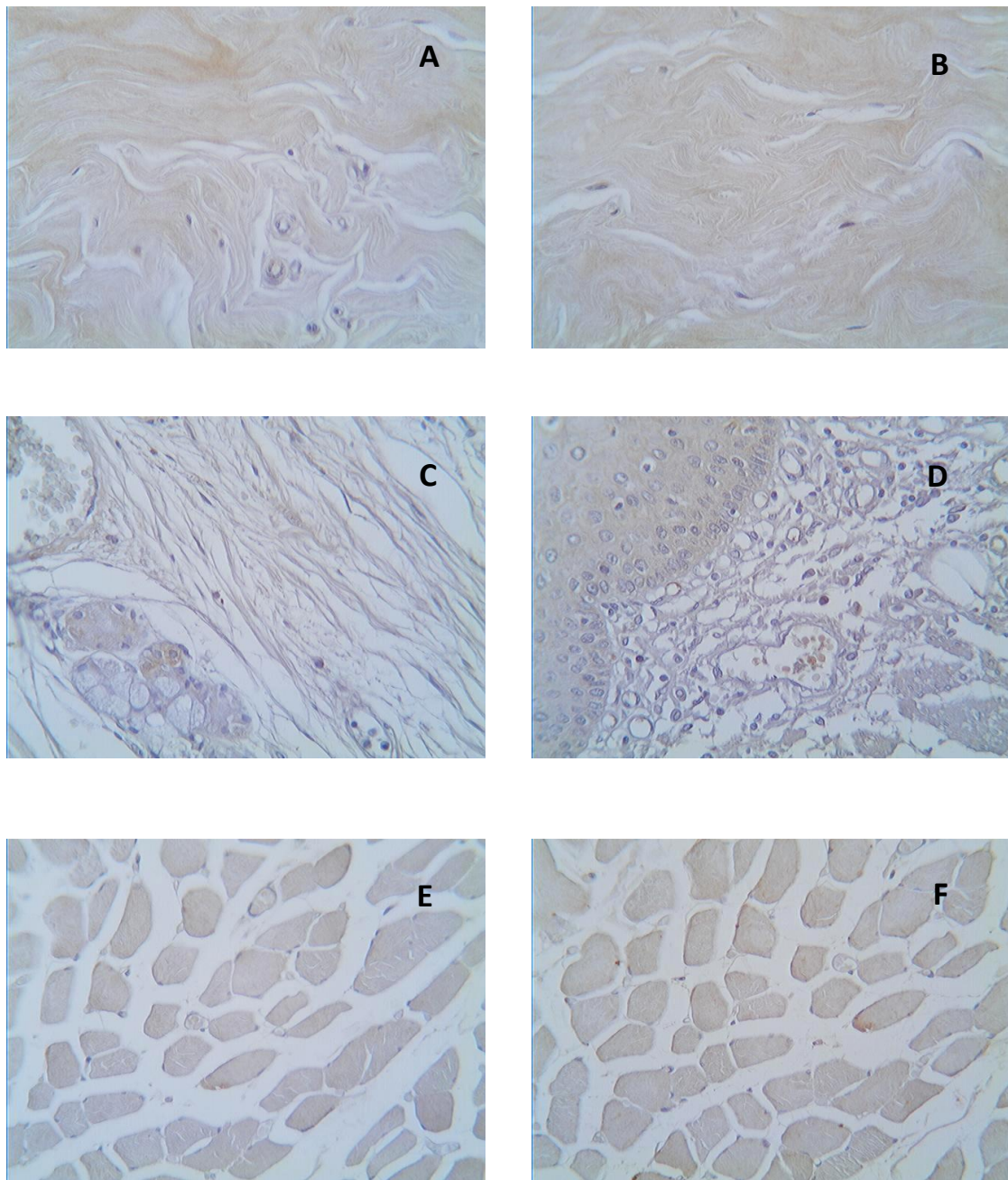


Fig.32. light micrographs of tissue microarray-Immunohistochemical assay with mAb 373E1 and mAb BCD4 (DAB, brown), X400.

(A): regular dense connective of resting mammary glands, mAb 373E1; (B): regular dense connective of resting mammary glands, with mAb BCD4 (C): loose connective that surround a mucous gland associated with bronchus with mAb 373E1; (D): loose connective of esophagus with mAb BCD4 (E): muscle skeletal fibers grouped into fascicles running longitudinally through the section with mAb 373E1; (F): muscle skeletal fibers grouped into fascicles running longitudinally through the section with mAb BCD-4.

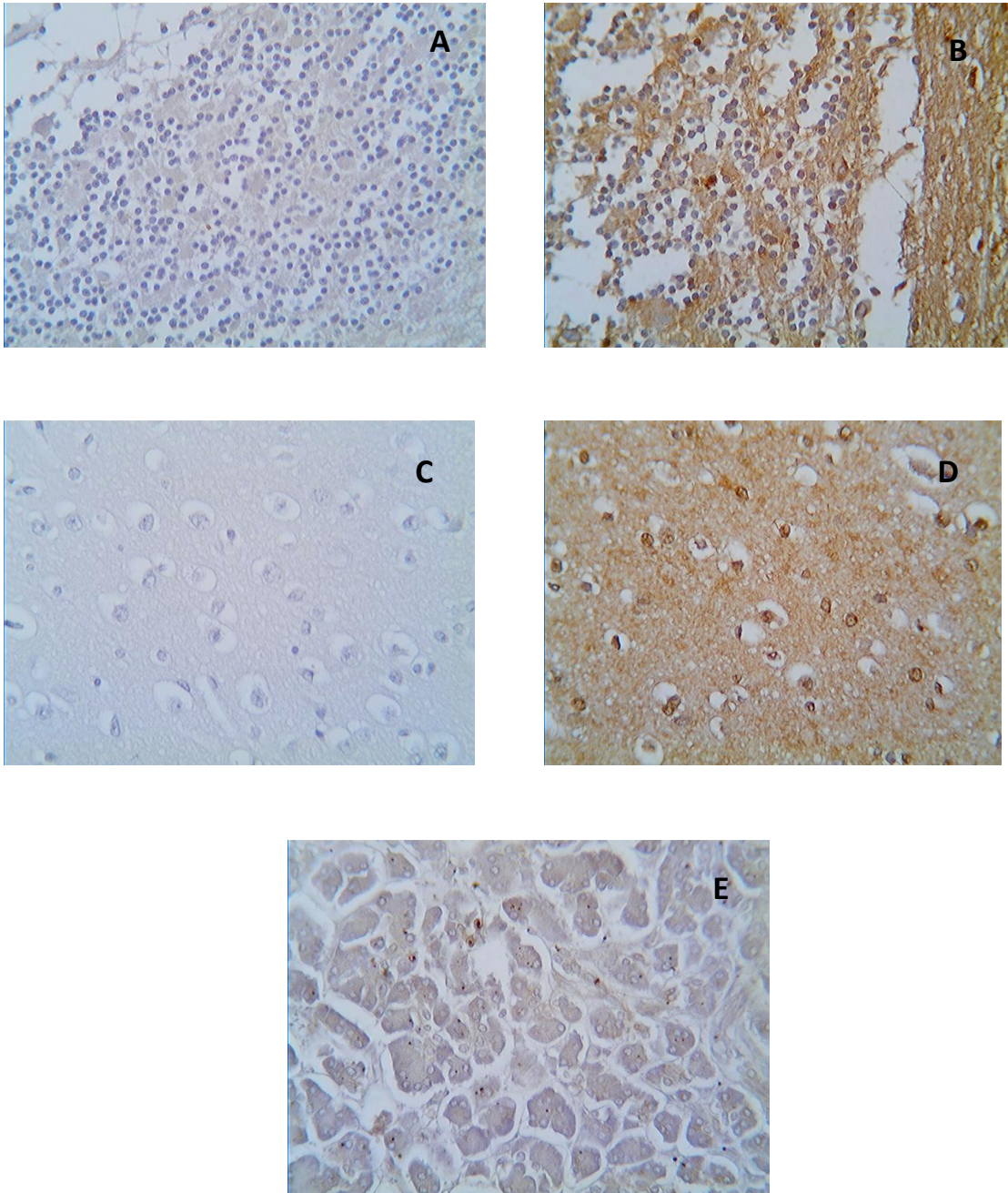


Fig. 33. light micrographs of tissue microarray-Immunohistochemical assay with mAb 373E1 and mAb BCD4 (DAB, brown), X400.

(A): white matter of cerebellum with mAb 373E1; (B): white and grey matter of cerebellum with mAb BCD4; (C): grey matter of cerebrum with mAb 373E1; (D): grey matter of cerebrum with mAb BCD4. (E): endocrine cells of pancreas with mAb 373E1.

4. DISCUSSION

The recent literature underlines as PGs may directly influence different cell functions, in normal as well as in pathological conditions. In particular recent works put the attention on the PGs involvement in the process of neoplastic transformation. Also if some PGs are well known to inhibit or to promote malignant transformation and tumor growth, others show a dual and controversial role: this is the case of the glypicans family. For example the inactivation of GPC3 and GPC5 genes seems to be related with an highly incidences of lung and breast carcinomas, mesothelioma and gastric cancer [Lin et al., 2012; Murthy et al., 2000; Xiang et al., 2001; Zhang et al., 2011; Zhu et al., 2002] while on the other hand genomic amplification of the 13q31.3 chromosome are suggested to be correlated with lymphomas [Yu et al., 2003] and rhabdomyosarcomas [Li et al., 2011; Williamson et al., 2007]. For this reason get off the hypothesis that role of GPCs in the tumorigenesis process may be specifically tumor-type correlated and may be influenced by their interactions with different ligands.

Glypicans are expressed in particular during development, suggesting that they play a central role in cell proliferation and morphogenesis and in regulating different heparin-binding growth factors in a tissue- and cell-specific manner. Among glypicans, GPC5 is the less well known, both for its involvement in normal and pathological conditions. Different studies correlated GPC5 expression modification with tumor progression [Li et al., 2011; Williamson et al., 2007; Yu et al., 2003; Zhang et al., 2011]. In this work we wanted to investigate the GPC5 role in the particular context of the soft tissue sarcomas, about that there are very few informations. After a deep study of the cell surface PG expression patterns of different sarcoma cell lines, we have identified a particular osteosarcoma cell line, 143B cells, characterized by a rather complex pattern of PG expression. We started with the construction of a cell model obtained by *de novo* surface expression of GPC5 and called 143B 5+. First we investigated the GPC5 cell surface localization by immunofluorescence and confocal analysis. The microscopic evaluation of GPC5 expressing cells suggest that the GPC5 localizes in particular cell surface regions that may correspond with reinforcement areas prevalently located on filopodia. This allow us to advance the hypothesis that GPC5 may be involved in cell adhesion and motility. The first evidence of this is the correlation between cytoskeletal organization and GPC5 localization. The study of the actin filaments network suggests that GPC5 is mainly distributed in specific membrane areas where actin forms reinforcing structures and that it may be involved in the cytoskeletal reorganization during cell movement. The investigation of GPC5-focal adhesion plaques correlation seems to support this hypothesis. We could observe that different focal adhesion molecules seems to colocalize with GPC5 and may be influenced by the presence of the PG. To deepen investigate the GPC5 involvement in the cell adhesion phenomena, we evaluate the ability of 143B 5+ cells to adhere on different ECM matrices

or in an anchorage-independent way. Our data suggest that GPC5 may affect cell ability to adhere on ECM components, such as collagen type III, collagen type VI, fibronectin and vitronectin. Probably GPC5 is involved in the interaction with particular integrin moieties that are related with the cell adhesion to these specific ECM matrices. In condition of anchorage independence, the presence of GPC5 on the cell surface seems to inhibit the cell growth capacity, prompting an inhibition influence of GPC5 on the survival of circulating cancer cells. Cell proliferation assays suggest us that GPC5 may be involved also in the proliferation capacity of 143B cells. More deeply, when GPC5 is expressed on the membrane, cells undergo a sensibly reducing in their proliferation rate, also in presence of growth factor such as VEGF, HGF or Wnt1. All these data support the idea that GPC5 may affect cell survival and proliferation, becoming a good candidate as tumor suppressor.

De novo expression of GPC5 was also tested in *in vivo* mouse models to investigate the influence of GPC5 on the whole tumor mass. The first important result obtained from *in vivo* inoculation of 143B 5+ and control cells, was that the presence of GPC5 on the injected cells seems to inhibit the tumor mass growth. Consequently vascularization of masses GPC5 positive results reduced respect to control, but the vascular perfusion does not appear altered suggesting that GPC5 does not influence the tumor vascular compartment. Immunostaining of the vascular network with marker for both endothelial and pericyte compartments, confirms that GPC5 probably does not influence the tumor vasculogenesis. To understand what is the basis of this anti-tumoral capacity, we investigated different aspects of tumorigenesis throughout immunostaining of the tumor masses. We observed that the human 143B 5+ cells injected in mouse have the possibility to survive in the murine environment and they may be observed within the murine masses. These cells seem to retain the same GPC5 membrane localization observed in *in vitro* assays. This data is confirmed also by gene transcript analysis. Interestingly, investigations on the proliferation rate of both human and murine cells and on the apoptotic rate do not show any particular differences between tumor masses obtained from 143B 5+ and control inocula.

Osteosarcoma cells transfected to over-express GPC6 show a behavior that is similar to what observed for control cells.

These data permit us to specifically ascribe to GPC5 expression all the characteristics of 143B 5+ cells.

We have therefore raised a unique anti-HS antibody denoted 4D1 that reacts with high affinity with heparin and highly sulfated HS variants and permits the immunolocalization of unique HS moieties in cells and tissues. The structural requirements of mAb 4D1 for antigen recognition

appear clearly distinct from those of several of the previously described anti-HS antibodies, including 10E4, 3G10, and HepSS1, although some overlapping traits were noted. Divergency for optimal antigen binding was observed with regard to sulfation degree, considering both 2-*O*- and 6-*O*-sulfation, and *N*-acetylation. The use of a panel of oligosaccharides of defined sizes and sulfation patterns further allowed us to establish that the epitope of mAb 4D1 must be contained within a tetrasaccharide HS unit. These observations lends further support to the notion that the epitope may be different than those recognized by the above previously described anti-HS antibodies, as well as by a number of phage display-generated anti-HS antibodies that have been published over the years [Lensen et al., 2005; Kurup et al., 2007; Smits et al., 2006; Thompson et al., 2009; van de Westerlo et al., 2002]. In accordance with its diverse epitope recognition, mAb 4D1 detected in a differentiated manner specific HS variants in healthy adult human tissues and its immunoreactive pattern was markedly different than that previously documented for other anti-HS antibodies. A first striking difference was the lack of mAb 4D1-reactive HS variants in basement membranes of epithelial tissues composing the majority of the organs of the body. This finding is consistent with the preferential staining of basement membranes by mAb 10E4 reported in previous investigations [David et al., 1992; van der Born et al., 2005] and further documented in this study. Why basement membranes would benefit from HSs with a lower sulfation degree remains an enigma. This in particular in light of the fact that no differences in the staining patterns of mAb 10E4 and 4D1 were observed in vascular structures; although light microscopy may not provide a sufficient high resolution for determining this aspect, it would appear that basement membranes of endothelial cells may contain HS with a spectrum of sulfation degrees. Differential expression of mAb 10E4- and HepSS1-reactive HS variants in basement membranes versus cell surfaces has also been documented in previous studies and parallels the analogous differential expression observed here between mAb 4D1 and mAb 10E4. Which cell surface-associated HSPGs actually carry the more highly sulfated HS moieties in different epithelial tissues remains to be further established. On the other hand it is likely that more sulfated HS chains may more effectively engage in growth factor sequestering on the cell membrane and optimally contribute to ternary complexes between these factors and their cognate receptors [Ashikari-Hada et al., 2004; Deakin et al., 2009; Guglier et al., 2008; Jastrebova et al., 2006; Jastrebova et al., 2010].

In parallel with mAb 4D1, a unique anti-KS was raised and called 373E1. This monoclonal antibody specifically react with a particular KS chemical structure. Thanks to the work of our collaborators of the Seikagaku biobusiness corporation, it is shown that this particular structure is characterized by an high concentration of sialic acid and fucose. The epitope necessary for 373E1

binding appear clearly distinct from those recognized from previously described anti-KS antibodies, such as BCD4. The differences in the binding site appear to involve the chemical structure of KS moiety. The distribution pattern of these particular KS structures generally results overlapping with that of KS recognized by BCD4. MAb 373E1 immunoreactivity appear to be intense in colon and intestine tissues and weakly in all the other tissues. Moreover 373E1-binding KS seems to be completely absent from all types of nervous tissues, suggesting that this mAb does not recognizes KS type III that is specifically distributed in all the nervous system. As KS is one of the most heterogeneous and less studied GAG moieties [Funderburgh, 2002], the characterization of these mAb may provide an additional tool for the study of this moiety.

5. ACKNOWLEDGEMENTS

I want to thank Prof. Roberto Perris for critical reading and valuable advice, Dr. Silvia Rossi for her help in preparing this work. I thank all the colleagues of the laboratory: Dr. Carlotta Alias, Dr. Alice Dallatomasina, Dr. Nicoletta Bertani, Dr. Domenica Mangieri and all the students that work with us.

I dedicate a special thank to all my family, my father, my mother and my brother Paolo, my wonderful grandmother and all my uncles and aunts. For their support and sacrifices.

I spend a greeting to all my unrivalled friends, my second family and my constant source of smiles.

6. BIBLIOGRAPHY

1. Anastasiou G, Gialeraki A, Merkouri E, Politou M, Travlou A. 2012. *Thrombomodulin as a regulator of the anticoagulant pathway: implication in the development of thrombosis*. Blood Coagul Fibrinolysis. 23, 1-10. Review.
2. Ashikari-Hada S, Habuchi H, Kariya Y, Itoh N, Reddi AH, Kimata K. 2004. *Characterization of growth factor-binding structures in heparin/heparan sulfate using an octasaccharide library*. J Biol Chem. 279, 12346-54.
3. Baghy K, Iozzo RV, Kovalszky I. 2012. *Decorin-TGF β axis in hepatic fibrosis and cirrhosis*. J Histochem Cytochem. 60, 262-8. Review.
4. Bezakova G, Ruegg MA. 2003. *New insights into the roles of agrin*. Nat Rev Mol Cell Biol. 4, 295-308. Review.
5. Bilandzic M, Stenvers KL. 2011. *Betaglycan: a multifunctional accessory*. Mol Cell Endocrinol. 339, 180-9. Review.
6. Bix G, Iozzo RV. 2008. *Novel interactions of perlecan: unraveling perlecan's role in angiogenesis*. Microsc Res Tech. 71, 339-48. Review.
7. Bleicher F, Couble ML, Buchaille R, Farges JC, Magloire H. 2001. *New genes involved in odontoblast differentiation*. Adv Dent Res. 15, 30-3. Review.
8. Chakravarti S. 2002. *Functions of lumican and fibromodulin: lessons from knockout mice*. Glycoconj J. 19,287-93. Review.
9. Choi Y, Chung H, Jung H, Couchman JR, Oh ES. 2011. *Syndecans as cell surface receptors: Unique structure equates with functional diversity*. Matrix Biol. 30, 93-9. Review.
10. Couchman JR. 2010. *Transmembrane signaling proteoglycans*. Annu Rev Cell Dev Biol. 26, 89-114. Review.
11. Datta S, Pierce M, Datta MW. 2006. *Perlecan signaling: helping hedgehog stimulate prostate cancer growth*. Int J Biochem Cell Biol. 38 ,1855-61. Review.
12. David G, Bai XM, Van der Schueren B, Cassiman JJ, Van den Berghe H. 1992. *Developmental changes in heparan sulfate expression: in situ detection with mAbs*. J Cell Biol. 119, 961-75.
13. Deakin JA, Blaum BS, Gallagher JT, Uhrín D, Lyon M. 2009. *The binding properties of minimal oligosaccharides reveal a common heparan sulfate/dermatan sulfate-binding site in hepatocyte growth factor/scatter factor that can accommodate a wide variety of sulfation patterns*. J Biol Chem. 284, 6311-21.
14. Desnoyers L, Arnott D, Pennica D. 2001. *WISP-1 binds to decorin and biglycan*. J Biol Chem. 276, 47599-607.

15. Evans MJ, Fanucchi MV, Plopper CG, Hyde DM. 2010. *Postnatal development of the lamina reticularis in primate airways*. *Anat Rec (Hoboken)*. 293, 947-54. Review.
16. Farach-Carson MC, Carson DD. 2007. *Perlecan--a multifunctional extracellular proteoglycan scaffold*. *Glycobiology*. 17, 897-905. Review.
17. Filmus J. 2001. *Glypicans in growth control and cancer*. *Glycobiology*. 11, 19R-23R. Review.
18. Funderburgh JL. 2002. *Keratan sulfate biosynthesis*. *IUBMB Life*. 54, 187-94. Review.
19. Gary SC, Hockfield S. 2000. *BEHAB/brevican: an extracellular matrix component associated with invasive glioma*. *Clin Neurosurg*. 47, 72-82. Review.
20. Guglier S, Hricovíni M, Raman R, Polito L, Torri G, Casu B, Sasisekharan R, Guerrini M. 2008. *Minimum FGF2 binding structural requirements of heparin and heparan sulfate oligosaccharides as determined by NMR spectroscopy*. *Biochemistry*. 47, 13862-9.
21. Haglund L, Tillgren V, Addis L, Wenglén C, Recklies A, Heinegård D. 2011. *Identification and characterization of the integrin alpha2beta1 binding motif in chondroadherin mediating cell attachment*. *J Biol Chem*. 286, 3925-34.
22. Happonen K.E., Fürst C.M., Saxne T., Heinegård D., Blom A.M. 2012. *PRELP protein inhibits the formation of the complement membrane attack complex*. *J. Biol. Chem*. 287, 8092-8100.
23. Hardingham TE, Fosang AJ. 1992. *Proteoglycans: many forms and many functions*. *FASEB J*. 6, 861-70. Review.
24. Hertweck MK, Erdfelder F, Kreuzer KA. 2011. *CD44 in hematological neoplasias*. *Ann Hematol*. 90, 493-508. Review.
25. Henríquez JP, Salinas PC. 2012. *Dual roles for Wnt signalling during the formation of the vertebrate neuromuscular junction*. *Acta Physiol (Oxf)*. 204, 128-36. Review.
26. Iozzo RV, Murdoch AD. 1996. *Proteoglycans of the extracellular environment: clues from the gene and protein side offer novel perspectives in molecular diversity and function*. *FASEB J*. 10, 598-614. Review.
27. Iozzo RV. 1998. *Matrix proteoglycans: from molecular design to cellular function*. *Annu Rev Biochem*. 67, 609-52. Review.
28. Iozzo RV, Sanderson RD. 2011. *Proteoglycans in cancer biology, tumour microenvironment and angiogenesis*. *J Cell Mol Med*. 15, 1013-31. Review.
29. Jastrebova N, Vanwildemeersch M, Rapraeger AC, Giménez-Gallego G, Lindahl U, Spillmann D. 2006. *Heparan sulfate-related oligosaccharides in ternary complex*

- formation with fibroblast growth factors 1 and 2 and their receptors.* J Biol Chem. 281, 26884-92.
30. Jastrebova N, Vanwildemeersch M, Lindahl U, Spillmann D. 2010. *Heparan sulfate domain organization and sulfation modulate FGF-induced cell signaling.* J Biol Chem. 285, 26842-51.
31. Jury EC, Kabouridis PS. 2010. *New role for Agrin in T cells and its potential importance in immune system regulation.* Arthritis Res Ther. 12, 205. Review.
32. Kalchishkova N, Fürst CM, Heinegård D, Blom AM. 2011. *NC4 Domain of cartilage-specific collagen IX inhibits complement directly due to attenuation of membrane attack formation and indirectly through binding and enhancing activity of complement inhibitors C4B-binding protein and factor H.* J Biol Chem. 286, 27915-26.
33. Karangelis DE, Kanakis I, Asimakopoulou AP, Karousou E, Passi A, Theocharis AD, Triposkiadis F, Tsilimingas NB, Karamanos NK. 2010. *Glycosaminoglycans as key molecules in atherosclerosis: the role of versican and hyaluronan.* Curr Med Chem. 17, 4018-26. Review.
34. Kinoshita, A., Sugahara, K., 1999. *Microanalysis of glycosaminoglycan-derived oligosaccharides labeled with a fluorophore 2-aminobenzamide by high-performance liquid chromatography: application to disaccharide composition analysis and exosequencing of oligosaccharides.* Anal. Biochem. 269, 367-378.
35. Knox SM, Whitelock JM. 2006. *Perlecan: how does one molecule do so many things?* Cell Mol Life Sci. 63, 2435-45. Review.
36. Knudson CB, Knudson W. 2001. *Cartilage proteoglycans.* Semin Cell Dev Biol. 12, 69-78. Review.
37. Kolset SO, Tveit H. 2008. *Serglycin--structure and biology.* Cell Mol Life Sci. 65, 1073-85. Review.
38. Kolset SO, Pejler G. 2011. *Serglycin: a structural and functional chameleon with wide impact on immune cells.* J Immunol. 187, 4927-33. Review.
39. Koutsi A, Papapanagiotou A, Papavassiliou AG. 2008. *Thrombomodulin: from haemostasis to inflammation and tumourigenesis.* Int J Biochem Cell Biol. 40, 1669-73. Review.
40. Kurpakus Wheeler M, Kernacki KA, Hazlett LD. 1999. *Corneal cell proteins and ocular surface pathology.* Biotech Histochem. 74,146-59. Review.
41. Kurup S, Wijnhoven TJ, Jenniskens GJ, Kimata K, Habuchi H, Li JP, Lindahl U, van Kuppevelt TH, Spillmann D. 2007. *Characterization of anti-heparan sulfate phage display antibodies AO4B08 and HS4E4.* J Biol Chem. 282, 21032-42.
42. Kwon MJ, Jang B, Yi JY, Han IO, Oh ES. 2012. *Syndecans play dual roles as cell adhesion receptors and docking receptors.* FEBS Lett. 586, 2207-11. Review.

43. Le Goff MM, Bishop PN. 2007. *Focus on molecules: opticin*. Exp Eye Res. 85, 303-4. Review.
44. Lensen JF, Rops AL, Wijnhoven TJ, Hafmans T, Feitz WF, Oosterwijk E, Banas B, Bindels RJ, van den Heuvel LP, van der Vlag J, Berden JH, van Kuppevelt TH. 2005. *Localization and functional characterization of glycosaminoglycan domains in the normal human kidney as revealed by phage display-derived single chain antibodies*. J Am Soc Nephrol. 16, 1279-88.
45. Li F, Shi W, Capurro M, Filmus J. 2011. *Glypican-5 stimulates rhabdomyosarcoma cell proliferation by activating Hedgehog signaling*. J Cell Biol. 192, 691-704.
46. Lin Q, Xiong LW, Pan XF, Gen JF, Bao GL, Sha HF, Feng JX, Ji CY, Chen M. 2012. *Expression of GPC3 protein and its significance in lung squamous cell carcinoma*. Med Oncol. 29, 663-9.
47. Louderbough JM, Schroeder JA. 2011. *Understanding the dual nature of CD44 in breast cancer progression*. Mol Cancer Res. 9, 1573-86. Review.
48. Marneros AG, Olsen BR. 2001. *The role of collagen-derived proteolytic fragments in angiogenesis*. Matrix Biol. 20, 337-45. Review.
49. Midorikawa Y, Ishikawa S, Iwanari H, Imamura T, Sakamoto H, Miyazono K, Kodama T, Makuuchi M, Aburatani H. 2003. *Glypican-3, overexpressed in hepatocellular carcinoma, modulates FGF2 and BMP-7 signaling*. Int J Cancer. 103, 455-65.
50. Morgan MR, Humphries MJ, Bass MD. 2007. *Synergistic control of cell adhesion by integrins and syndecans*. Nat Rev Mol Cell Biol. 8, 957-69. Review.
51. Morgenstern DA, Asher RA, Fawcett JW. 2002. *Chondroitin sulphate proteoglycans in the CNS injury response*. Prog Brain Res. 137, 313-32. Review.
52. Multhaupt HA, Yoneda A, Whiteford JR, Oh ES, Lee W, Couchman JR. 2009. *Syndecan signaling: when, where and why?* J Physiol Pharmacol. 60 Suppl 4, 31-8. Review.
53. Murthy SS, Shen T, De Rienzo A, Lee WC, Ferriola PC, Jhanwar SC, Mossman BT, Filmus J, Testa JR. 2000. *Expression of GPC3, an X-linked recessive overgrowth gene, is silenced in malignant mesothelioma*. Oncogene. 19, 410-6.
54. Myhre K, Blobe GC. 2009. *Proteoglycan signaling co-receptors: roles in cell adhesion, migration and invasion*. Cell Signal. 21, 1548-58. Review.
55. Neame PJ, Tapp H, Azizan A. 1999. *Noncollagenous, nonproteoglycan macromolecules of cartilage*. Cell Mol Life Sci. 55, 1327-40. Review.
56. Oohira A, Shuo T, Tokita Y, Nakanishi K, Aono S. 2004. *Neuroglycan C, a brain-specific part-time proteoglycan, with a particular multidomain structure*. Glycoconj J. 21, 53-7. Review.

57. Pejler G, Abrink M, Wernersson S. 2009. *Serglycin proteoglycan: regulating the storage and activities of hematopoietic proteases*. *Biofactors*. 35, 61-8. Review.
58. Pugia MJ, Valdes R Jr, Jortani SA. 2007. *Bikunin (urinary trypsin inhibitor): structure, biological relevance, and measurement*. *Adv Clin Chem*. 44, 223-45. Review.
59. Rahmani M, Wong BW, Ang L, Cheung CC, Carthy JM, Walinski H, McManus BM. 2006. *Versican: signaling to transcriptional control pathways*. *Can J Physiol Pharmacol*. 84, 77-92. Review.
60. Rauch U, Feng K, Zhou XH. 2001. *Neurocan: a brain chondroitin sulfate proteoglycan*. *Cell Mol Life Sci*. 58, 1842-56. Review.
61. Ricciardelli C, Sakko AJ, Ween MP, Russell DL, Horsfall DJ. 2009. *The biological role and regulation of versican levels in cancer*. *Cancer Metastasis Rev*. 28, 233-45. Review.
62. Röhl S, Seul J, Paulsson M, Hartmann U. 2006. *Testican-1 is dispensable for mouse development*. *Matrix Biol*. 25, 373-81. Review.
63. Rucci N, Rufo A, Alamanou M, Capulli M, Del Fattore A, Ahrman E, Capece D, Iansante V, Zazzeroni F, Alesse E, Heinegård D, Teti A. 2009. *The glycosaminoglycan-binding domain of PRELP acts as a cell type-specific NF-kappaB inhibitor that impairs osteoclastogenesis*. *J Cell Biol*. 187, 669-83.
64. Roughley PJ. 2006. *The structure and function of cartilage proteoglycans*. *Eur Cell Mater*. 12, 92-101. Review.
65. Sasaki T, Hohenester E, Timpl R. 2002. *Structure and function of collagen-derived endostatin inhibitors of angiogenesis*. *IUBMB Life*. 53, 77-84. Review.
66. Sasisekharan R, Raman R, Prabhakar V. 2006. *Glycomics approach to structure-function relationships of glycosaminoglycans*. *Annu Rev Biomed Eng*. 8, 181-231. Review.
67. Schick BP. 2010. *Serglycin proteoglycan deletion in mouse platelets: physiological effects and their implications for platelet contributions to thrombosis, inflammation, atherosclerosis, and metastasis*. *Prog Mol Biol Transl Sci*. 93, 235-87. Review.
68. Seidler DG, Dreier R. 2008. *Decorin and its galactosaminoglycan chain: extracellular regulator of cellular function?* *IUBMB Life*. 60, 729-33. Review.
69. Silbert JE, Sugumaran G. 2002. *Biosynthesis of chondroitin/dermatan sulfate*. *IUBMB Life*. 54, 177-86. Review.
70. Singla S, Hu C, Mizeracki A, Mehta JL. 2011. *Decorin in atherosclerosis*. *Ther Adv Cardiovasc Dis*. 5, 305-14. Review.
71. Smits NC, Lensen JF, Wijnhoven TJ, Ten Dam GB, Jenniskens GJ, van Kuppevelt TH. 2006. *Phage display-derived human antibodies against specific glycosaminoglycan epitopes*. *Methods Enzymol*. 416, 61-87.

72. Stallcup WB, Huang FJ. 2008. *A role for the NG2 proteoglycan in glioma progression*. Cell Adh Migr. 2, 192-201. Review.
73. Tan AM, Zhang W, Levine JM. 2005. *NG2: a component of the glial scar that inhibits axon growth*. J Anat. 207, 717-25. Review.
74. Teng YH, Aquino RS, Park PW. 2012. *Molecular functions of syndecan-1 in disease*. Matrix Biol. 31, 3-16. Review.
75. Thompson SM, Fernig DG, Jesudason EC, Losty PD, van de Westerlo EM, van Kuppevelt TH, Turnbull JE. 2009. *Heparan sulfate phage display antibodies identify distinct epitopes with complex binding characteristics: insights into protein binding specificities*. J Biol Chem. 284, 35621-31.
76. Tkachenko E, Rhodes JM, Simons M. 2005. *Syndecans: new kids on the signaling block*. Circ Res. 96, 488-500. Review.
77. Trowbridge JM, Gallo RL. 2002. *Dermatan sulfate: new functions from an old glycosaminoglycan*. Glycobiology. 12, 117R-25R. Review.
78. Ueno, M., Yamada, S., Zako, M., Bernfield, M., and Sugahara, K., 2001. *Structural characterization of heparan sulfate and chondroitin sulfate of syndecan-1 purified from normal murine mammary gland epithelial cells. Common phosphorylation of xylose and differential sulfation of galactose in the protein linkage region tetrasaccharide sequence*. J. Biol. Chem. 276, 29134-29140
79. van den Born J, Salmivirta K, Henttinen T, Ostman N, Ishimaru T, Miyaura S, Yoshida K, Salmivirta M. 2005. *Novel heparan sulfate structures revealed by monoclonal antibodies*. J Biol Chem. May 27;280(21):20516-23.
80. van de Westerlo EM, Smetsers TF, Dennissen MA, Linhardt RJ, Veerkamp JH, van Muijen GN, van Kuppevelt TH. 2002. *Human single chain antibodies against heparin: selection, characterization, and effect on coagulation*. Blood. 99, 2427-33.
81. Wadhwa S, Embree MC, Bi Y, Young MF. 2004. *Regulation, regulatory activities, and function of biglycan*. Crit Rev Eukaryot Gene Expr. 14,301-15. Review.
82. Wight TN. 2008. *Arterial remodeling in vascular disease: a key role for hyaluronan and versican*. Front Biosci. 13, 4933-7. Review.
83. Williamson D, Selfe J, Gordon T, Lu YJ, Pritchard-Jones K, Murai K, Jones P, Workman P, Shipley J. 2007. *Role for amplification and expression of glypican-5 in rhabdomyosarcoma*. Cancer Res. 67, 57-65.
84. Whitelock JM, Melrose J, Iozzo RV. 2008. *Diverse cell signaling events modulated by perlecan*. Biochemistry. 47, 11174-83. Review.
85. Wu YJ, La Pierre DP, Wu J, Yee AJ, Yang BB. 2005. *The interaction of versican with its binding partners*. Cell Res. 15, 483-94. Review.

86. Wu Y, Belenkaya TY, Lin X. 2010. *Dual roles of Drosophila glypican Dally-like in Wingless/Wnt signaling and distribution*. Methods Enzymol. 480, 33-50. Review.
87. Xiang YY, Ladedo V, Filmus J. 2001. *Glypican-3 expression is silenced in human breast cancer*. Oncogene. 20, 7408-12.
88. Xu JP, Zhao J, Li S. 2011. *Roles of NG2 glial cells in diseases of the central nervous system*. Neurosci Bull. 27, 413-21. Review.
89. Yamada, S., Okada, Y., Ueno, M., Iwata, S., Deepa, S. S., Nishimura, S., Fujita, M., Van Die. I., Hirabayashi, Y., Sugahara, K., 2002. *Determination of the glycosaminoglycan-protein linkage region oligosaccharide structures of proteoglycans from Drosophila melanogaster and Caenorhabditis elegans*. J. Biol. Chem. 277, 31877-31886.
90. Yamaguchi Y. 1996. *Brevican: a major proteoglycan in adult brain*. Perspect Dev Neurobiol. 3, 307-17. Review.
91. Yan D, Wu Y, Feng Y, Lin SC, Lin X. 2009. *The core protein of glypican Dally-like determines its biphasic activity in wingless morphogen signaling*. Dev Cell. 17, 470-81.
92. Young MF, Bi Y, Ameye L, Chen XD. 2002. *Biglycan knockout mice: new models for musculoskeletal diseases*. Glycoconj J. 19, 257-62. Review.
93. Yoneda A, Lendorf ME, Couchman JR, Multhaupt HA. 2012. *Breast and ovarian cancers: a survey and possible roles for the cell surface heparan sulfate proteoglycans*. J Histochem Cytochem. 60, 9-21. Review.
94. Yu W, Inoue J, Imoto I, Matsuo Y, Karpas A, Inazawa J. 2003. *GPC5 is a possible target for the 13q31-q32 amplification detected in lymphoma cell lines*. J Hum Genet. 48, 331-5.
95. Zaucke F, Grässel S. 2009. *Genetic mouse models for the functional analysis of the perifibrillar components collagen IX, COMP and matrilin-3: Implications for growth cartilage differentiation and endochondral ossification*. Histol Histopathol. 24, 1067-79. Review.
96. Zhang C, Zhang S, Zhang D, Zhang Z, Xu Y, Liu S. 2011. *A lung cancer gene GPC5 could also be crucial in breast cancer*. Mol Genet Metab. 103, 104-5.
97. Zhu Z, Friess H, Kleeff J, Wang L, Wirtz M, Zimmermann A, Korc M, Büchler MW. 2002. *Glypican-3 expression is markedly decreased in human gastric cancer but not in esophageal cancer*. Am J Surg. 184, 78-83.
98. Zhuo L, Salustri A, Kimata K. 2002. *A physiological function of serum proteoglycan bikunin: the chondroitin sulfate moiety plays a central role*. Glycoconj J. 19, 241-7. Review.